

G9116

HYDRODYNAMIC STUDY OF SWIRLING FLUIDIZED BED AND THE ROLE OF DISTRIBUTOR

**THESIS SUBMITTED TO
THE COCHIN UNIVERSITY OF SCIENCE AND TECHNOLOGY
IN PARTIAL FULFILMENT OF THE
REQUIREMENTS FOR THE AWARD OF THE DEGREE OF
DOCTOR OF PHILOSOPHY**

BY

PAULOSE M. M.

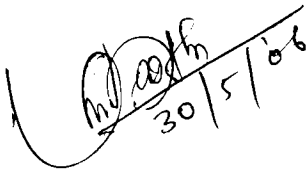


**SCHOOL OF ENGINEERING
COCHIN UNIVERSITY OF SCIENCE AND TECHNOLOGY
KOCHI- 682 022, KERALA, INDIA**

May - 2006

CERTIFICATE

This is to certify that the thesis entitled **HYDRODYNAMIC STUDY OF SWIRLING FLUIDIZED BED AND THE ROLE OF DISTRIBUTOR** is based on the original work done by Sri Paulose M.M. under our supervision and guidance in School of Engineering, Cochin University of Science and Technology. No part of this thesis has been presented for any other degree from any other institution.



Dr. Narayanan Namboothiri V.N,
Lecturer,
Division of Mechanical Engineering,
School of Engineering,
Cochin University of Science and
Technology, Kochi- 22



Dr Sreejith P.S,
Professor,
Division of Mechanical Engineering,
School of Engineering,
Cochin University of Science and
Technology, Kochi- 22

Kochi-22
30-05-2006

ABSTRACT

In spite of the wide industrial applications of swirling fluidized bed, critical review of the available literature on the hydrodynamic characteristics of fluidized bed reveals that, a systematic study is limited, particularly on the influence of the angle of air injection, area of opening and the useful area of the distributor on the hydrodynamic characteristics of the swirling fluidized bed.

For the present, it has been proposed to study the hydrodynamic characteristics of swirling fluidized bed, using large particles (Geldart D-type) selected from locally available agricultural produce (coffee beans and black pepper). The important variables considered in the present study include percentage area of opening, angle of air injection and the percentage useful area of the distributor.

A total of seven distributors have been designed and fabricated for a bed column of 300 mm, namely single row vane type distributors (15° and 20° vane angle), inclined hole type distributors (15° and 20° hole angle), three row vane type distributors (15° and 20° vane angle) and perforated plate distributors. The useful area of distributor of single row vane type, three row vane- type and inclined hole- type distributors are respectively 64 %, 91 % and 94 %.

Detailed experimental studies have been carried out using seven different distributors. The hydrodynamic parameters considered in the present study include distributor pressure drop, air velocity, minimum fluidizing velocity, bed pressure drop, bed height and the bed behaviour.

It has been observed that, in general, the distributor pressure drop decreases with an increase in the percentage area of opening. Further, an increase in the area of opening above 17 % will not considerably reduce the distributor pressure drop. In the present study, for the distributor with an area of opening 17 %, and corresponding to the

maximum measured superficial velocity of 4.33 m/s, the distributor pressure drop obtained was 55.25 mm of water.

Lower percentage of the useful area of distributor in single row vane type distributors can be improved using multiple rows of vanes. So, the three row vane type distributors show better performance compared to the other type of distributors considered.

Based on the study of empty bed it could be observed that the radial component of velocity, which supports the radial mixing of the particles decreases with an increase in radial distance. On the other hand, the tangential component of velocity, which causes swirl motion, increases with an increase in radial distance.

The study on the bed behaviour revealed that, in a swirling fluidized bed, once swirl motion starts, the bed pressure drop increases with superficial velocity in the outer region and it decreases in the inner region. This means that, with higher superficial velocity, the air might get by-passed through the inner boundary of the bed (around the cone). So, depending on the process for which the bed is used, the maximum superficial velocity is to be limited to have an optimum bed performance.

The superficial velocity corresponding to the beginning of wave and swirl motion increases with an increase in the bed weight and after a certain bed weight, they become constant and are independent of bed weight. Identification of the constant superficial velocity corresponding to the wave and swirl motion in a fluidized bed is important for determining the optimum bed weight, particularly for processes like drying of agricultural produces.

TABLE OF CONTENTS

CERTIFICATE	i
ACKNOWLEDGMENS	ii
ABSTRACT	iii
TABLE OF CONTENTS	v
LIST OF TABLES	ix
LIST OF FIGURES	x
ABBREVIATIONS	xvi
NOMENCLATURE	xvii
CHAPTER 1 INTRODUCTION	1
1.1 GENERAL	1
1.2 SCOPE OF THE THESIS	3
CHAPTER 2 LITERATURE REVIEW	4
2.1 INTRODUCTION	4
2.2 DISTRIBUTOR PRESSURE DROP	4
2.3 BED PRESSURE DROP	10
2.4 EFFECT OF TEMPERA ^T URE IN BED HYDRODYNAMICS	11
2.5 CENTRIFUGAL FLUIDIZED BED	12
2.6 FLUIDIZED BED DRYING	14
2.7 SWIRLING FLUIDIZED BED	16
2.8 DISCUSSION	18
2.9 OBJECTIVES OF THE PRESENT STUDY	19
CHAPTER 3 DESIGN AND FABRICATION OF DISTRIBUTORS	20
3.1 INTRODUCTION	20

3.2	SINGLE ROW VANE TYPE DISTRIBUTORS	20
3.2.1	Design	20
3.2.2	Fabrication	24
3.3	INCLINED HOLE TYPE DISTRIBUTORS	25
3.3.1	Design	25
3.3.2	Fabrication	26
3.4	THREE ROW VANE TYPE DISTRIBUTORS	28
3.4.1	Design	29
3.4.2	Fabrication	29
3.5	PERFORATED PLATE DISTRIBUTOR	30
3.6	CONCLUSION	30
CHAPTER 4 EXPERIMENTAL SET UP AND PROCEDURE		32
4.1	INTRODUCTION	32
4.2	EXPERIMENTAL SET-UP	32
4.3	EXPERIMENTAL PROCEDURE	35
4.3.1	Determination of Physical Properties of Bed Particles	35
4.3.1.1	Mean particle size	35
4.3.1.2	Bed density	36
4.3.1.3	Particle density	36
4.3.1.4	Bed voidage	37
4.3.1.5	Particle specification	38
4.3.2	Determination of Distributor Pressure Drop	38
4.3.3	Determination of Minimum Fluidizing Velocity	39
4.3.4	Measurement of Air Velocity in Empty Bed	40
4.3.5	Determination of Bed Pressure Drop	42

4.3.6	Determination of Bed Height	42
4.3.7	Identification of Different Regimes	43
4.3.8	Determination of Bed Pressure Drop along Radial Direction	43
4.4	CONCLUSION	43
CHAPTER 5 RESULTS AND DISCUSSION		45
5.1	INTRODUCTION	45
5.2	DISTRIBUTOR PRESSURE DROP	45
5.3	AIR VELOCITY IN EMPTY BED	48
5.4	MINIMUM FLUIDIZING VELOCITY OF VANE TYPE DISTRIBUTORS	56
5.5	VARIATION OF BED PRESSURE DROP WITH SUPERFICIAL VELOCITY	60
5.5.1	Behaviour of Single Row Vane Type Distributor	61
5.5.2	Behaviour of Inclined Hole Type Distributor	70
5.5.3	Behaviour of Three Row Vane Type Distributor	74
5.6	VARIATION OF BED PRESSURE DROP WITH SUPERFICIAL VELOCITY ALONG RADIAL DIRECTION FOR THREE ROW VANE TYPE DISTRIBUTORS	86
5.7	VARIATION OF BED HEIGHT WITH SUPERFICIAL VELOCITY IN INCLINED HOLE TYPE DISTRIBUTORS	91
5.8	BED BEHAVIOUR IN THREE RAW VANE TYPE DISTRIBUTORS	94
5.9	CONCLUSIONS	99
5.9.1	Distributor pressure drop	100
5.9.2	Air velocity in empty bed	100
5.9.3	Minimum fluidizing velocity of vane type distributors	101
5.9.4	Variation of bed pressure drop with superficial velocity	101
5.9.5	Variation of bed Pressure drop With superficial velocity	102

along radial direction	
5.9.6 Variation of bed height with superficial velocity	103
5.9.7 Bed behaviour in three row vane type distributors	103
CHAPTER 6 CONCLUSIONS	104
6.1 INTRODUCTION	104
6.2 CONCLUSIONS	104
6.3 SUGGESTIONS FOR FUTURE WORK	106
APPENDIX A CALIBRATION OF THREE HOLE PROBE	108
APPENDIX B CALIBRATION CERTIFICATE OF MICRO-MANOMETER	111
APPENDIX C UNCERTAINTY ANALYSIS	112
APPENDIX D VIDEO CLIPPINGS	120
REFERENCES	121

LIST OF TABLES

Table No.	Table Title	Page No.
3.2.1	Design details of single row vane-type distributors	23
3.3.1	Distribution of holes in inclined hole distributors	26
3.4.1	Distributor details of three row vane type distributors	29
4.3.1	Mean particle size of coffee beans	36
4.3.2	Calculation of bed density	37
4.3.3	Particle density of coffee beans	37
4.3.4	Particle density of pepper	38
4.3.5	Physical properties of particles	38
5.2.1	Variation of distributor pressure drop with superficial velocity	47
5.4.1	Comparison of minimum fluidizing velocity	60
5.8.1	Superficial velocity corresponding to the starting of wave motion and swirl motion	99

LIST OF FIGURES

Fig. No.	Figure Title	Page No.
3.2.1	Geometric relationship of vanes in single row vane type distributor	22
3.2.2	Photograph of single row vane type distributor	24
3.3.1	Three dimensional view of the fixture	27
3.3.2	Photograph of inclined hole type distributor	28
3.4.1	Photograph of three row vane type distributor	30
4.2.1	Schematic diagram of the experimental set-up	32
4.2.2	Photograph of the experimental set-up	33
4.2.3	Three hole probe and its holder	35
5.2.1	Variation of distributor pressure drop with superficial velocity	46
5.3.1	Variation of velocity with flow rate in three row vane type distributor -probe at 5 mm height and at 143 mm radial distance	49
5.3.2	Variation of velocity with flow rate in three row vane type distributor- probe at 5 mm height and at 133 mm radial distance	50
5.3.3	Variation of velocity with flow rate in three row vane type distributor- probe at 5 mm height and at 123 mm radial distance	50
5.3.4	Variation of velocity with flow rate in three row vane type distributor -probe at 5 mm height and at 113 mm radial distance	51
5.3.5	Variation of velocity with flow rate in three row vane type distributor- probe at 5 mm height and at 103 mm radial distance	51
5.3.6	Variation of velocity with flow rate in three row vane type distributor- probe at 5 mm height and at 93 mm radial distance	52
5.3.7	Variation of velocity with flow rate in three row vane type distributor - probe at 5 mm height and at 83 mm radial distance	53

5.3.8	Variation of velocity at different radial distances in three row vane type distributor -probe at 5 mm height and airflow rate- 0.124 m ³ /s	53
5.3.9	Variation of velocity at different radial distances in three row vane type distributor - probe at 5 mm height and at airflow rate - 0.175 m ³ /s	54
5.3.10	Variation of velocity at different radial distances in three row vane type distributor - probe at 10 mm height and airflow rate - 0.124 m ³ /s	54
5.3.11	Variation of velocity at different radial distances in three row vane type distributor - probe at 10 mm height and airflow rate - 0.175 m ³ /s	55
5.3.12	Plot showing boundary of region having swirl motion of air in empty bed for a three row vane type distributor	56
5.4.1	Minimum fluidizing velocity in beds with conventional bed – bed material - coffee beans	58
5.4.2	Minimum fluidizing velocity in beds with single row vane type distributor- vane angle – 20 ° and bed material - coffee beans	58
5.4.3	Minimum fluidizing velocity in beds with single row vane type distributor- vane angle -15 ° and bed material - coffee beans	59
5.4.4	Minimum fluidizing velocity in beds with three row vane type distributor -vane angle - 20 ° and bed material – pepper	59
5.4.5	Minimum fluidizing velocity in beds with three row vane type distributor – vane angle – 15 ° and bed material – pepper	60
5.5.1	Comparison of the variation of bed pressure drop with superficial velocity in beds with single row vane type distributor having vane angle $\theta = 15^{\circ}$ and in conventional distributor (bed material- 2 kg coffee beans)	62
5.5.2	Single row vane-type distributor showing separation of particles from the cone	63
5.5.3	Comparison of the variation of bed pressure drop with superficial velocity in beds with single row vane type distributor having vane angle $\theta = 15^{\circ}$ and conventional distributor (bed material- 2 kg pepper)	64
5.5.4	Comparison of the variation of bed pressure drop with superficial velocity in beds with single row vane type distributor having vane angle $\theta = 20^{\circ}$ and conventional distributor (bed material- 2 kg coffee beans)	64

5.5.5	Comparison of the variation of bed pressure drop with superficial velocity in beds with single row vane type distributor having vane angle $\theta = 20^{\circ}$ and conventional distributor (bed material-2 kg pepper)	65
5.5.6	Effect of bed weight in beds with single row vane type distributor having vane angle $\theta = 15^{\circ}$ (bed material – coffee beans)	66
5.5.7	Effect of bed weight in beds with single row vane type distributor having vane angle $\theta = 20^{\circ}$ (bed material – coffee beans)	66
5.5.8	Effect of bed weight in beds with single row vane type distributor having vane angle $\theta = 15^{\circ}$ (bed material – pepper)	67
5.5.9	Effect of bed weight in beds with single row vane type distributor having vane angle $\theta = 20^{\circ}$ (bed material – pepper)	67
5.5.10	Comparison of the variation of bed pressure drop with superficial velocity between 15° and 20° single row vane type distributors (bed material -1.5 kg coffee beans)	68
5.5.11	Comparison of the variation of bed pressure drop with superficial velocity between 15° and 20° single row vane type distributors (bed material –2.0 kg coffee beans)	69
5.5.12	Comparison of the variation of bed pressure drop with superficial velocity between 15° and 20° single row vane type distributors (bed material –1.5 kg pepper)	69
5.5.13	Comparison of the variation of bed pressure drop with superficial velocity between 15° and 20° single row vane type distributors (bed material –2.0 kg pepper)	71
5.5.14	Effect of bed weight in inclined hole type distributor having vane angle $\theta = 15^{\circ}$ (bed material – coffee beans)	71
5.5.15	Effect of bed weight in inclined hole type distributor having vane angle $\theta = 15^{\circ}$ (bed material – pepper)	72
5.5.16	Effect of bed weight in inclined hole type distributor having vane angle $\theta = 20^{\circ}$ (bed material – coffee beans)	73
5.5.17	Effect of bed weight in inclined hole type distributor having vane angle $\theta = 20^{\circ}$ (bed material – pepper)	73
5.5.18	Inclined hole type distributor showing bypassing of air	74
5.5.19	Comparison of the variation of bed pressure drop with	75

	superficial velocity in three row vane type distributor having vane angle $\theta = 15^0$ and conventional distributor (bed material- 2 kg coffee beans)	
5.5.20	Comparison of the variation of bed pressure drop with superficial velocity in three row vane type distributor having vane angle $\theta = 15^0$ and conventional distributor (bed material- 2 kg pepper)	75
5.5.21	Comparison of the variation of bed pressure drop with superficial velocity in three row vane type distributor having vane angle $\theta = 20^0$ and conventional distributor (bed material- 2 kg coffee beans)	76
5.5.22	Comparison of the variation of bed pressure drop with superficial velocity in three row vane type distributor having vane angle $\theta = 20^0$ and conventional distributor (bed material- 2 kg pepper)	76
5.5.23	Effect of bed weight on bed pressure drop in three row vane type distributor having vane angle $\theta = 15^0$ (bed material – coffee beans)	77
5.5.24	Effect of bed weight on bed pressure drop in three row vane type distributor having vane angle $\theta = 15^0$ (bed material – pepper)	78
5.5.25	Effect of bed weight on bed pressure drop in three row vane type distributor having vane angle $\theta = 20^0$ (bed material – coffee beans)	78
5.5.26	Effect of bed weight on bed pressure drop in three row vane type distributor having vane angle $\theta = 20^0$ (bed material – pepper)	79
5.5.27	Comparison of the variation of bed pressure drop with superficial velocity between 15^0 and 20^0 three row vane type distributors (bed material –1.5 kg coffee beans)	80
5.5.28	Comparison of variation of the bed pressure drop with superficial velocity between 15^0 and 20^0 three row vane type distributors (bed material –2.0 kg coffee beans)	80
5.5.29	Comparison of variation of the bed pressure drop with superficial velocity between 15^0 and 20^0 three row vane type distributors (bed material –1.5 kg pepper)	81
5.5.30	Comparison of variation of the bed pressure drop with superficial velocity between 15^0 and 20^0 three row vane type distributors (bed material –2.0 kg pepper)	81

5.5.31	Comparison of variation of the bed pressure drop with superficial velocity between single row and three row vane type distributors with vane angle 15° (bed material –1.5 kg coffee beans)	82
5.5.32	Comparison of variation of the bed pressure drop with superficial velocity between single row and three row vane type distributors with vane angle 15° (bed material –2.0 kg coffee beans)	82
5.5.33	Comparison of variation of the bed pressure drop with superficial velocity between single row and three row vane type distributors with vane angle 15° (bed material –1.5 kg pepper)	83
5.5.34	Comparison of variation of the bed pressure drop with superficial velocity between single row and three row vane type distributors with vane angle 15° (bed material –2.0 kg pepper)	83
5.5.35	Comparison of variation of the bed pressure drop with superficial velocity between single row and three row vane type distributors with vane angle 20° (bed material –1.5 kg coffee beans)	84
5.5.36	Comparison of variation of the bed pressure drop with superficial velocity between single row and three row vane type distributors with vane angle 20° (bed material –2.0 kg coffee beans)	84
5.5.37	Comparison of variation of the bed pressure drop with superficial velocity between single row and three row vane type distributors with vane angle 20° (bed material –1.5 kg pepper)	85
5.5.38	Comparison of variation of the bed pressure drop with superficial velocity between single row and three row vane type distributors with vane angle 20° (bed material –2.0 kg pepper)	85
5.6.1	Variation of bed pressure drop with superficial velocity at different radial positions in three row vane-type distributor - vane angle 15° and bed material – 1.5 kg coffee beans	87
5.6.2	Variation of bed pressure drop with superficial velocity at different radial positions in three row vane-type distributor - vane angle 15° and bed material – 2.0 kg coffee beans	87
5.6.3	Variation of bed pressure drop with superficial velocity at different radial positions in three row vane type distributor -	88

vane angle 15° and bed material – 2.5 kg coffee beans

5.6.4	Variation of bed pressure drop with superficial velocity at different radial positions in three row vane type distributor - vane angle 15° and bed material – 3.0 kg coffee beans	88
5.6.5	Variation of bed pressure drop with superficial velocity at different radial positions in three row vane type distributor - vane angle 20° and bed material – 1.5 kg coffee beans	89
5.6.6	Variation of bed pressure drop with superficial velocity at different radial positions in three row vane type distributor - vane angle 20° and bed material – 2.0 kg coffee beans	89
5.6.7	Variation of bed pressure drop with superficial velocity at different radial positions in three row vane type distributor vane angle 20° and bed material – 2.5 kg coffee beans	90
5.6.8	Variation of bed pressure drop with superficial velocity at different radial positions in three row vane type distributor - vane angle 20° and bed material – 3.0 kg coffee beans	90
5.7.1	Variation of bed height with superficial velocity in inclined hole type distributors – bed material - 2 kg coffee beans	92
5.7.2	Variation of bed height with superficial velocity in inclined hole type distributors- bed material - 2 kg pepper	93
5.8.2	Different regimes in three row vane type distributor - vane angle 15° and bed material coffee beans	97
5.8.3	Different regimes in three row vane type distributor - vane angle 20° and bed material coffee beans	97
5.8.4	Different regimes in three row vane type distributor - vane angle 15° and bed material pepper	98
5.8.5	Different regimes in three row vane type distributor - vane angle 20° and bed material pepper	98

ABBREVIATIONS

HJIS	Horizontal jet and inclined surface
IHD	Inclined hole distributor
IH15	Inclined hole distributor with 15 degree inclination
IH20	Inclined hole distributor with 20 degree inclination
LT15	Beginning of lift in 15 degree inclined distributor
LT20	Beginning of lift in 20 degree inclined distributor
PPD	Perforated plate distributor
SIH15	Beginning of swirl in 15 degree inclined hole distributor
SIH20	Beginning of swirl in 20 degree inclined hole distributor
SRVD	Single row vane type distributor
SRVD15	Single row vane type distributor with 15 degree inclination
SRVD20	Single row vane type distributor with 20 degree inclination
SS15	Beginning of swirl in 15 degree inclined distributor
SS20	Beginning of swirl in 20 degree inclined distributor
TRVD	Three row vane type distributor
TRVD15	Three row vane type distributor with 15 degree inclination
TRVD20	Three row vane type distributor with 20 degree inclination
WS15	Beginning of wave in 15 degree inclined distributor
WS20	Beginning of wave in 20 degree inclined distributor

NOMENCLATURES

A	Cross-sectional area of the bed
a	Length inserted in the vane holder on one side
A_r	Arcamides number
C	Constant
D	Diameter of the bed
D_c	Diameter of the cone
d	Diameter of hole in the perforated plate distributor
d_i	Average diameter of two consecutive sieve size
d_m	Mean diameter of the particle
g	Acceleration due to gravity
H_{mf}	Height of bed at minimum fluidizing velocity
l	Over lapping length of the blade
M	Mass of bed
N	Number of blades
n	Number of holes
ΔP_b	Bed pressure drop
ΔP_d	Distributor pressure drop
ΔP_v	Venturimeter pressure drop
Q	Volume flow rate of air
R	Ratio of the distributor pressure drop to bed pressure drop
R^2	Coefficient of determination
Re_{mf}	Reynolds number at minimum fluidizing velocity

R_c	Critical stability condition of fluidized bed
r	Radial position in the distributor
r_i	Inner radius of the vane
r_o	Outer radius of the vane
T	Temperature
t	Thickness of the Vane
U_{mf}	Minimum fluidizing velocity
U_M	Superficial velocity at which all the orifices in a distributor become operative
U	Superficial velocity
U_t	Terminal velocity of the particle
W_r	Width of vane at radius r
x_o	Cord length of arc at outer radius of the vane
x_i	Fraction of mass retained by a particular aperture size
Z	Bed height
δ_i	Gap width between adjacent vanes at inner radius
δ_o	Gap width between adjacent vanes at outer radius
ε	Voidage
θ	Inclination of the vane with the horizontal
ρ_b	Density of bed
ρ_g	Density of gas
ρ_p	Density of particle
ϕ	Angle between two vanes

CHAPTER 1

INTRODUCTION

1.1 GENERAL

Fluidization is a process by which solid particles are made to behave like a fluid by suspending them in a gas or a liquid. This is achieved by passing the fluid through a bed of particles.

A fluid flowing through the interstices of particles exerts a drag force on the particles and as the fluid flow increases, this force may be large enough to disturb the arrangements of particles within the bed. When the upward velocity of the fluid through the bed is raised progressively, a situation will eventually arise where the fluid drag exerted on the bed of particles is just sufficient to support its entire weight. The bed is then said to be incipiently fluidized and it exhibits fluid like properties.

This method of solid-fluid contacting has certain useful characteristics. Owing to the rapid mixing of solids, near-isothermal conditions prevail throughout the bed. Rates of heat transfer and mass transfer are higher, compared to other methods of contact. The containment of well-mixed solid particles at a uniform temperature resists sharp temperature fluctuations, thereby allowing highly exothermic reactions to be carried out without the problem of temperature runaway. The smooth flow of particles in the bed can be used for continuous operations. Due to the above advantages, fluidized beds are widely used in many applications such as heat recovery, treatment of metal surfaces, heat exchangers, gasification, combustion of solid fuels, endothermic and exothermic reactions, waste treatment, drying, coating of pellets, etc.

Conventional fluidized beds, wherein perforated or porous plate distributors are used, have certain limitations such as slugging, channeling, elutriation of solid particles and

limitation in the size of the particle. Many attempts have been made to improve the performance of the conventional fluidized bed. This has resulted in the development of a variety of fluidized beds such as circulating fluidized bed, centrifugal fluidized bed, vibro-fluidized bed, magneto-fluidized bed, tapered fluidized bed, spouted fluidized bed, swirling fluidized bed, etc.

The swirling fluidized bed is a relatively new variant of the fluidized bed. In a swirling fluidized bed, the air enters the bed at an angle through the inclined openings of the distributor. The vertical component of the air velocity causes fluidization and the horizontal component causes swirl motion. The bed, if shallow, swirls as a single mass. On the other hand, as the bed height increases, two layers will form with a swirling bottom layer and a bubbling top layer.

Swirling fluidized beds have several advantages over conventional fluidized beds. Quality fluidization with distributors having low distributor pressure drop is possible in a swirling fluidized bed. Due to the cross flow of the particles, no stable jet formation occurs in the swirling fluidized bed. The toroidal motion in the bed mixes the particles in the radial direction. The gas velocity can be increased to high values with little elutriation.

Large particles (Geldart 'D' type), which are difficult to fluidize in a conventional bed, can be effectively fluidized in swirling fluidized beds. So, swirling fluidized beds have distinct advantages in drying of agricultural produce such as cardamom, black pepper, coffee beans, cocoa beans, etc. as well as Ayurvedic tablets.

However, the swirling fluidized bed has limitations too. In general only an annular area of the distributor is used in swirling fluidized bed, which causes restriction in its size. The inclination of the air jet is an important factor which influences the minimum fluidization velocity as well as swirl velocity. At high air velocity, a portion

of the air may get by-passed through the inner region of the distributor.

Even though swirling fluidized beds are commercially available, only limited study has been reported in literature about their hydrodynamic behaviour. So, a detailed hydrodynamic study on the swirling fluidized bed is necessary and the present investigation has been framed to address some of the limitations of the existing swirling fluidized bed.

1.2 SCOPE OF THE THESIS

The details of the chapters included in this thesis are as follows.

Chapter 1 contains a general introduction. Chapter 2 contains a brief review of literature on the hydrodynamic characteristics of fluidized bed and objective of the present investigation is presented. Chapter 3 contains the design details of seven distributors fabricated for the purpose of present study. Chapter 4 contains details of the experimental set-up and procedure. Chapter 5 contains results obtained and discussions based on the present investigation. Chapter 6 contains major conclusions drawn from the present investigation along with some suggestions for the further work.

Chapter 6 is followed by list of references, appendices A, B and C. Appendix A contains calibration details of the three-hole probe. Appendix B contains uncertainty analysis. A video presentation comparing the bed performance of different types of distributors is given in appendix C.

CHAPTER 2

LITERATURE REVIEW

2.1 INTRODUCTION

This chapter presents a critical review of the available literature on the hydrodynamic characteristics of a fluidized bed, which are relevant to the scope of the present study. The review of literature is presented based on the various parameters that influence the fluidized bed.

2.2 DISTRIBUTOR PRESSURE DROP

The most important function of a gas distributor, as the name indicates, is the uniform distribution of air in the bed. Design of a good gas distributor is essential for the satisfactory performance of any fluidized bed. Successful industrial application of a fluidized bed depends on its performance.

A good gas distributor shall possess the following qualities:

- 1 Have low distributor pressure drop at the operating velocity so as to minimize the power consumption
- 2 Be strong enough to withstand both thermal and mechanical stresses
- 3 Ability to prevent particle flow back to the plenum chamber at low airflow
- 4 Have minimum particle attrition
- 5 Ability to prevent distributor erosion.

Some of these qualities are contradictory and their relative importance may change with the type of process for which the distributor is meant for.

There are oscillations in the local pressure drop at the distributor in the conventional fluidized bed due to bubbling action. Further, if the distributor pressure drop is very low, the air will enter the bed in a zone of lowest pressure drop and thereby there will be a non-uniform distribution of airflow within the bed. Therefore, to overcome the

small local pressure disturbances, the distributor pressure drop has to be large enough in conventional fluidized bed. Botterill (1975) considered the distributor pressure drop as an important factor, which influences the uniform and stable fluidization.

Ratio of the distributor pressure drop to the bed pressure drop (R) is generally considered for the design of distributors in conventional bed. This ratio is influenced by different parameters such as distributor type, particles fluidized, bed depth, superficial gas velocity, etc. For deep beds or for high density materials, Agarwal et al. (1962) recommend a minimum value of 0.10 for the ratio R . On the other hand, for shallow beds a minimum distributor pressure drop of 350 mm of water is recommended. For a porous distribution plate, to have a uniform fluidization, Hiby (1967) suggested a minimum value of 0.3 for R . He reported that the required minimum ratio R for a uniform fluidization increased moderately with particle size. For a porous distribution plate, to have a uniform fluidization, Siegel (1976) recommended a minimum values of 0.25 and 0.15 for R respectively for large particles (496 μm) and small particles (23 μm). Whitehead (1971) observed that, depending on the process involved, the industrial fluidized bed installations use a variety of distributor pressure drop with values of R ranging from 0.02 to 0.5. So, it could be seen from the literature that for stable fluidization in a conventional fluidized bed, different investigators have suggested different minimum values of R ranging from 0.02 to 0.50.

Saxana (1979) conducted experiments in a 305 mm \times 305 mm square bed using Johnson screen type, porous plate and conical bubble cap type distributors. He observed that the value of R at minimum fluidization depends on the bed height and this value increased rapidly with increase in fluidization velocity. Further, the distributor pressure drop was found to increase with fluidizing velocity, to decrease

with percentage open area of the distributor plate, and to be independent of the bed weight or height for a given distributor design. He has reported that a distributor with greater pressure drop across it gives rise to smaller bubbles for the same excess fluidizing velocity than a distributor with smaller pressure drop.

Sathiyamoorthy et al. (1978) carried out experiments using plus type and Y type distributors in a 100 mm diameter bed with particle size varying from 70 μm to 200 μm . They observed that the number of operating orifices is determined by the gas flow rate, bed height, bed material and the type of distributor. It has also been observed that a higher pressure drop across the distributor would be required to operate all orifices in fluidizing fine size particles.

Many researchers considered the ratio of distributor pressure drop to bed pressure drop as a design criterion and suggested that there should be some minimum value for the uniform distribution of air. Hiby (1967) suggested that the minimum ratio of the distributor to bed pressure drop depends not only on the type of distributor but also on the particles fluidized, the bed depth, the superficial gas velocity, and bed aspect ratio. Qureshi and Creasy (1979) proposed, based on the available data from commercial fluidized beds, the following empirical relation for the ratio of distributor pressure drop to bed pressure drop at critical stability condition of fluidized beds (R_c).

$$R_c = 0.01 + 0.2 \left[e^{\left(-0.5 \times \frac{D}{Z} \right)} \right] \quad (2.1)$$

Geldart and Baeyens (1985) state that the equation (2.1) for R gives too low values of R_c for low aspect ratio beds. They suggested a more conservative approach to be used for $H_{mf}/D < 0.5$ and proposed the following equation.

$$R_c = e^{(3.8 \times H_{mf}/D)} \quad (2.2)$$

Shi and Fan (1984) contradicted the Siegel's model at the onset of fluidized bed channeling and established the condition under which channeling occurs in the bed for both porous distributor and perforated distributor. They concluded that the non-occurrence of channeling cannot ensure the uniform fluidization and stated that the criterion for it should be based on the condition of full fluidization in the bed.

Different researchers proposed different types of design for gas distributors in conventional fluidized bed such as multi-orifice type, perforated plate type, bubble cap type, stand pipe type, and ball distributor. These designs were studied with respect to its applications, fluidization uniformity, gas jetting characteristics, bubble behaviour, existence of dead zone and solid motion at the distributor, size, spacing and orientation of orifices and solids flow back.

Fakhimi (1983) studied the behaviour of multi-orifice distributor in gas fluidized bed, giving importance to the height of the entrance effect and the mechanics of gas solids flow in the region immediately above the distributor plate. He found that the principal factors influencing the height of the entrance effect were the incipient fluidizing velocity, mean particle size, orifice spacing and gas flow rate.

Sathiyamoorthy and Rao (1978) studied the effect of bed height and bed materials on the number of operating orifices in multi-orifice plate distributors. They reported that the number of operating orifices is a function of gas velocity and the ratio of distributor pressure drop to the bed pressure drop.

In a uniformly fluidized bed, Sathiyamoorthy and Rao (1981) suggested the following equation to determine the superficial gas velocity at which all the orifices in a distributor become operative (U_M).

$$U_M = U_{mf} \times \left(2.65 + 1.24 \times \log_{10} \frac{U_t}{U_{mf}} \right) \quad (2.3)$$

Once U_M is determined, the ratio of bed pressure drop to the distributor pressure drop can be determined from the following expression, wherein the value of C is taken as 2

$$\frac{\Delta P_d}{\Delta P_b} = C \left(\frac{U_{mf}}{U_M - U_{mf}} \right)^C \quad (2.4)$$

Otero and Munoz (1974) studied the fluidization quality, pressure drop and solids flow back through the bubble cap type plate distributor. They reported that the solids flow back is due to the bed pulsations and depends on the particle size and the diameter and inclination of the holes in the cap.

Whitehead et al. (1967) investigated the effect of two types of multi-tiered gas distributor and two silica sands with different size distributions on fluidization characteristics in a bed of 1219.2 mm (4 feet) square and up to 2743.2 mm (9 feet) deep. They concluded that a complex gas distributor did not produce significantly better gas dispersion than a simple one in the upper regions of the bed.

Yacono and Anyelino (1978) studied the bubble behavior in a ball distributor in comparison with porous plate distributor. They observed that ball distributor has the advantage of submitting the gas to a very small pressure drop while promoting, under certain conditions, a very homogenous fluidization and has interesting features which include high permeability to dust transported by the gas stream. However, the main draw back of this distributor is that it will get destroyed by accidentally fluidizing the balls.

Wen et al. (1978) studied the dead zone heights near the distributor plate in two-dimensional and three-dimensional fluidized bed. They reported that gas velocity,

distributor type, orifice pitch, orifice diameter and particle size have significant effects on dead zone height in the case of two-dimensional bed. They have identified the importance of orifice pitch in three-dimensional bed and reported that the behaviour of the two-dimensional bed cannot be readily extrapolated quantitatively to three dimensional cases.

Chyang and Huang (1991) studied the behaviour of pressure drop across a perforated plate distributor in the absence and presence of a bed material. They observed that the pressure drop across a perforated plate distributor measured in the presence of bed material was higher than that measured in an empty column at low gas velocities and was significantly affected by the locations of pressure taps corresponding to the orifice layout on the perforated plate.

Brik et al. (1990) designed a distributor with horizontal jets and inclined surfaces (HJIS) to eliminate severe agglomeration problems in a process for reactive modification of a polymer in an industrial fluidized bed. Sufficient mixing of the gas and the particles were to be ensured while designing this distributor so as to eliminate both the mass and the heat transfer problems. With a properly designed HJIS distributor, the polymer particles were not allowed to be stagnant on the exposed surfaces of the gas distributor due to two factors. First, the inclined surfaces or “tents” utilized gravity and the angle of repose of the particles to ensure that there was no stagnation of polymer above those areas. Second, there was no stagnation in the other flat areas between those “tents” due to the sweeping action of the horizontal jets before they dissipated and the gas entered the bulk of the bed to fluidize the particles. They present a design procedure and equations which allow the size and location of the “tents” and their orifices to be calculated to produce uniformly active jets and prevent powder stagnation and gas distributor blockages.

2.3 BED PRESSURE DROP

The bed pressure drop (ΔP_b) versus superficial gas velocity diagram is used to determine the minimum fluidization velocity (U_{mf}). This diagram is particularly useful to assess the quality of fluidization in conventional fluidized bed.

When gas is passed upwards through a packed bed, the pressure drop rises with flow rate, reaching a maximum value at the point of incipient fluidization. In conventional bed, an increase in the velocity above the minimum fluidizing velocity does not result in an increase in bed pressure drop. Once the bed is fluidized, the pressure drop across it (ΔP_b) is sufficient to support the full weight of the particles so that

$$\Delta P_b = \left(\frac{M}{\rho_p - A} \right) (\rho_p - \rho_g) \times g \quad (2.5)$$

Equation 2.5 implies that either there is no interaction between the particles and bed wall or there is no energy degradation in the bed. Howard (1989) suggested that degradation of energy can occur due to collision between two particles or between a particle and bed wall and this energy degradation can cause increased bed pressure drop across the bed than the value calculated based on the equation 2.5.

Botterill et al. (1982), Mathur et al. (1986), Nakamura et al. (1985) and Saxena et al. (1990), have studied the variation of bed pressure drop with superficial velocity. Each investigator studied the influence of different parameters such as distributor type, bed geometry, particle size and size distribution, bed temperature and bed pressure. These researchers have reported that the bed pressure drop is constant at a gas velocity greater than the minimum fluidizing velocity.

For higher superficial velocity than the minimum fluidization velocity, Upadhyay

et al. (1981), Yang et al. (1987) and Bouratoua et al. (1993) reported a lower bed pressure drop than the value obtained based on equation 2.5.

According to Bouratoua et al. (1993), the lower pressure drop after minimum fluidization is due to the existence of an additional force along the walls, contributing to support the fluidized solids. Such a force can be due to the wall friction exerted on particles down flowing along the walls in compensation of up flow of particles in the wake of the bubbles.

Upadhyay et al. (1981) reported a reduction in bed pressure drop by about 15-20% than the static bed pressure. They attribute this difference to a partially fluidized bed and pointed out that 15-20% of the bed was not fluidized.

Sutherland (1964) explained the method of measuring the bed pressure drop in a conventional fluidized bed and suggested that a rise in pressure drop with increasing gas flow over the fluidized region can be taken as an indicative of slugging, while a decrease in the pressure drop leads to channeling.

2.4 EFFECT OF TEMPERATURE IN BED HYDRODYNAMICS

As the temperature of the bed changes, the obvious changes are in the properties of the fluidizing medium. When gas is used for fluidizing, its density decreases with increase in temperature, while its viscosity increases. At low Reynolds number, viscous effects predominate. On the other hand, at high Reynolds number inertia effects predominate.

Singh et al. (1973) observed that the minimum fluidizing velocity is inversely proportional to the viscosity of gas in the laminar region.

Desai et al. (1977) have observed that for laminar flow the minimum fluidizing velocity decreases with an increase in temperature of the gas. On the other hand, in transition and turbulent regions, minimum fluidizing velocity becomes less dependent

on temperature.

Sadasivan (1980) observed that the minimum fluidizing velocity decreases with increase in temperature for small particles and increases in the case of large particles.

Botterill et al. (1982) used a slowly responding differential pressure probe for the measurement of the average bed voidage at a given gas flow rate above minimum fluidizing velocity. The voidage has been calculated using the following equation.

$$\bar{\epsilon} = 1.0 - \left(\frac{l}{\rho_s - \rho_g} \times \frac{\Delta p}{\Delta H} \right) \quad (2.6)$$

They observed a decrease in voidage with an increase in particle size distribution. Further, for a bed of Geldart “B” type particles, the voidage at minimum fluidizing velocity increased with temperature.

Wu and Baeyens (1991) experimentally investigated the effect of temperature on the minimum fluidizing velocity of beds of different materials. They compared their data with different correlations and proposed the following correlation.

$$Re_{mf} = 7.33 \times 10^{-5} + 10 \left[(8.241 \times \log_{10} A_r) \right]^{1.2} \quad (2.7)$$

It is to be noted that while Singh et al. (1973) and Sadasivan (1980) observed no influence in voidage due to change in temperature, Vreedenberg (1958) and Botterill et al. (1982) observed an increase in voidage with temperature.

2.5 CENTRIFUGAL FLUIDIZED BED

In processes such as coal combustion, zinc roasting, etc., it is preferred to have high superficial gas velocity for reducing the reactor size. However, if large amount of excess aeration is introduced in a conventional fluidized bed, it leads to the formation of large bubbles or slugging and particle elutriation. In such cases, gas solid contact

becomes rather poor. Hence, in processes where high superficial gas velocity is required, conventional bed becomes handicapped and as a result, the concept of centrifugal fluidized bed is introduced.

A centrifugal fluidized bed is a cylindrical bucket, rotating about its axis of symmetry, with aeration introduced in the radially inward direction to fluidize the particles. Instead of having a fixed gravitational field as in the case of conventional bed, the body force in a centrifugal bed becomes an adjustable parameter which is determined by the speed of rotation and the bucket radius. By using a strong centrifugal field much greater than gravity, the bed particle is able to withstand a large amount of aeration without serious formation of large bubbles and thus the gas solid contact at a high aeration rate is improved.

Kroger et al. (1979) proposed equations predicting the pressure drop and radial flow distribution in a centrifugal fluidized bed and validated their theory using their experimental results.

Takahashi et al. (1984) conducted experiments in a horizontal rotating fluidized bed with different particle densities and size distribution. They reported that, unlike conventional fluidized bed, the bed pressure drop in centrifugal fluidized bed does not remain essentially unchanged; it attains a maximum value at minimum fluidizing velocity. A further increase in gas velocity results in a slight decrease in the bed pressure drop.

Fan et al. (1985) proposed a model for the determination of incipient fluidization in a centrifugal fluidized bed and validated their model with their experimental results obtained from a horizontal rotating fluidized bed. They concluded that the characteristics of centrifugal fluidized beds are substantially different from those of conventional fluidized beds and hence the known hydrodynamic relations of the latter

cannot be applied to the former.

Chen (1987) proposed a theoretical model for the fluidizing phenomena of a centrifugal fluidized bed. According to him, unlike the conventional bed, the centrifugal fluidized bed fluidizes layer by layer from the inner free surface to outwards, in a range of aeration rates.

It is to be noted that unlike Takahashi et al. (1984), Chen (1987) predicted a constant bed pressure drop after fluidization in centrifugal fluidized bed. On the other hand, Kao et al. (1987) reported that, depending on the bed thickness, the pressure drop versus superficial velocity curve can exhibit either a plateau or a maximum.

2.6 FLUIDIZED BED DRYING

Agricultural produce which are seasonal and available in plenty in peak season are required to be dried for storing. Different investigators have attempted to study the drying characteristics of various agricultural produces in fluidized beds.

Hatamipour and Mowla (2002) studied the drying characteristics of root vegetable using cylindrically shaped carrot in a conventional fluidized bed. They reported that the air velocity has no significant influence on rate of drying.

Niamnuay and Devahastin (2004) studied the drying characteristics of coconut chips in conventional fluidized bed. They reported that an increase in inlet air velocity as well as air temperature increases the rate of drying. However, they observed that, the quality of the dried product, based on the colour and quantity of oil on the surface, is affected when higher air temperature or air velocity is used.

Prakash et al. (2004) compared the quality of carrot dried in three different types of driers, namely conventional fluidized bed, microwave oven and solar cabinet. They found that the rehydration property and β -carotene content was the highest when fluidized bed was used as the drier.

Senadeera et al. (2003) studied the effect of shape of materials on drying rate in a conventional fluidized bed. They considered cylindrical beans with different length to diameter ratios and solid potatoes with different aspect ratios. They observed that the drying rate decreased as the length to diameter ratio or aspect ratio, as the case may be, is increased.

Topuz et al. (2004) conducted experimental and numerical studies on drying of hazelnuts in a conventional fluidized bed. They observed that the rate of drying increases with increase in temperature. Further, they have reported a decrease in the drying rate with an increase in the air velocity and suggested that this phenomenon was due to the slugging.

Shi et al. (2000) studied heat and mass transfer characteristics of wet material in a centrifugal fluidized bed. They observed that the drying rate increases with increase in the superficial gas velocity and particle diameter and with decrease in bed rotation speed and initial bed thickness. They stated that the drying rate of food products depends on the shape, dimensions and material of the drying products, as well as the operational conditions.

Özbey and Söylemez (2004) studied the drying characteristics of wheat grains in a swirling fluidized bed. Axial guide vane type swirl generator was used in their study. They reported that a swirling flow field enhances the drying performance of wheat grains compared to a non-swirling flow field. Also, the drying performance increased with “swirl number”, which is defined as the ratio of the angular momentum flux to the axial momentum flux of the swirling flow. They have further reported that the temperature of air has more important effect on drying compared with that of the mass flow rate.

2.7 SWIRLING FLUIDIZED BED

Swirling fluidized bed is a novel variant of fluidized bed featuring an annular bed and inclined injection of gas through the distributor. The gas entering into the bed will have two components- horizontal and vertical. The vertical component supports fluidization while the horizontal component supports the swirling motion in the bed. Even though commercial products are available in the market the available literature on a systematic study of swirling fluidized bed is scanty.

Ouyang and Levenspiel (1986) proposed a spiral distributor for swirl motion. They evaluated and compared the characteristics of this distributor, such as pressure drop, quality of fluidization and heat transfer coefficient with that of sintered- plate distributor. The spiral distributor was made of overlapping vanes, shaped as sectors of a circle with a gap between the vanes. The gap between the adjacent vanes was maximum at the outer periphery and zero at the center of the distributor. They arranged the vanes in such a way that the air leaving from the gap of the vanes is tangential. However, they have not reported the angle of inclination of the vane. They reported that the inclined jet from the opening impart a swirling motion in a shallow bed while in deep bed, the swirling motion is restricted to the lower portion of the bed and that bubbling occurs in the region above the swirling region. Their comparison of pressure fluctuation across the fluidized bed supported by a spiral plate and a porous plate shows that, for low density solids, the sintered plate gives better fluidization at low superficial velocity. On the other hand, at high superficial velocities, the performance is better in spiral distributor. However for high density solids, the spiral distributor seems to give a better quality of fluidization at all gas velocities. They also reported that the distributor pressure drop across the spiral distributor is from 1 to 2 orders of magnitude smaller than for the sintered plate distributor. Virr (1985)

described the behaviour of a shallow bed heat exchanger working on the swirling bed principle. Binod and Raghavan (2002) studied the hydrodynamic characteristics of fluidized bed with annular spiral distributors. The distributors were made by placing inclined vanes at an angle of 12° with the horizontal over an annular region with the help of outer and inner holders made of Plexiglas. As the air flow rate was increased, they observed different bed behaviour like bubbling, wave motion and swirl motion. When the static bed height was higher than 45 mm, they observed two-layer fluidization with a continuously swirling lower layer and a vigorously bubbling top layer. They have reported that the superficial velocity required for stable swirl is higher for higher bed weight. Further, in the stable swirl zone, they have noticed an increase in bed-pressure drop with airflow rate and have suggested the effect of wall friction as the reason for this increase. Shu et al. (2000) studied the hydrodynamics of a toroidal fluidized bed (torbed) reactor using fine particles and compared its performance with that of the conventional bed. An annular ring gas distributor with vanes fixed at 25° with horizontal was used in their study. They suggested that, for shallow torbed, the vertical component of the process gas velocity head should be considered to compare with the minimum fluidization velocity in conventional bed. Vikram et al. (2003) developed an analytical model for the prediction of hydrodynamic characteristics of swirling fluidized bed. An annular distributor with a central cone was used for their study. According to them, the swirl velocity increases linearly and bed pressure drop increases parabolically with superficial velocity. They reported that the vane angle has a considerable influence on the bed characteristics such as bed pressure drop and swirl velocity, while the effect of cone angle is negligible. They further reported that swirl velocity as well as bed pressure drop decreases with increase in vane angle.

2.8 DISCUSSION

It can be observed that different types of distributors are developed for different processes. For a stable fluidization in deep fluidized bed, different investigators suggested different minimum values for the ratio of distributor pressure drop to the bed pressure drop, which ranges from 0.02 to 0.50. On the other hand, Agarwal et al. (1962) recommended a minimum distributor pressure drop of 350 mm of water for shallow conventional beds. A lower distributor pressure drop may cause non uniform distribution of air while a higher distributor pressure drop leads to higher energy loss. An optimum design of distributor should ensure uniform distribution of air with minimum distributor pressure drop. However, only limited information is available on the influence of the distributor pressure drop on the bed behaviour of swirling fluidized bed.

For conventional fluidized bed, almost all researchers agree that the bed pressure drop becomes constant at gas velocity greater than minimum fluidizing velocity and variation in the pressure drop after fluidization is an indicative of undesirable characteristics such as slugging or channeling. On the other hand, there is a difference in opinion in the case of centrifugal fluidized bed. While some researchers reported a constant bed pressure drop, some others reported a decrease in the bed pressure drop after minimum fluidization. In the case of swirling fluidized bed, Binod and Raghavan (2002) reported that there is an increase in the bed pressure drop with the superficial velocity in the swirl regime. However, information available about the influence of bed pressure drop variation on the behaviour of swirling fluidized bed is limited.

Irrespective of the type of fluidized bed, it can be concluded that temperature of air is the primary factor in the drying process. Cardamom, an agricultural produce and several ayurvedic tablets cannot be dried in sunlight as this will degrade the quality of

the end product. Unlike conventional fluidized bed, swirling fluidized beds can be effectively used to fluidize large particles (Geldart D type). Özbey and Söylemez (2004) reported that the swirl flow enhances the drying performance of particles. Drying of agricultural produces using swirling fluidized bed is a potential area wherein, most of the particles fall in the group of "Geldart D" type. However, a systematic study on the hydrodynamic characteristics of swirling fluidized bed with particles as agricultural produces is limited.

It can further be concluded that, in spite of the wide industrial applications of swirling fluidized bed, systematic study is limited, particularly on the influence of the angle of air injection, area of openings and percentage useful area of the distributor on the hydrodynamic characteristics of the fluidized bed.

2.9 OBJECTIVES OF THE PRESENT STUDY

Based on the brief review of the available literature, the following objectives have been proposed for the present study.

1. To study the basic hydrodynamic characteristics of swirling fluidized bed using large particles selected from locally available agricultural produce and by considering the following major variables
 - a. Percentage area of opening
 - b. Angle of air injection
 - c. Percentage useful area of the distributor

CHAPTER 3

DESIGN AND FABRICATION OF DISTRIBUTORS

3.1 INTRODUCTION

The most important part of a fluidized bed is its distributor. A distributor, as the name implies, distributes the air uniformly to the bed. In a conventional fluidized bed, air is admitted vertically upwards to the bed. On the other hand, in a swirling fluidized bed, air enters the bed at an angle and this is achieved by providing inclined holes or inclined slots in the distributor. It is a well accepted fact that high distributor pressure drop is required for good fluidization in conventional fluidized beds. On the other hand, quality fluidization can be achieved in a swirling fluidized bed with a comparatively lower distributor pressure drop.

This chapter deals with the design and fabrication of the following types of distributors.

1. Single row vane type distributor
2. Inclined hole type distributor
3. Three row vane type distributor
4. Perforated plate distributor.

For all other types except the perforated plate distributor, two distributors were fabricated with vane/hole angles of 15° and 20° .

3.2 SINGLE ROW VANE TYPE DISTRIBUTORS

3.2.1 Design

Single row vane type distributors were made by a number of overlapping vanes, shaped as truncated sectors of a circle with a gap between the vanes. The vanes are made from truncated sectors to form an annular region of airflow between the outer

and inner diameters of the distributor. The opening between vanes is of trapezoidal shape and its area is dependent on the vane angle, the gap width between the vanes and the vane thickness. The number of vanes required in the annular region depends on the vane angle and the gap width between the vanes. Hence the design is essentially the determination of the number of vanes and percentage area of opening in a distributor for a known set of parameters.

Consider top edge of two adjacent vanes at its outer radius (r_o). The distance between these two points (a and c in figure 3.2.1b) is given by the relation

$$x_o = r_o \times \sqrt{2 \times (1 - \cos \phi)} \quad (3.1)$$

The gap width between the vane (δ_o) at radius r_o is given by

$$\delta_o = r_o \times \sqrt{2 \times (1 - \cos \phi)} \times \sin \theta - t \quad (3.2)$$

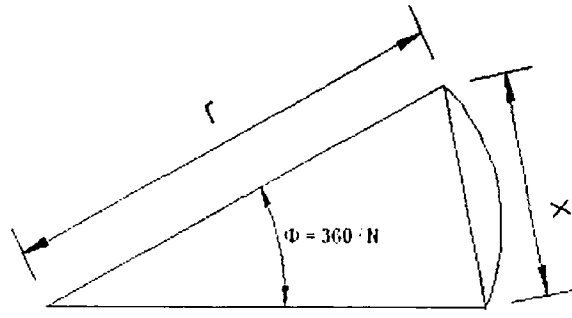
The number of vanes can be calculated from equation 3.2 as

$$N = \frac{360}{\cos^{-1} \left[1 - \frac{\left(\frac{\delta_o + t}{r_o \sin \theta} \right)^2}{2} \right]} \quad (3.3)$$

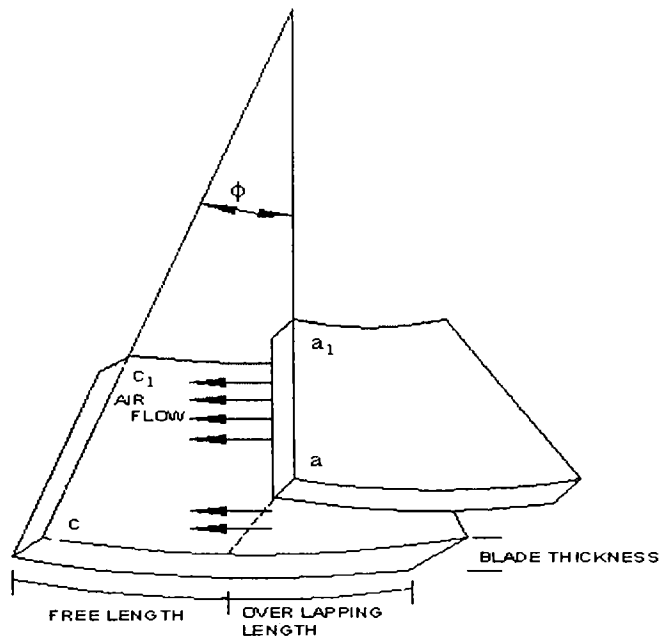
$$\text{Area of one trapezoidal opening} = \frac{(\delta_i + \delta_o)}{2} (r_o - r_i) \quad (3.4)$$

$$= \left[\frac{[r_o \times \sqrt{2 \times (1 - \cos \phi)} \times \sin \theta - t + r_i \times \sqrt{2 \times (1 - \cos \phi)} \times \sin \theta - t](r_o - r_i)}{2} \right]$$

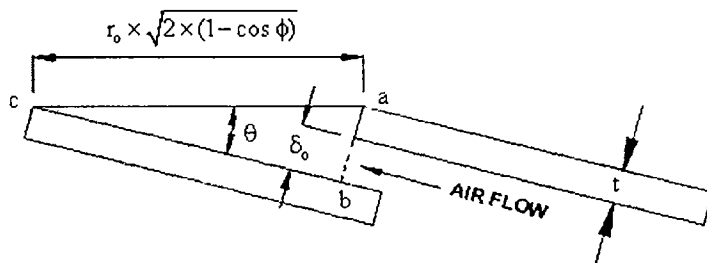
$$= \left[\frac{\sqrt{2 \times (1 - \cos \phi)}}{2} \times \sin \theta \times (r_o^2 - r_i^2) - t \times (r_o - r_i) \right] \quad (3.5)$$



(a)



(b)



(c)

Figure 3.2.1 Geometric relationship of vanes in single row vane type distributor

$$\text{Total area of opening} = N \times \left[\frac{\sqrt{2 \times (1 - \cos \phi)}}{2} \times \sin \theta \times (r_o^2 - r_i^2) - t \times (r_o - r_i) \right] \quad (3.6)$$

$$\text{Percentage area of opening} = \frac{N \times \left[\frac{\sqrt{2 \times (1 - \cos \phi)}}{2} \times \sin \theta \times (r_o^2 - r_i^2) - t \times (r_o - r_i) \right]}{\pi \times (r_o^2 - r_i^2)} \times 100 \quad (3.7)$$

$$\text{Percentage useful area of the distributor} = \frac{(D^2 - D_c^2)}{D^2} \times 100 \quad (3.8)$$

$$\text{Length of vane} = (r_o - r_i) + 2a \quad (3.9)$$

where, the length inserted in the vane holder on one side, $l = 5 \text{ mm}$

$$\text{Width of the vane at radius } r, W_r = r \times \sqrt{2 \times (1 - \cos \phi)} \times \cos \theta + l \quad (3.10)$$

where, the overlapping length of the vane, $l = 15 \text{ mm}$

Based on the above relations, single row vane type distributors were designed with 15° and 20° vane angles. The design details of single row vane type distributors are given in Table 3.2.1

Table 3.2.1 Design details of single row vane type distributors

Sl. No	Particulars	Vane angle(θ)	
		15°	20°
1	Maximum gap width between vanes, (δ) mm	3	3
2	Vane thickness, (t) mm	0.8	0.8
3	Outer radius, (r_o) mm	150	150
4	Inner radius, (r_i) mm	90	90
5	Number of vanes, (N)	64	85
6	Width of vane at r_o , mm	37	37
7	Width of vane at r_i , mm	30	30
8	Percentage area of opening	19	25
9	Percentage useful area of the distributor	64	64

3.2.2 Fabrication

A square perspex plate of size 400 mm and 10 mm thickness was used to make the distributor. An annular ring having 180 mm inner diameter and 300 mm outer diameter was cut off from this plate, thereby a square plate having a circular hole of 300 mm diameter and a circular disc of 180 mm diameter was obtained. Based on the number of vanes to be used, the outside of the circular disc as well as the inside of the square plate was divided equally and marked with the help of a template. Through these markings inclined grooves corresponding to the vane angle (15° and 20° with horizontal) were cut using a hacksaw. A fixture was specially designed and used for ensuring accuracy while making the inclined grooves. The grooved circular disc and square plate were then screwed to a plywood base in such a way that the 300 mm diameter hole of the square plate and circular disc were concentric.

Vanes were made as per the design using 0.8 mm thick steel plate. These vanes were inserted into the grooves in such a manner that the top edge of each vane was flush with the surface of the distributor and was in the radial direction. The vanes were then fixed in position with epoxy resin. Figure 3.2.2 shows the photograph of a single row vane type distributor fabricated

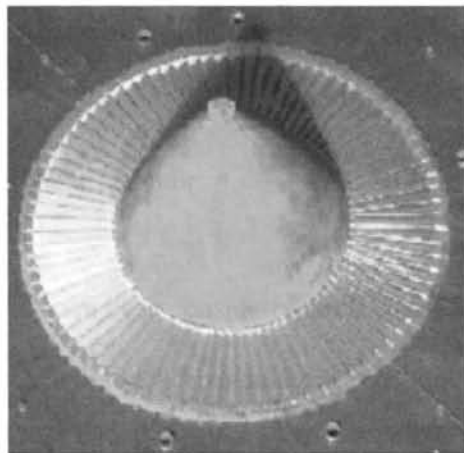


Figure 3.2.2 Photograph of single row vane type distributor

3.3 INCLINED HOLE TYPE DISTRIBUTORS.

In general, there is practical difficulty in increasing the useful area of single row vane type distributors beyond a certain limit. This is because, the gap width between two adjacent vanes decreases inwards as the radius reduces and as a result, the fabrication of a full spiral distributor is difficult. However, instead of trapezoidal openings, if circular openings are provided in the distributor, the useful area of the distributor can be increased. This thinking lead to the design of inclined hole type distributor. The following section deals with the design and fabrication of inclined hole type distributors

3.3.1 Design

The following factors were considered for the design of inclined hole type distributor.

1. Size of hole – governed by the minimum size of bed particle.
2. Radial pitch of hole – selected to achieve the maximum percentage area of opening
3. Circular pitch of hole –selected to achieve the maximum percentage area of opening which depends on the inclination of the hole.

The percentage area of opening and percentage useful area of the distributors can be calculated from the following expressions.

$$\text{Percentage area of opening} = \frac{(d^2 \times n)}{(D^2 - D_c^2)} \times 100 \quad (3.11)$$

$$\text{Percentage useful area of the distributor} = \frac{(D^2 - D_c^2)}{D^2} \times 100 \quad (3.12)$$

The following parameters have been considered for the present study.

1. Inclination of hole to the horizontal (θ) = 15° and 20°
2. Diameter of the distributor (D) = 300 mm

3. Diameter of the hole (d) = 3 mm
4. Radial Pitch = 10 mm
5. Thickness of the distributor (t) = 10 mm
6. Diameter of the cone (D_c) = 75 mm

Based on the above parameters, two distributors have been designed and details of the distribution of holes within the distributor are given in Table 3.3.1

Table 3.3.1 Distribution of holes in inclined hole type distributors

Sl.No.of Concentric ring	Ring diameter (mm)	Number of holes on the ring	
		$\theta = 15^\circ$	$\theta = 20^\circ$
1	80	9	20
2	100	13	24
3	120	16	30
4	140	20	34
5	160	23	39
6	180	26	43
7	200	29	48
8	220	32	53
9	240	36	58
10	260	39	63
11	280	42	68
Total number of holes		285	480

3.3.2 Fabrication

Due to the difficulties in drilling holes at low angles (15° and 20° to the horizontal), tubes with appropriate inner diameter have been considered for holes. Accordingly, brass tubes with 5 mm outer diameter and 3 mm inner diameter were selected and it was proposed to place these tubes at an appropriate angle and cast them in resin, to make the inclined hole type distributors

For accurate cutting of tubes with required angle and length, special fixtures were

fabricated. The fixture essentially consists of a 90 mm long HCHC steel with a square cross section of side 25 mm. A 5 mm diameter hole was drilled centrally in the axial direction of the fixture. One end of the fixture was shaped to the required angle. Parallel to the shaped face of the fixture and at a distance of 10 mm from it, a slot with 0.8 mm width and 16 mm depth was made. Provision was made in the fixture to hold the tube in position during the cutting operation. A three dimensional view of the fixture is shown in figure 3.3.1



Figure 3.3.1 Three dimensional view of the fixture

The fixture was first fixed in a bench vice. One end of the tube was inserted through the hole and was fixed in position with the bolt provided. The tube was then cut through the slot of the fixture with a hacksaw so as to obtain the required angle (15° or 20°) on one end of the tube. The tube was then advanced through the hole and the cut end of the tube was made flush with the inclined surface and fixed. Now, cutting the tube through the slot of the fixture will give one piece of the tube with the designed dimensions.

Concentric circles were drawn with a radial pitch of 10 mm, starting from a radius of 80 mm to 280 mm on the drawing sheet which was fixed to plywood with adhesive. On each circle, markings were made based on the radial pitch. The tube pieces were

aligned and fixed on the markings with adhesive. While fixing the tubes, they were aligned tangential to the circles drawn with a fixture. A metallic ring of 330 mm inside diameter and 10 mm height was fixed on the drawing sheet in such a way that the ring and the circles drawn on the sheet were concentric. The space within the metallic ring was carefully filled with epoxy. The whole set-up was kept undisturbed for 24 hours. Distributor faces were polished to have an even surface. A cone (75 mm base diameter and 60° apex angle) was fixed at the center of the distributor by bolts. Figure 3.3.2 shows the photograph of the distributor thus fabricated.

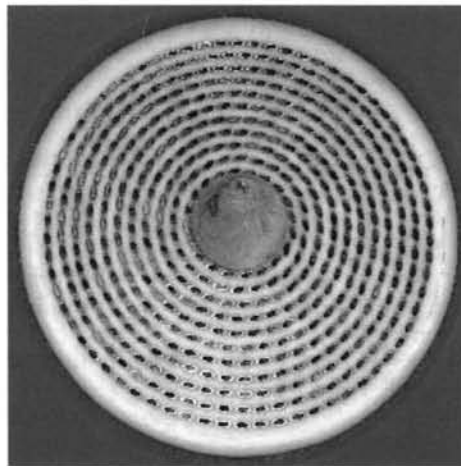


Figure3.3.2 Photograph of inclined hole type distributor

While the percentage useful area of both the distributors came to 94, the percentage area of opening for the distributors with 15° and 20° hole angle works out to be 3 and 5 respectively.

3.4 THREE ROW VANE TYPE DISTRIBUTORS

It is felt that without much reduction from the percentage area of opening of a single row vane type distributor, the percentage useful area of the distributor can be increased by arranging the vanes in the form of circular rows. This is a new method proposed by the investigator.

3.4.1 Design

In the present study, an attempt has been made to arrange vanes in three rows. Each row of the distributor can be designed similar to that of single row vane type distributor. The following parameters were selected for this design.

1. Length of opening in each row = 30 mm
2. Maximum gap width between vanes = 3 mm
3. Vane thickness, t = 0.8 mm
4. Width of vane holder = 8 mm
5. Vane angle = 15° and 20°

Based on the above parameters, two distributors were designed and the details are given in Table 3.4.1

Table 3.4.1 Distributor details of three row vane type distributors

Sl.No	Particulars	Vane angle(θ)	
		15°	20°
1	Diameter of the distributor, mm	300	300
2	Number of vanes in the outer row	64	85
3	Number of vanes in the middle row	48	63
4	Number of vanes in the inner row	32	41
5	Diameter of the cone, (D_c), mm	88	88
6	Percentage area of opening	17	22
7	Percentage useful area of the distributor	91	91

3.4.2 Fabrication

A 10 mm thick mild steel plate was used to fabricate the vane holders. The vane holders are in the form of three annular rings and a circular disc. Three 8 mm wide metallic rings were cut from a 10 mm thick metallic plate. Depending on the number of vanes to be provided in each row, markings were made on the periphery of the rings or disc, as the case may be, using a template. Through these markings, inclined

grooves corresponding to the designed vane angles were cut using hacksaw. A fixture was designed and used for ensuring accuracy while making inclined grooves. The rings and circular disc were screwed concentrically on a plywood sheet and vanes were fixed in their corresponding slots with epoxy. Figure 3.4.1 shows the photograph of one of the distributors fabricated

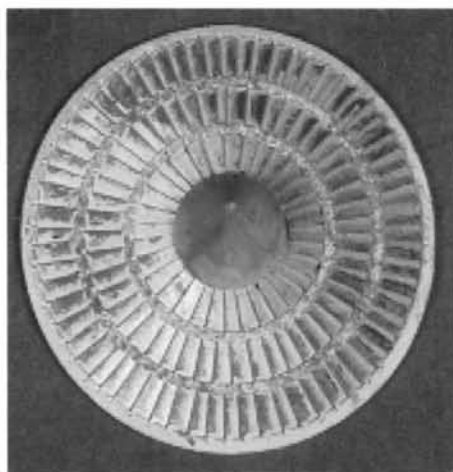


Figure 3.4.1 Photograph of three row vane type distributor

3.5 PERFORATED PLATE DISTRIBUTOR

A perforated plate distributor was fabricated for the purpose of determining the minimum fluidization velocity of bed materials. Perspex sheet of 10 mm thickness was used for the distributor and circular holes were drilled. The fabrication details are presented below.

Diameter of the distributor (D) = 300 mm

Diameter of hole (d) = 2.5 mm

No. of holes (n) = 1258

Percentage area of opening $\approx 9\%$

3.6 CONCLUSIONS

A total of seven distributors have been designed and fabricated namely single row vane type distributors (15° and 20° vane angle), inclined hole type distributors (15°

and 20° hole angle), three row vane type distributors (15° and 20° vane angle) and perforated plate distributors. The useful area of distributor of single row vane type, three row vane type and inclined hole type distributors are 64 %, 91 % and 94 % respectively. The method of fabrication, and design details have been explained for each distributor.

CHAPTER 4

EXPERIMENTAL SET-UP AND PROCEDURE

4.1 INTRODUCTION

This chapter presents details of the experimental set-up and describes the procedure adopted to determine various parameters. Procedure for the determination of various physical properties of bed particles such as bed density, particle density, particle size and voidage is explained. Procedure to determine distributor pressure drop, minimum fluidizing velocity, air velocity in empty bed, bed pressure drop, bed height, different operating regimes of the bed is discussed in detail in this chapter.

4.4 EXPERIMENTAL SET-UP

The schematic diagram shown in Figure 4.2.1 describes important parts of the experimental set-up and the photograph of the complete view of the experimental set-up is presented in figure 4.2.2.

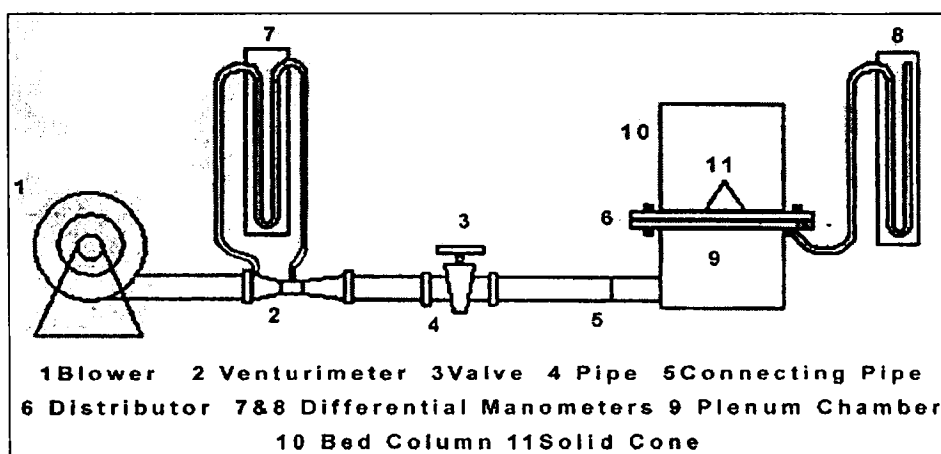


Figure 4.2.1 Schematic diagram of the experimental set-up

A blower supplies air to the plenum chamber through a 125 mm diameter pipe. The air flow rate can be controlled by the gate valve. The flow rate can be calculated from the water column manometer connected to the venturimeter. The venturimeter is fixed

at a distance of 1000 mm away from the outlet of the blower and the gate valve is located at 1000 mm down stream with respect to the venturimeter. This ensures a uniform flow in the venturimeter.

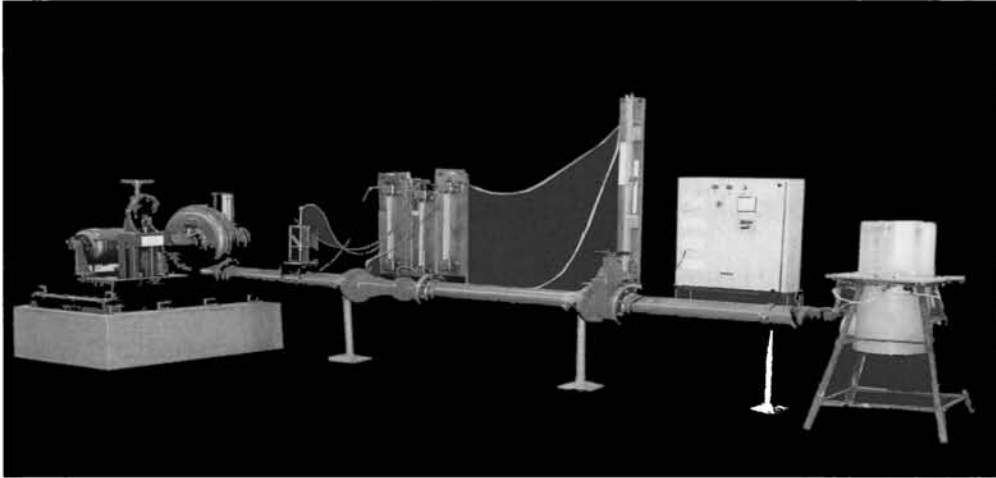


Figure 4.2.2 Photograph of the experimental set-up

A pointer attached to a rack and pinion arrangement helps to measure the readings on the manometer without parallax error. The entry of air in to the plenum chamber is made tangential to it so as to have a clockwise air circulation within this chamber.

This is to reduce the pressure loss at entry in the distributor, as the inclined vane/hole type distributors were also designed to have a clockwise air entry into the bed.

The cylindrical mild steel plenum chamber has an internal diameter of 300 mm and height of 600 mm. A flange has been provided on the top of the plenum chamber for attaching the bed column.

The cylindrical bed column has an internal diameter of 300 mm and a height of 600 mm. This is made of perspex cylinder so as to have visual observations while conducting experiments. A flange, made of 10 mm thick perspex, was made at the bottom of the bed column for fixing it to the plenum chamber.

A distributor holder has been made to place the distributor in position. This is made from a 12 mm thick perspex square plate of size 450 mm and is provided with a

300 mm diameter central opening and an inner annular groove (10 mm depth and 15 mm width). Rubber packing provided at top and bottom of the distributor ensures an airtight assembly of the distributor.

A calibrated temperature sensor of type K thermocouple (Alumel-Chromel) has been located within the pipe just before the venturimeter, for the purpose of measuring the temperature of air flowing through the venturimeter. This temperature can be measured to an accuracy of 0.1 °C with a digital temperature indicator.

Three 0.8 mm diameter pressure tapings, equally spaced around the circumference of the plenum chamber, have been provided just below the distributor to measure the distributor pressure drop. These tapings are connected through a piezometric ring to one limb of a U-tube manometer. In a similar manner, four pressure tapings are provided just above the distributor in the bed column. These tapings are also connected through a piezometric ring to the other limb of the manometer. Now, the distributor pressure drop can be obtained directly from the difference in the manometer readings.

The bed pressure drop can be obtained by connecting the pressure tapings from the bed to the positive terminal of the digital micro manometer (FCO 520 air pro) and leaving the negative terminal open to the atmosphere. The digital micro manometer has a least count of 0.01 mm of water and is capable of measuring a maximum pressure of 60 mm of water. A 2.6 mm diameter three-hole probe is used to measure the two-dimensional air velocity in the empty bed. The projected area of the probe is approximately 2.4 percent of the flow area and hence the influence of the probe on the flow field is negligible. A probe holder, fixed to the flange of the bed column, holds the three-hole probe. Figure 4.2.3 shows the photograph of the probe and its holder.

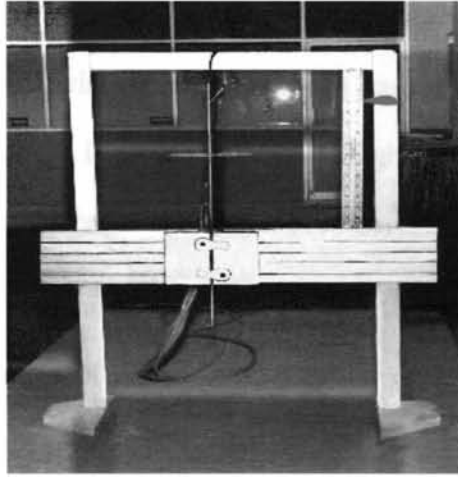


Figure 4.2.3 Three hole probe and its holder

The probe can be fixed in the vertical slot of the holder with two knobs and is free to rotate about the vertical axis in the slot. The direction of air flow at the point of measurement with respect to the tangential position can be obtained from a protractor attached to the probe. The probe can be moved along the vertical and horizontal directions in the probe holder and its position can be located with the help of attached scales. The calibration details of the three-hole probe is given in appendix A.

4.3 EXPERIMENTAL PROCEDURE

4.3.1 Determination of Physical Properties of Bed Particles

The mean particle size, bed density, particle density and bed voidage are the physical properties determined to specify the bed material.

4.3.1.1 Mean particle size

The mean particle size of the bed material can be determined by sieve analysis and from the relation

$$d_m = \left\{ \sum \frac{x_i}{d_i} \right\}^{-1} \quad (4.1)$$

Two types of bed materials have been considered in the present experimental

investigation, namely pepper and coffee beans. These materials were properly dried and weighed. The entire material was sieved through standard IS sieves using a sieve shaker. The particles retained in each sieve were weighed accurately and from this data, mean particle size of the bed materials has been arrived at.

Mean diameter of pepper calculated is 4.38 mm and 100 % particles were passing 4.75 mm sieve and retaining 4.00 mm sieve.

Details of sieve analysis carried out for coffee beans are presented in Table 4.3.1. The mean diameter of coffee beans calculated is 8.78 mm

Table 4.3.1 Sieve analysis details of coffee beans

Sieve size (mm)		d_i (mm)	x_i	x_i / d_i	$d_m = \left\{ \sum \frac{x_i}{d_i} \right\}^{-1}$
Passing	Retaining				
12.5	10	11.25	0.224	0.0199	8.78 mm
10	9	9.50	0.334	0.0352	
9	8.5	8.75	0.089	0.0102	
8.5	7	7.75	0.213	0.0275	
7	6.3	6.65	0.140	0.0211	

4.3.1.2 Bed density

As-poured density of bed material was determined using a 3 litre calibrated container. The material filling the container was weighed to an accuracy of 0.1 gram with a calibrated digital balance. Table 4.3.2 shows the details of the observations made in connection with the bed density calculation.

4.3.1.3 Particle density

Particle density was determined using a standard pycnometer. Distilled water was used in the pycnometer. Mass measurement was made to an accuracy of 0.1 g using a digital weighing machine. Table 4.3.3 and 4.3.4 presents the details of observation

made for the determination of particle density in the case of coffee beans and pepper respectively.

Table 4.3.2 Calculation of bed density

Sl.No	Bed particle	Pepper	Coffee beans
1	Volume of container (l)	3.0	3.0
2	Mass of particle in container (g)		
	Trial --1	1802.3	1398.6
	Trial --2	1797.2	1403.5
	Trial --3	1801.5	1401.2
3	Average mass of particle (g)	1800.3	1400.4
4	Bed density (kg/m ³)	600	470

Table 4.3.3 Particle density of coffee beans

Sl. No.	Description	Trial number			Average
		1	2	3	
1	Mass of pycnometer, M ₁ (g)	467.8	467.3	467.5	-
2	Mass of pycnometer + particle, M ₂ (g)	925.2	885.0	910.6	-
3	Mass of pycnometer + particle+water, M ₃ (g)	1112.1	1125.4	1140.2	-
4	Mass of pycnometer+ water, M ₄ (g)	1265.7	1266.5	1265.3	-
5	Particle density of coffee beans, (M ₂ -M ₁) / [(M ₄ -M ₁) - (M ₃ -M ₂)] (g/cc)	0.75	0.76	0.78	0.76

4.3.1.4 Bed voidage

Once particle density and bed density of bed particles were determined, the bed voidage (ϵ) can be calculated from the relation

$$\epsilon = 1 - \frac{\rho_b}{\rho_p} \quad (4.2)$$

Table 4.3.4 Particle density of pepper

Sl. No.	Description	Trial number			Average
		1	2	3	
1	Mass of pycnometer, M_1 (g)	467.9	467.3	467.6	-
2	Mass of pycnometer + particle, M_2 (g)	991.5	1019.9	1031.5	-
3	Mass of pycnometer + particle + water, M_3 (g)	1345.1	1357.5	1367.2	-
4	Mass of pycnometer + water, M_4 (g)	1265.4	1265.2	1265.4	-
5	Particle density of pepper, $(M_2 - M_1) / [(M_4 - M_1) - (M_3 - M_2)]$ (g/cc)	1.18	1.20	1.22	1.20

4.3.1.5 Particle specification

Table 4.3.5 gives the various physical properties determined in the case of the two bed materials, namely coffee beans and pepper.

Table 4.3.5 Physical properties of particles

Sl. No.	Property	Coffee beans	Pepper
1	Average Particle diameter (mm)	8.78	4.38
2	Average Particle density (kg/m^3)	760	1200
3	Bed density (kg/m^3)	470	600
4	Bed Voidage (%)	39	50

4.3.2 Determination of Distributor Pressure Drop

Distributor pressure drop is one of the important parameters, which influences the fluidization quality as well as energy consumption and it varies with the superficial velocity. Distributor pressure drop can be determined by observing the pressure difference across the distributor in an empty bed.

The distributor was fixed in position between the plenum chamber and the bed column by bolting and a leak proof joint was ensured. Horizontality of the distributor

was ensured with the help of a spirit level. Pressure tapping from the top and bottom of the distributor was connected to the U-tube differential water column manometer.

For a particular value of venturimeter reading, (venturimeter pressure drop, ΔP_v) the distributor pressure drop (ΔP_d) and temperature of air (T) were observed. The measurements were made only after the readings were stabilized in each case. The observations were made at regular increments of the venturimeter readings, starting from zero, by operating the gate valve.

The volume flow rate of air (Q) can be calculated using the equation

$$Q = 0.021 \sqrt{\Delta P_v \times \frac{\rho_w}{\rho_a} \times \left(\frac{273 + T}{273} \right)} \quad (4.3)$$

From the volume flow rate, the superficial velocity (U) can be calculated using the equation

$$U = \frac{4 \times V}{\pi(D^2 - D_c^2)} \quad (4.4)$$

4.3.3 Determination of Minimum Fluidizing Velocity

Minimum fluidizing velocity of the bed is dependent on the physical properties of the particles and is an important parameter for the design of fluidized beds.

The bed pressure drop was measured with a calibrated digital micro manometer, the details of which are given in appendix B. The positive terminal of the manometer was connected to the pressure tapping from the top of the distributor and the negative terminal was left open to the atmosphere. Since bed pressure drop fluctuates, average of ten readings, taken at an interval of ten seconds was considered as the bed pressure drop. The time interval was correctly set with the help of a buzzer.

Two kilograms of bed material was placed in the bed column. The gate valve was initially opened to such an extent that the bed fluidized vigorously and the corresponding venturimeter reading (venturimeter pressure drop, ΔP_v), bed pressure drop (ΔP_b) and temperature of air (T) were observed. The observations were taken only after stabilization of the readings. The experiment was repeated for lower air flow rates by controlling the gate valve opening.

4.3.4 Measurement of Air Velocity in Empty Bed

Inclined hole/vane type distributors cause air to swirl in the bed. Hence at any point in a plane parallel to the distributor, the air velocity will have radial and tangential component. While the radial component contributes to the radial mixing of the particles, tangential component leads to swirl motion. Measurement of air velocity at different planes will give an insight in to the bed behaviour.

A three hole probe was used to measure the air velocity and it's direction in the horizontal plane. A reference radial line was drawn on the distributor. Markings were made on this line at regular interval of 5 mm within the radial distance from 53 mm to 143 mm. Concentric circles were marked on the distributor through these markings. The probe holder was fixed across the bed column in such a way that the tip of the probe will move in the line of the radius drawn when the protractor is set at zero angle. A five limb inclined water column manometer (30° inclination with the horizontal) was used to measure the pressure developed in the three hole probe. Each hole of the probe was connected to separate limb of the manometer with flexible rubber hose. The other two limbs were left open to the atmosphere.

Constant airflow was ensured by the venturimeter readings, which in turn is adjusted by the gate valve. The temperature of the air was noted. The plane in which measurements are to be taken was set with the help of the vertical scale fitted to the

probe holder.

In the plane considered, the probe tip was set at the marked radial distance with zero reading in the protractor (this ensures the orientation of the probe tip in the tangential direction). Air pressures in the left and right holes were balanced to the maximum extent possible by rotating the probe about its vertical axis. The small variation in the radial distance caused due to the above said rotation of the probe was then adjusted. This rotation of probe and adjustment of the radial distance was repeated till the tip of the probe was set at the radial distance considered with the left and right probe pressures balanced. The manometer readings corresponding to the air pressure at all the three holes and the rotation of the probe (from the protractor) were noted. From these readings, the tangential and radial components of the air velocities at the set point can be calculated. The flow rate was calculated from the venturimeter readings and the temperature of the air. Measurements were made at marked radial distances and for different air flow. The experiment was conducted for probe positions at the top of the distributor and at planes located at distances 5, 10, and 15 mm above the distributor.

Vortex formation due to the swirl motion causes the formation of a central region without airflow. The above experimental set-up was used to locate this region in a typical swirl bed and the procedure is explained below.

Constant airflow was maintained and the corresponding air temperature was noted. The plane in which measurements have been taken was set with the help of the vertical scale fitted to the probe holder. The probe was initially fixed in a plane located at 5 mm above the distributor. The probe tip was set with zero reading in the protractor to ensure the orientation of the probe tip in the tangential direction and was placed near the bed wall. The probe was then moved slowly towards the center and

the manometer reading corresponding to the air pressure in the three holes was continuously monitored. The radial position of the probe corresponding to zero pressure at the probe holes was noted. The experiment was repeated in planes located at different distances from the distributor.

4.3.5 Determination of Bed Pressure Drop

Variation of bed pressure drop with superficial velocity is one of the important parameters for assessing the quality of fluidization. The bed pressure drop can be determined by observing the pressure difference across the bed.

The distributor selected was fixed in position as explained in section 4.3.2. Pressure tapping from the top of the distributor was connected to the positive terminal of the digital micro-manometer and the negative terminal was left open to the atmosphere. Average of ten micro-manometer readings, taken at intervals of ten seconds, was considered as the bed pressure drop (ΔP_b) in the present study.

A specified mass of bed material was placed in the bed column. For a fixed value of venturimeter reading, starting from zero (venturimeter pressure drop, ΔP_v) the bed pressure drop (ΔP_b) and temperature of air (T) were observed. The observations were made only after the readings were stabilized in each case. The experiment was repeated at regular increments of the venturimeter readings by operating the gate valve. Volume flow rate of air and superficial velocity can be calculated using equation 4.3 and 4.4. The entire experiment was repeated for different distributors fabricated by varying the bed material and bed weight.

4.3.6 Determination of Bed Height

Three scales, symmetrically attached to the outer periphery of the bed column were used to measure the bed height. The least count of these scales was 1.0 mm and the average of three scale readings, rounded to 1.0 mm accuracy, was considered as the

bed height. Accurate measurement of the bed heights was not possible in the case of vane type distributors, as the bed height was not steady in the wave region.

4.3.7 Identification of Different Regimes

As the superficial velocity is increased from zero to the maximum, in general, the swirling fluidized bed may undergo three different stages namely stagnant, wave motion and swirl motion. Different processes need different types of bed behaviour and hence it is important to identify the velocity regime over which these behaviors occur.

For a particular bed material and bed weight, the airflow was increased slowly from zero by opening the gate valve until wave motion is observed in the bed. Venturimeter reading corresponding to the starting of this wave motion was recorded. The airflow was further increased until swirl motion is observed in the bed and the corresponding venturimeter reading was also recorded. This experiment was conducted for different bed weights, which varied from 500g to 1300g at an increment of 100g, for both coffee beans and pepper. The superficial velocity corresponding to the starting of wave motion and swirl motion can be calculated from the corresponding venturimeter readings.

4.3.8 Determination of Bed Pressure Drop along Radial Direction

Bed pressure drop may vary along the radial direction in a swirling fluidized bed. This variation may affect the efficiency of the process in the bed, particularly for drying processes. In the present study, the bed pressure drop variation along the radial direction was observed in the case of three row vane type distributors with coffee beans as the bed material.

Pressure tappings were made at four points along the radial direction in the distributor. Holes were drilled through the rings of the distributor or through the inner disc, as the case may be. Pressure tappings were made by inserting copper tubes through these holes. While top of the tube was kept in flush with the top of the distributor, its bottom was connected to flexible tubes and these tubes were taken out through the bottom of the plenum chamber. A digital micro-manometer was used to measure the bed pressure drop at each pressure tapping.

The experimental procedure to determine the bed pressure drop at each pressure tapping was similar to that explained in section 4.3.5. The bed pressure drop was determined along the radius of the bed for different airflow rates and different bed weights.

4.4 CONCLUSIONS

Details of the experimental set-up have been explained. The procedure adopted to determine various physical properties of bed particles and the bed parameters have been discussed.

CHAPTER 5

RESULTS AND DISCUSSION

5.1 INTRODUCTION

This chapter deals with the results obtained and discussions made based on the experimental studies carried out in the case of seven different distributors. The following hydrodynamic parameters were studied.

1. Distributor pressure drop
2. Air velocity
3. Minimum fluidizing velocity
4. Bed pressure drop
5. Bed height

Conclusions arrived at, based on the discussions carried out are also presented in this chapter.

5.2 DISTRIBUTOR PRESSURE DROP

Distributor pressure drop is an important parameter, which influences the energy consumption and the fluidization quality. In general, a higher distributor pressure drop leads to higher energy consumption. It has been reported that a minimum distributor pressure drop as high as 350 mm of water is required for a uniform fluidization in a shallow conventional bed and a lower distributor pressure drop than this may cause non-uniform distribution of air in the bed [Agarwal (1962)]. However, in the case of swirling fluidized bed, a uniform fluidization can be achieved even with lower distributor pressure drop [Binod and Raghavan (2002)], which is a distinct advantage of such beds.

Distributor pressure drop can be determined by observing the pressure difference across the distributor in an empty bed and the detailed procedure for the determination of distributor pressure drop is explained in section 4.3.2.

Figure 5.2.1 shows the variation of distributor pressure drop with superficial velocity in the case of all the seven distributors. The curves presented are the best fit polynomials and are marked in ascending order based on the percentage area of opening of the distributor, starting from the lowest value. Table 5.2.1 gives the expression for each curve and its coefficient of determination (R^2).

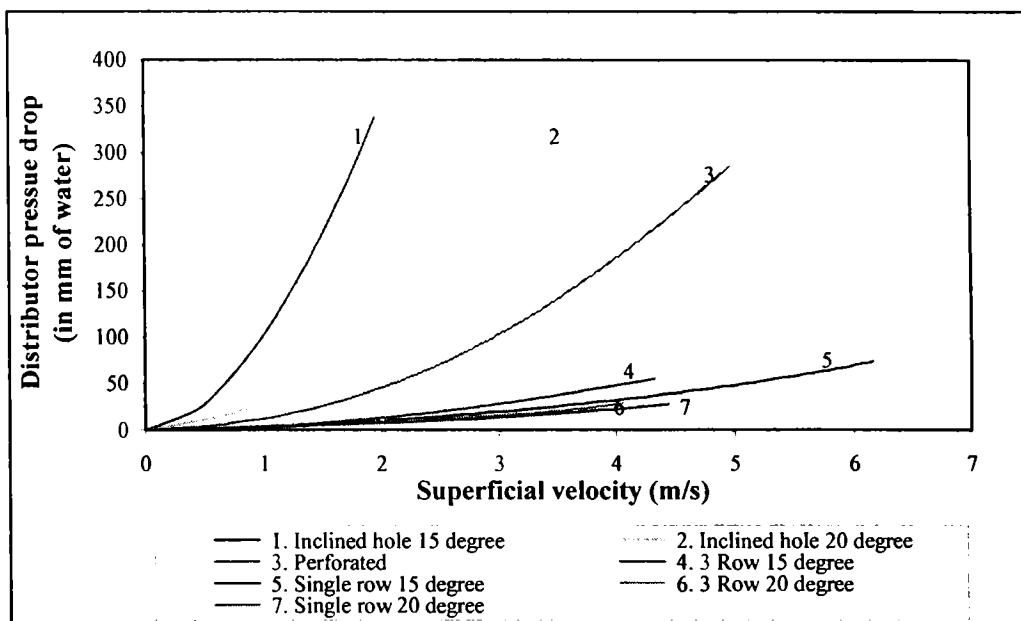


Figure 5.2.1 Variation of distributor pressure drop with superficial velocity

Inclined hole type distributors have a limitation in increasing the percentage area of opening. On the other hand, a higher percentage area of opening can be achieved with inclined vane type distributors. In the present study, a total of four vane type distributors with area of openings varying from 17 % to 25 % have been considered against two inclined hole type distributors with area of openings 3% and 5%.

Table 5.2.1 Variation of distributor pressure drop with superficial velocity

Sl. No	Type of distributor	% area of opening	Equation of the curve	R ² value
1	Inclined hole 15 degree	3	$\Delta P_d = 6.3806U^4 - 32.865U^3 + 127.32U^2 + 1.6558U$	0.999
2	Inclined hole 20 degree	5	$\Delta P_d = -0.4156U^4 + 3.2U^3 + 16.364U^2 + 11.154U$	0.999
3	Perforated	9	$\Delta P_d = -0.1868U^4 + 1.9226U^3 + 5.4593U^2 + 5.5393U$	0.999
4	3 Row 15 degree	17	$\Delta P_d = -0.088U^4 + 0.7281U^3 + 0.7857U^2 + 2.8572U$	0.999
5	Single row 15 degree	19	$\Delta P_d = 0.0404U^4 - 0.4383U^3 + 3.0699U^2 + 0.2285U$	0.998
6	3 Row 20 degree	22	$\Delta P_d = 0.2101U^4 - 1.375U^3 + 3.5178U^2 + 1.3582U$	0.997
7	Single row 15 degree	25	$\Delta P_d = -0.366U^4 + 5313U^3 - 1.2379U^2 + 4.4676U$	0.998

Curve 1 and 2 represent the variation of distributor pressure drop for inclined-hole type distributor with 15° and 20° hole angle respectively. Their percentage area of openings is 3% and 5% respectively. Curve 3 corresponds to perforated plate distributor with a percentage area of opening 9. Curve 4 and 6 represent three row vane type distributors with vane angle 15° and 20° respectively and their corresponding percentage area of opening is 17 and 22. Curve 5 and 7 represent single row vane type distributors with vane angle of 15° and 20° with a percentage area of opening of 19 and 25. The results show that for a given superficial velocity, the distributor pressure drop is lower for a distributor with higher percentage area of opening. For a given superficial velocity, as the percentage area of opening reduces, the air jet passing through a single opening will have higher velocity. This higher velocity causes higher pressure loss through the openings. Further, for the same

percentage area of opening, if the area of a single opening is reduced, the pressure loss through the opening increases. The individual or combined effect of the above two, as the case may be, ultimately causes a higher distributor pressure drop with a lower percentage area of opening of the distributor.

5.3 AIR VELOCITY IN EMPTY BED

In a shallow conventional fluidized bed the air velocity is primarily in the vertical direction and hence the radial and axial mixing of particles is generated by the gas bubbles within the bed. On the other hand, in inclined hole/vane type distributor air will swirl in the bed. Because of this swirling, at any point in a plane parallel to the distributor, the air will have radial and tangential components of velocity. While the radial component contributes to the radial mixing of the particles, tangential component leads to swirl motion. The variation in the radial component of the air velocity along the radius influences lateral mixing. Similarly, the tangential component causes vortex formation.

Since three row vane type distributors have a high useful area with low distributor pressure drop, the variation of air velocity of different planes in a bed has been studied in an empty bed for this kind of distributor with vane angle 15° as a typical case. The detailed procedure for the measurement of air velocity is presented in section 4.3.4.

The variation of radial and tangential components of velocities with volume flow rate of air at different radial distances and at different planes above the distributor was studied. Different planes considered were at an incremental distance of 5.0 mm from the distributor. The readings at the top surface of distributor showed non uniform variation. Further, the readings in a plane located ≥ 15 mm from the distributor revealed that the airflow was actually taking place over a small outer annular space.

Here, the readings obtained from two planes, located at 5 mm and 10 mm above the distributor, were considered. In a given plane, measurements were taken at different radial distances at an interval of 10 mm from 143 mm to 83 mm. It is to be noted that at radial distances 73 mm, the air flow was not significant and hence measurements were not taken for the values of radial distances lower than 83 mm. The variation of radial and tangential components of velocities with volume flow rate of air at different radial distances in a plane located at 5 mm above the distributor was studied and the details are presented in figures 5.3.1 to 5.3.7.

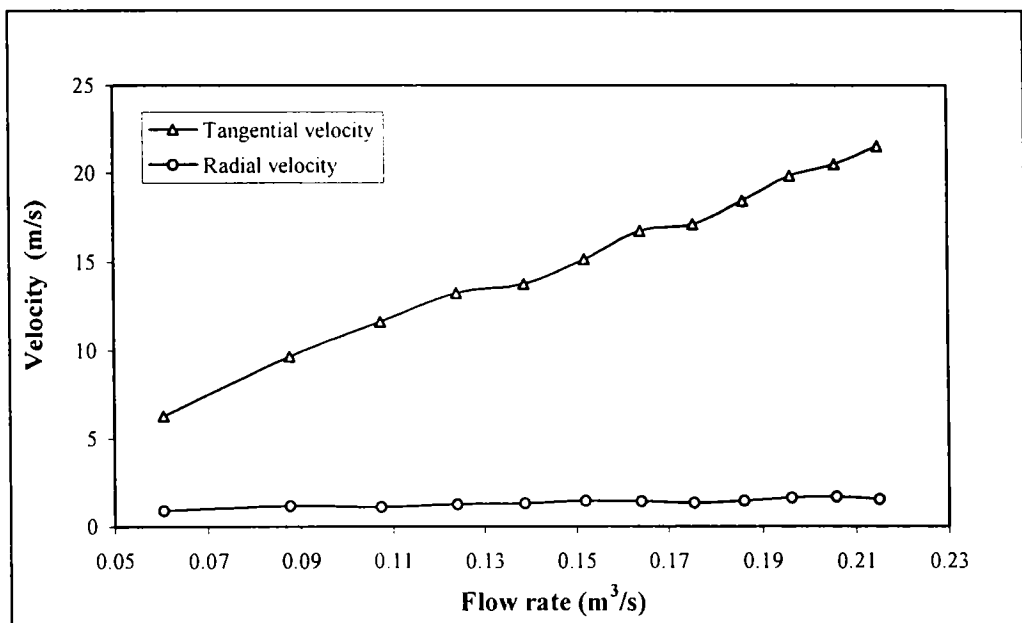


Figure 5.3.1 Variation of velocity with flow rate in three row vane type distributor- probe at 5 mm height and at 143 mm radial distance

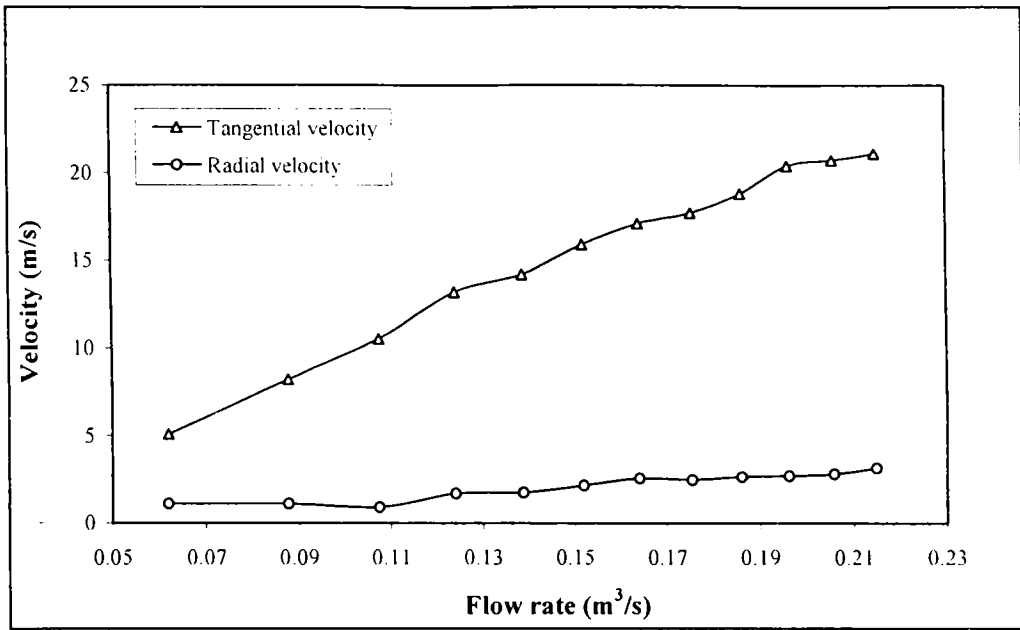


Figure 5.3.2 Variation of velocity with flow rate in three row vane type distributor- probe at 5 mm height and at 133 mm radial distance

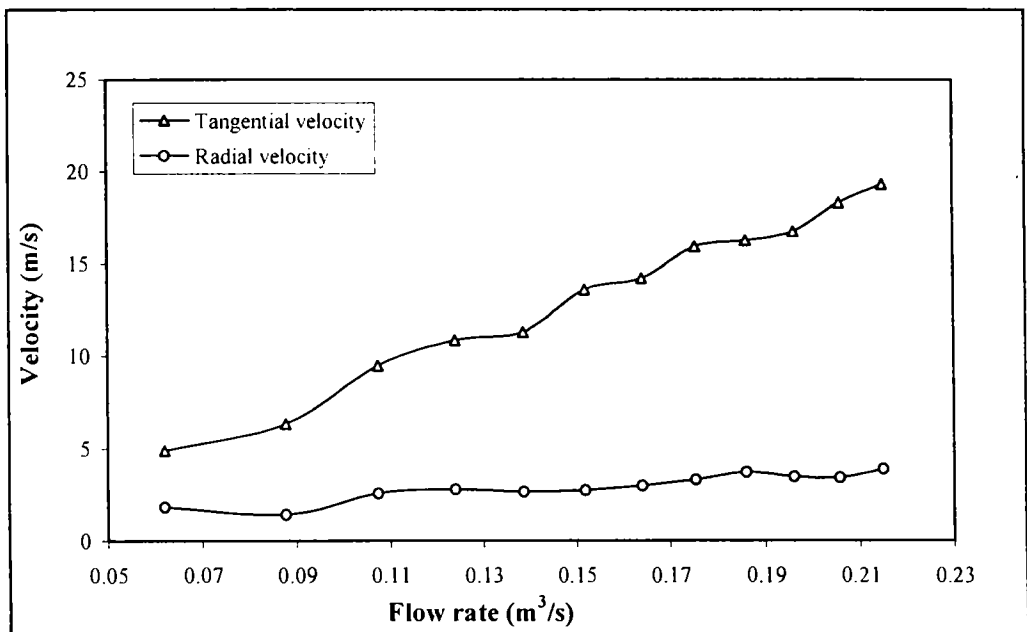


Figure 5.3.3 Variation of velocity with flow rate in three row vane type distributor- probe at 5 mm height and at 123 mm radial distance

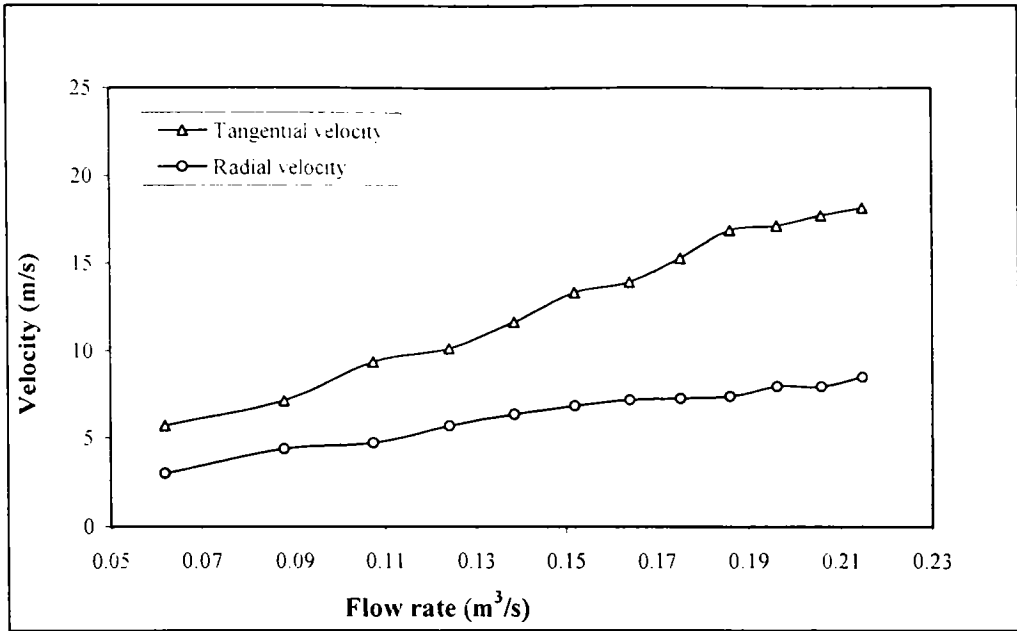


Figure 5.3.4 Variation of velocity with flow rate in three row vane type distributor -probe at 5 mm height and at 113 mm radial distance

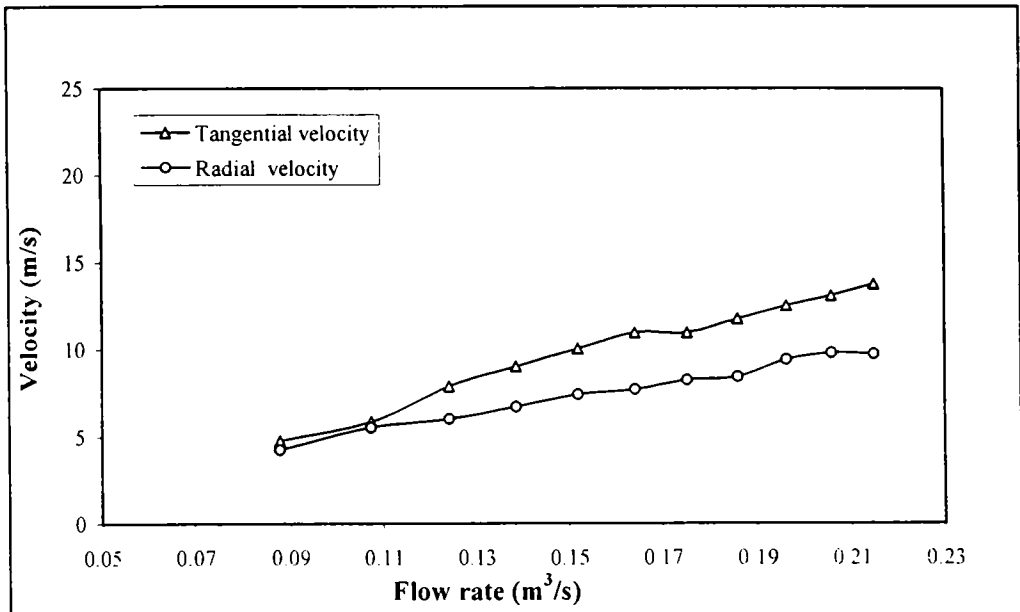


Figure 5.3.5 Variation of velocity with flow rate in three row vane type distributor- probe at 5 mm height and at 103 mm radial distance

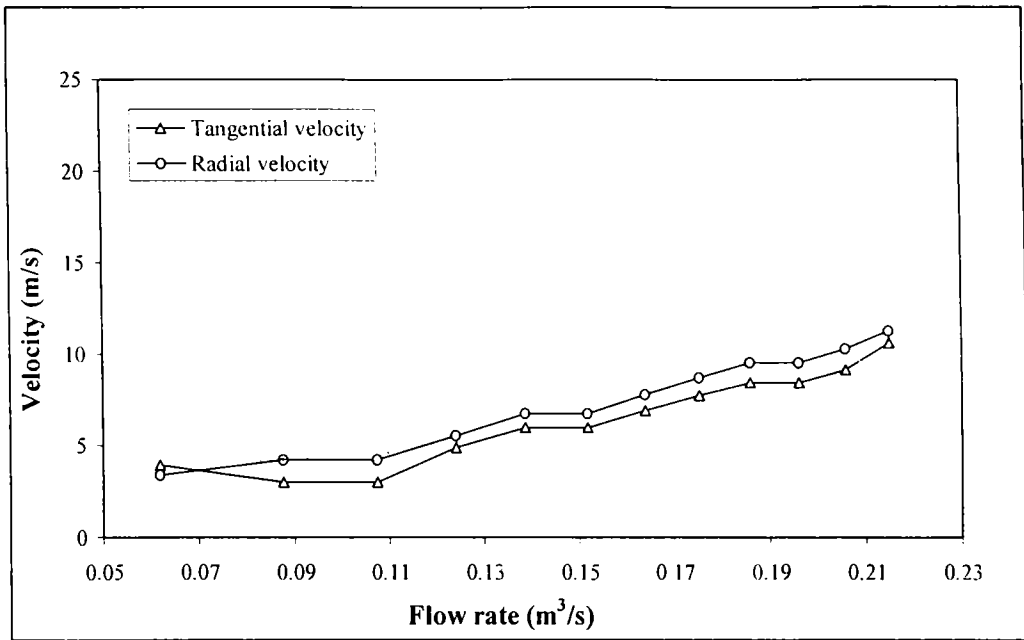


Figure 5.3.6 Variation of velocity with flow rate in three row vane type distributor- probe at 5 mm height and at 93 mm radial distance

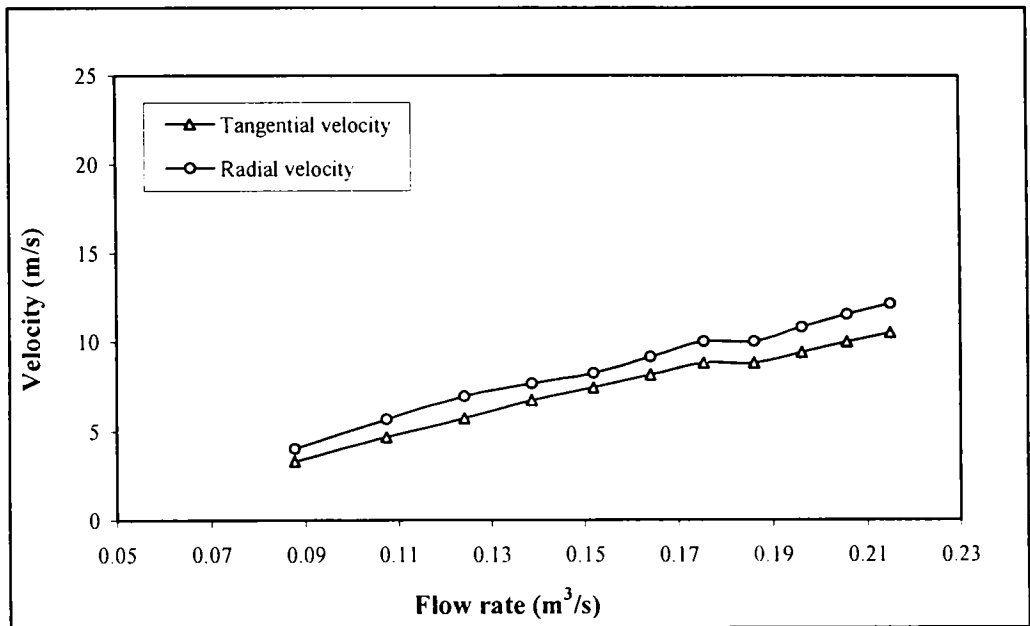


Figure 5.3.7 Variation of velocity with flow rate in three row vane type distributor - probe at 5 mm height and at 83 mm radial distance

The tangential component of velocity is seen to be higher at a radial distance of 143 mm for all flow rates compared to the radial component. As the radial distance reduces, the difference between the tangential component and radial component of the velocity reduces. For a radial distance of 93 mm and lower, the radial component of velocity is higher than the tangential component.

The variation of radial and tangential components of velocity along the radial direction for two different air flow rates ($0.124 \text{ m}^3/\text{s}$ and $0.175 \text{ m}^3/\text{s}$) are shown in figures 5.3.8 to 5.3.11. While figures 5.3.8 and 5.3.9 correspond to the readings at a plane 5 mm above the distributor, figures 5.3.10 and 5.3.11 correspond to the readings at a plane 10 mm above the distributor.

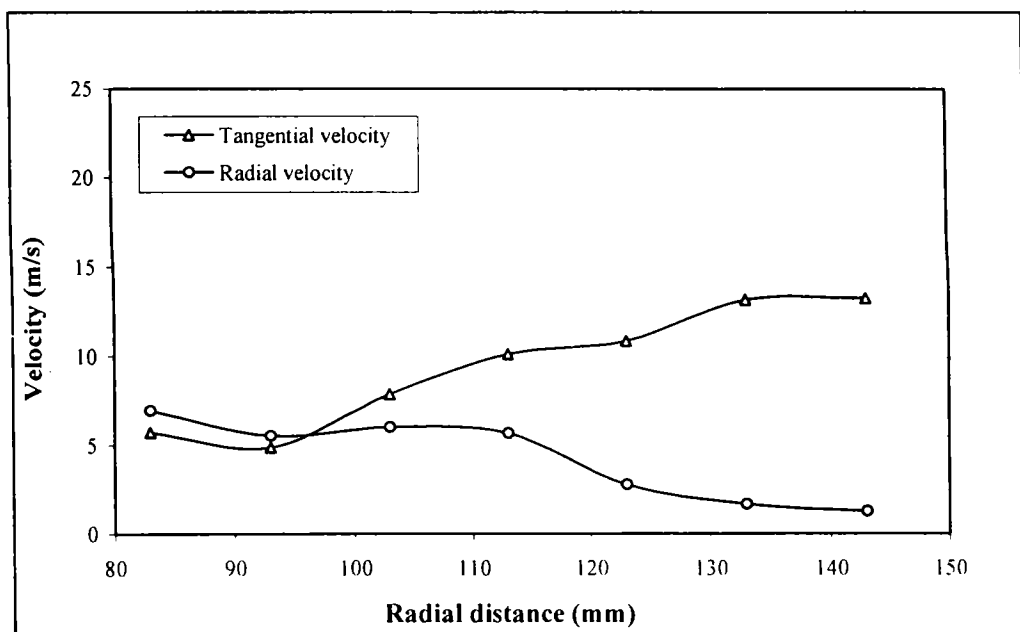


Figure 5.3.8 Variation of velocity at different radial distances in three row vane type distributor -probe at 5 mm height and airflow rate- $0.124 \text{ m}^3/\text{s}$

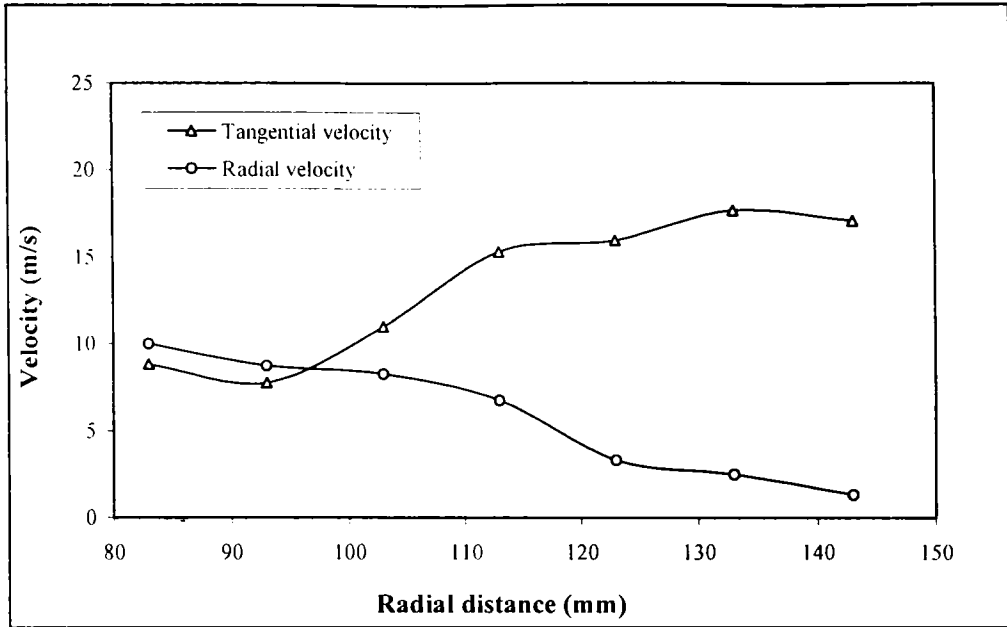


Figure 5.3.9 Variation of velocity at different radial distances in three row vane type distributor - probe at 5 mm height and airflow rate - $0.175 \text{ m}^3/\text{s}$

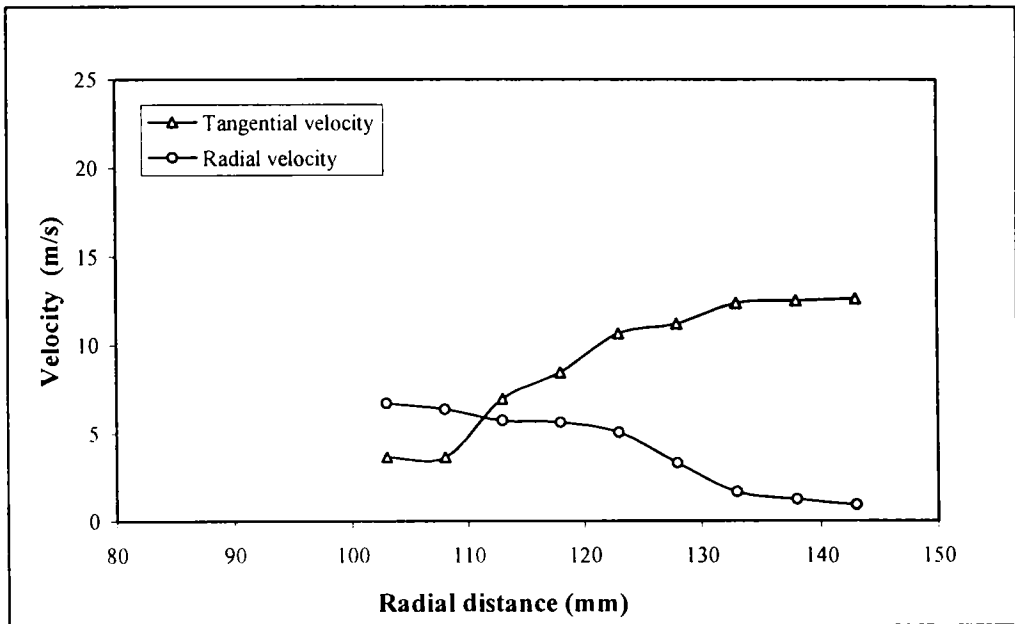


Figure 5.3.10 Variation of velocity at different radial distances in three row vane type distributor - probe at 10 mm height and at airflow rate - $0.124 \text{ m}^3/\text{s}$

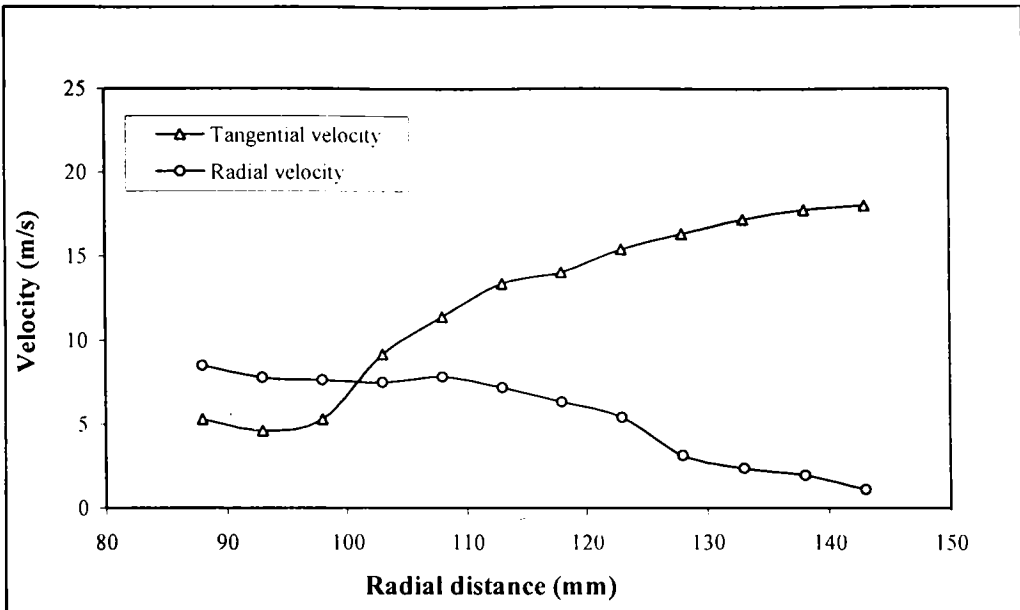


Figure 5.3.11 Variation of velocity at different radial distances in three row vane type distributor - probe at 10 mm height and airflow rate - $0.175 \text{ m}^3/\text{s}$

From the figures 5.3.8 to 5.3.11, it can be observed that, in general, while the radial component of velocity decreases, the tangential component increases with an increase in the radial distance.

Once vortex is formed in the bed, two regions can be identified based on the flow of air. There is an inner region where the air is practically stagnant and an outer region where the air will have a swirl motion. Figure 5.3.12 shows the locus of points which identifies the boundary of the above two regions for two typical flow rates. The coordinates of the points in the curves correspond to the horizontal distance from the center of the distributor and vertical distance from the top of the distributor. For a particular bed height, up to the radial distance identified by the curve there is little air flow and beyond this radial distance, the air swirls.

The air flow is available over the full radial distance up to a certain height above the distributor and beyond this height, the air swirls within a narrow annular width at the

outer boundary. It can be concluded that there is a limitation over the maximum height of bed material which may swirl effectively in a swirling fluidized bed, which depends to some extent on the particle characteristics. Further, it is expected to have a non swirling top layer region in the bed if the bed height is more than a certain value.

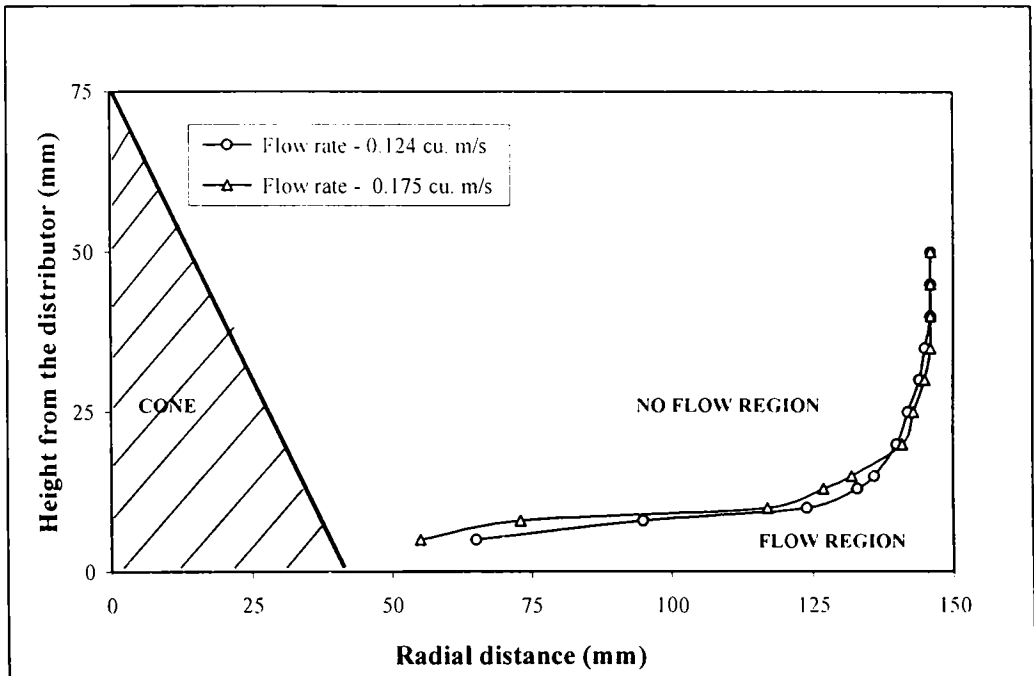


Figure 5.3.12 Plot showing boundary of region having swirl motion of air in empty bed for a three row vane type distributor

5.4 MINIMUM FLUIDIZING VELOCITY OF VANE TYPE DISTRIBUTORS

It is clear from the present study that the bed has to first fluidize and the particles have to unlock before swirling can begin, as otherwise the interparticle friction will be too great to permit relative movement of particles. The minimum fluidizing velocity, U_{mf} , can be defined as the minimum superficial velocity at which the pressure drop through the bed is equal to the bed weight per unit cross-section. There exist many empirical relations to predict U_{mf} in a conventional bed, but no such relation is

available in a swirling fluidized bed.

The minimum fluidizing velocity was determined experimentally in the case of vane type distributors. Two types of particles namely coffee beans and pepper, both coming under “D type” particles as per Geldart’s classification [Howard, 1985], were used for this study. For inclined hole type distributors the minimum fluidizing velocity was not a unique value and hence this distributor was not considered for the determination of U_{mf} .

The U_{mf} can be determined from a plot showing the variation of bed pressure drop with superficial velocity and the methods of determination of these values are described in section 4.3.3. The minimum fluidizing velocity is the superficial velocity corresponding to the intersection of two straight lines drawn appropriately on the above plot. One horizontal line is drawn based on the constant bed pressure values after the fluidization. The other straight line is drawn by considering the last few points before fluidization (in the packed region). Only the last few points are considered to draw the second line due to the fact that the shape of the curve in the packed region is not a straight line. It has been reported that for “D type” particles, the graph in the packed bed region will be non-linear as the flow of gas in the interstices is no more laminar [Howard (1985)] and the same behaviour was observed in the present study also.

Typical graphs showing minimum fluidizing velocity of beds with different distributors and bed materials are presented in figures 5.4.1 to 5.4.5. The minimum fluidizing velocity determined for five distributors are compared in table 5.4.1.

From table 5.4.1, it can be observed that the U_{mf} is lowest for perforated plate distributor and highest for single row vane type distributors. For vane type distributors, the minimum fluidizing velocity is higher for a low vane angle. For the

bed particles considered, the vane type distributors give a higher minimum fluidizing velocity compared to perforated type distributors.

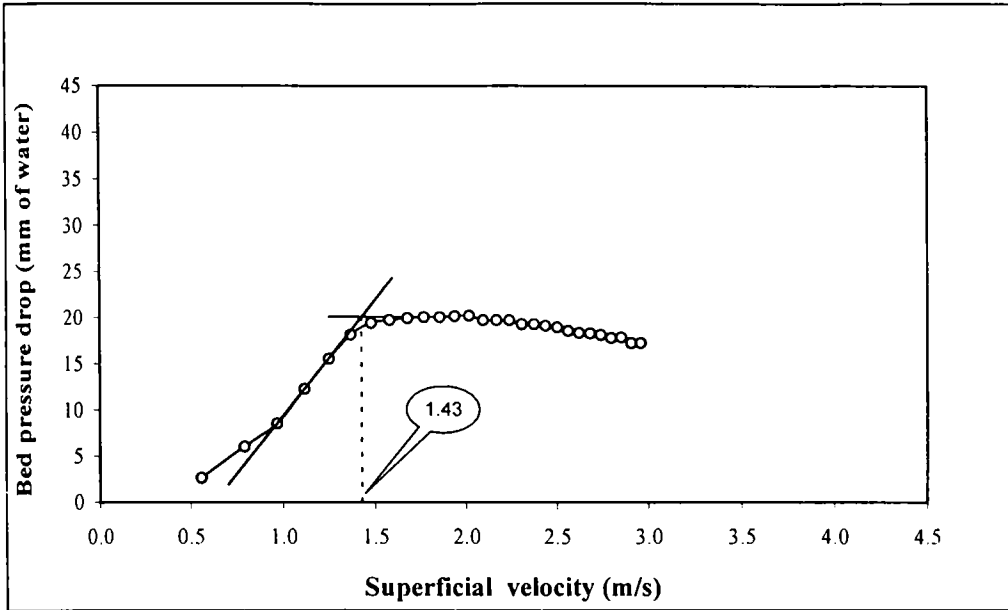


Figure 5.4.1 Minimum fluidizing velocity in beds with conventional bed – bed material - coffee beans

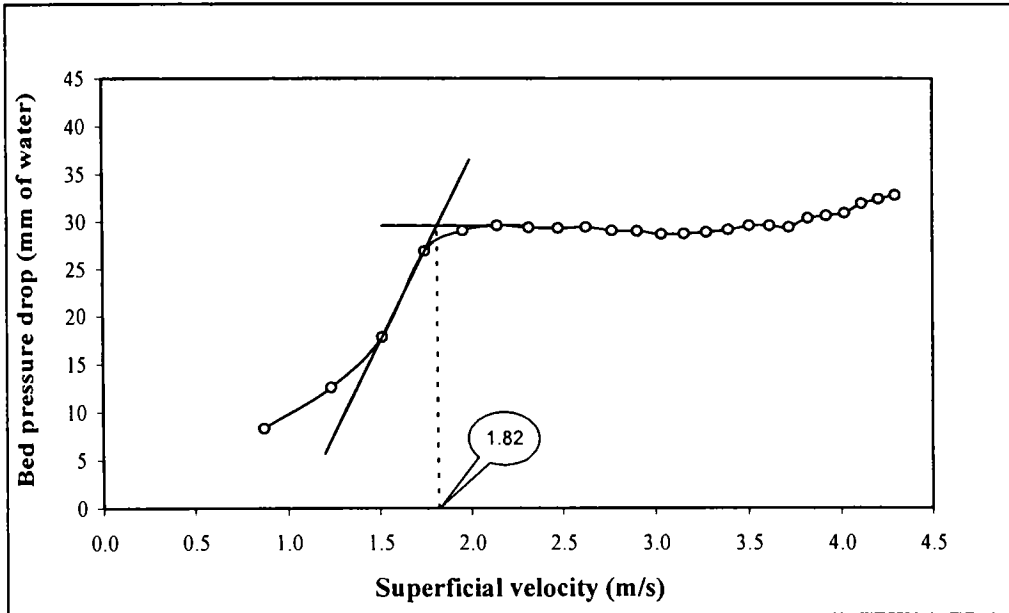


Figure 5.4.2 Minimum fluidizing velocity in beds with single row vane type distributor- vane angle – 20 ° and bed material - coffee beans

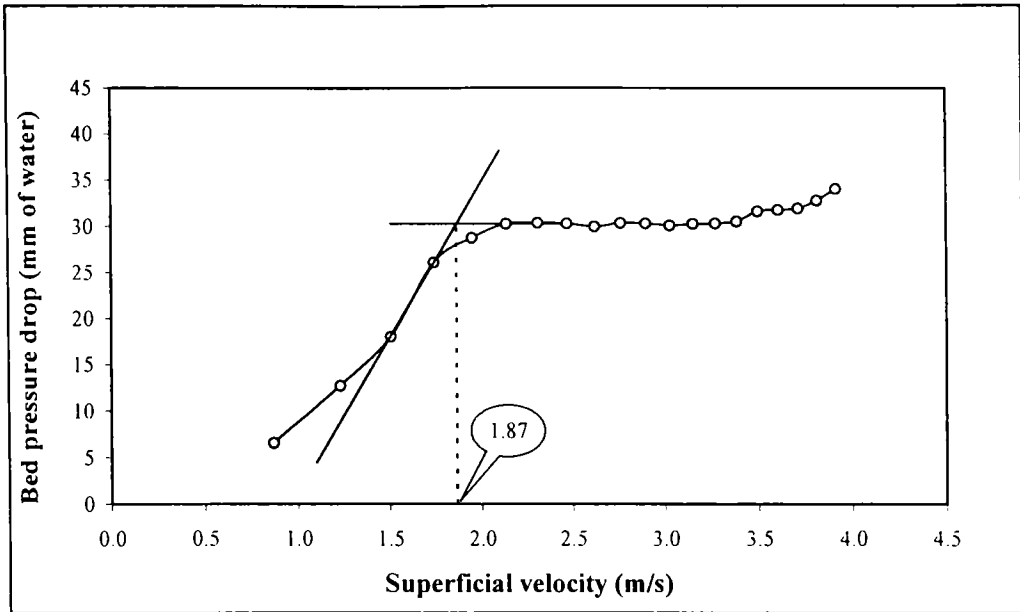


Figure 5.4.3 Minimum fluidizing velocity in beds with single row vane type distributor- vane angle -15 ° and bed material - coffee beans

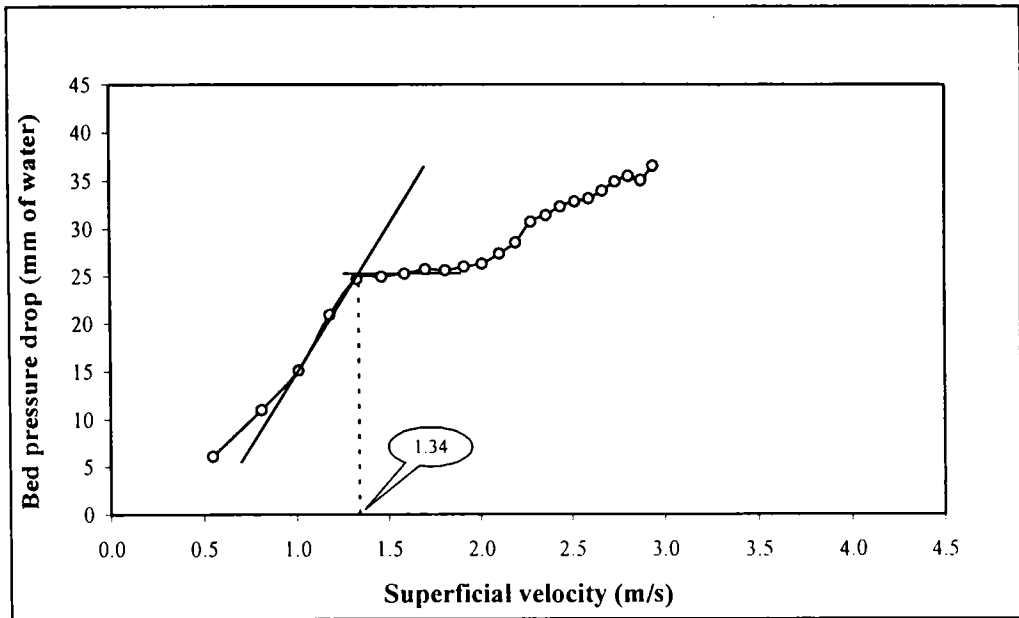


Figure 5.4.4 Minimum fluidizing velocity in beds with three row vane type distributor- vane angle - 20 ° and bed material - pepper

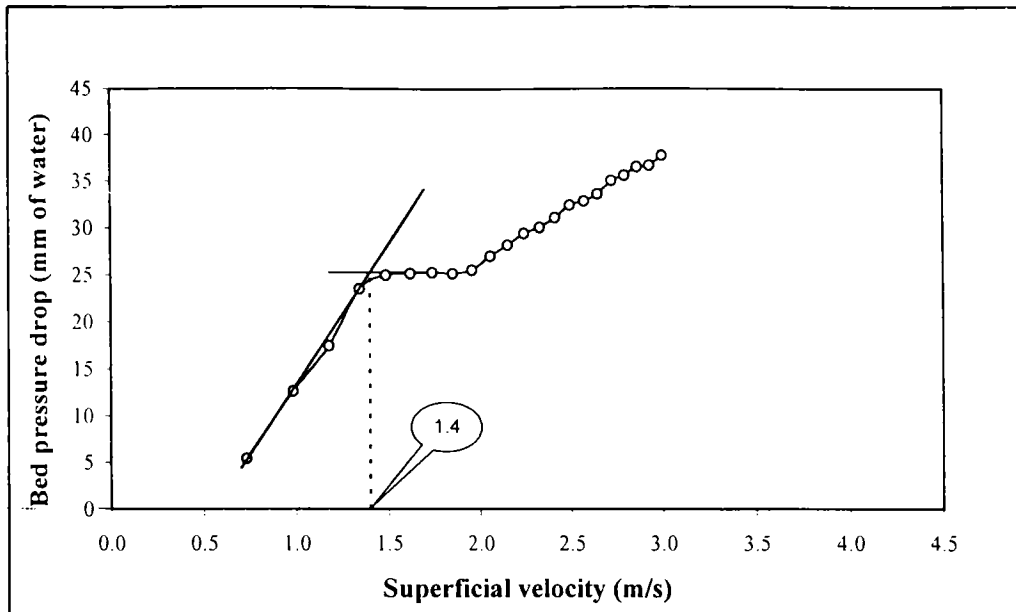


Figure 5.4.5 Minimum fluidizing velocity in beds with three row vane type distributor – vane angle – 15 ° and bed material - pepper

Table 5.4.1 Comparison of minimum fluidizing velocity

Sl. No.	Distributor Type	U_{mf} (m/s)	
		Coffee Beans	Pepper
1	Perforated Plate	1.43	1.28
2	Three Row - 20° Vane Angle	1.59	1.34
3	Three Row - 15° Vane Angle	1.64	1.40
4	Single Row - 20° Vane Angle	1.82	1.42
5	Single Row - 15° Vane Angle	1.87	1.49

The U_{mf} also depend on the vane angle. Compared to perforated plate distributor, a variation as high as 30.8 % has been observed (for single row - 15° vane angle- coffee beans) in the present study.

5.5 VARIATION OF BED PRESSURE DROP WITH SUPERFICIAL VELOCITY.

Bed pressure drop is an important parameter, which gives an insight into the quality of fluidization. From the initial experiments it was seen that swirl velocity, relative velocity of particles, lateral mixing of particles, and toroidal motion are factors which

determine the behavior of the swirling fluidized bed. But up to date no experimental data is available on these parameters. Hence, an attempt has been made to study some of these parameters based on visual observation.

The variation of bed pressure drop with superficial velocity has been studied in the case of seven distributors. The distributors are classified into four groups, viz

- Single row vane type (15° and 20°)
- Inclined hole type (15° and 20°)
- Three row vane type (15° and 20°)
- Perforated plate (conventional)

Coffee beans and pepper were used as bed materials and the bed weights considered were 1.5 kg and 2.0 kg. Based on a preliminary study, it has been observed that a bed weight lower than 1.5 kg causes an early separation of particles from the central cone in inclined hole type as well as in three row vane type distributors. On the other hand, a bed weight higher than 2.0 kg causes spouting and slugging in single row vane type distributor. Based on these factors, 1.5 kg and 2.0 kg bed weights have been selected.

5.5.1 Behaviour of Single Row Vane type Distributor

Figure 5.5.1 compares the variation of bed pressure drop with superficial velocity for single row vane type distributor having vane angle $\theta = 15^{\circ}$ (SRVD15) with perforated plate distributor (PPD). In both the cases, the bed material used was 2 kg of coffee beans. The percentage area utilized in SRVD15 distributor was 64% while that for PPD was 100%. Accordingly, the static bed height for SRVD15 was 65 mm and that for conventional bed was 62 mm.

The velocity corresponding to the beginning of both wave and swirl motion in the bed was visually observed for SRVD and the corresponding velocities were identified as WS and SS respectively [Figure 5.5.1]. Approximate velocity for the onset of wave

motion in SRVD15 was 2.5 m/s and that for swirl motion was 3.2 m/s. It is also observed that, as superficial velocity increases, the swirl motion, which starts from the outer region of the bed, progresses towards the inner region.

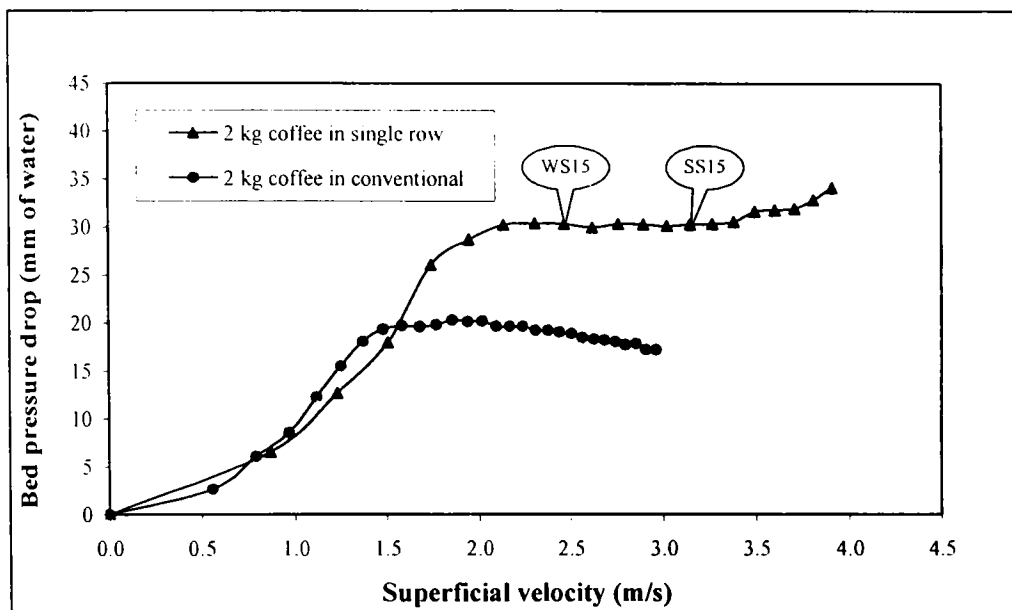


Figure 5.5.1 Comparison of the variation of bed pressure drop with superficial velocity in beds with single row vane type distributor having vane angle $\theta = 15^\circ$ and conventional distributor (bed material- 2 kg coffee beans)

In a conventional fluidized bed, slugging as well as formation of large bubbles has been observed when coffee beans were used. This is clearly the typical behaviour of conventional fluidized beds with Geldart D type particles.

Compared to the conventional bed, the bed pressure drop for SRVD15 is higher in the fluidized region (Figure 5.5.1) This difference in pressure drop is due to a higher bed height in SRVD15. Further, the bed pressure drop in SRVD15 is almost constant for superficial velocity ranging from about 2.2 m/s to 3.5 m/s and thereafter, a slight increase is seen. This increase in bed pressure drop is due to the combined effect of particle-wall friction and vortex formation. It was observed that when the velocity was increased beyond 3.5 m/s, particles separated from the cone at the centre of the

distributor and air bypasses through an annulus at the inner region of the bed. For conventional bed, the bed pressure drop decreases when the superficial velocity is increased beyond about 2 m/s. This behaviour is due to the formation of large bubbles.

A typical case of particle separation and the corresponding phenomena of air bypassing at higher superficial velocity in SRVD15 is shown in figure 5.5.2. It is clear that the particle separation starts from the cone at the center. The bed particle used in this case was 2.0 kg coffee beans.

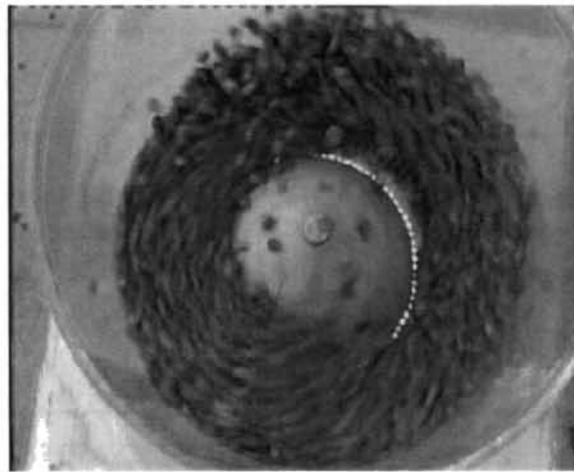


Figure 5.5.2 Single row vane type distributor showing separation of particles from the cone

Experiments were also carried out to study the variation of bed pressure drop with superficial velocity using a different bed particle (pepper), as well as with different distributor vane angle (20°). The results of this study can be compared similar to that in figure 5.5.1 and these details are presented in figures 5.5.3 to 5.5.5.

In conventional fluidized bed, the bed pressure drop increases with superficial velocity in the packed bed region and reaches a maximum value at the minimum fluidizing velocity (U_{mf}). An increase in the superficial velocity above U_{mf} does not result in an increase in bed pressure drop. In the case of swirling beds with single

row vane type distributors, up to the formation of the wave motion, the variation of bed pressure drop is similar to that of the conventional bed.

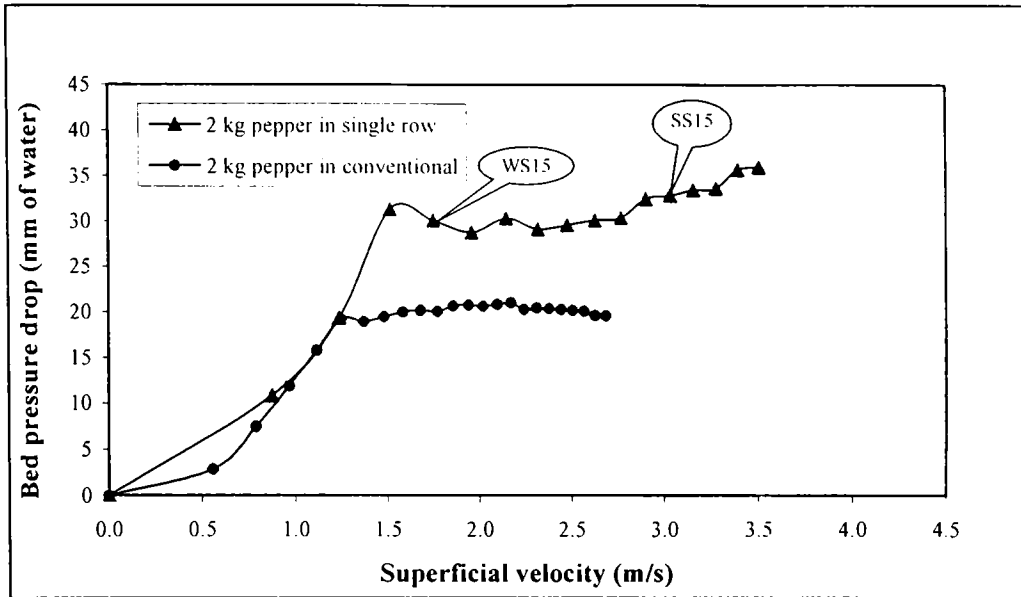


Figure 5.5.3 Comparison of the variation of bed pressure drop with superficial velocity in beds with single row vane type distributor having vane angle $\theta = 15^{\circ}$ and conventional distributor (bed material- 2 kg pepper)

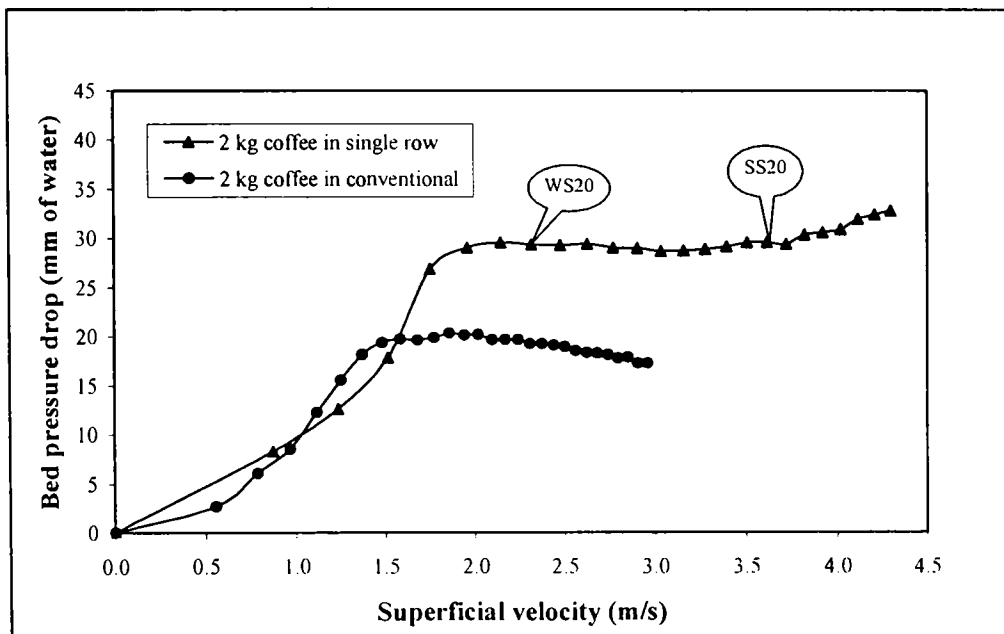


Figure 5.5.4 Comparison of the variation of bed pressure drop with superficial velocity in beds with single row vane type distributor having vane angle $\theta = 20^{\circ}$ and conventional distributor (bed material- 2 kg coffee beans)

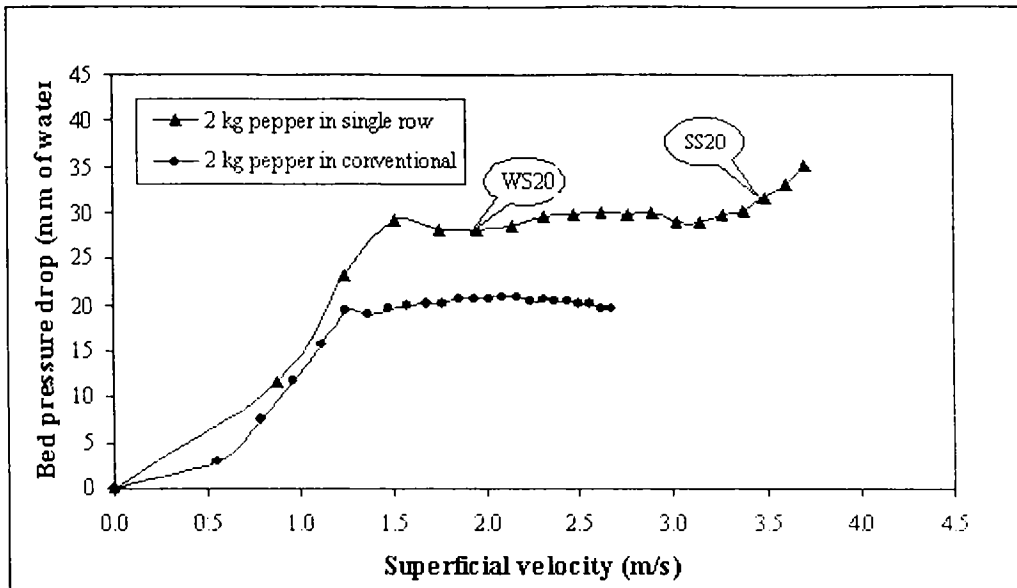


Figure 5.5.5 Comparison of the variation of bed pressure drop with superficial velocity in beds with single row vane type distributor having vane angle $\theta = 20^\circ$ and conventional distributor (bed material-2 kg pepper)

In the wave region, the bed pressure drop is almost constant over the initial region and it increases towards the end. In the swirl region, however, the bed pressure drop increases with an increase in the superficial velocity.

The influence of bed weight on bed pressure drop is compared in figures 5.5.6 to 5.5.9 for two bed weights, namely 2.0 kg and 1.5 kg in SRVD15 and SRVD20 with two types of particles (coffee beans and pepper).

For single row vane type distributor with a bed weight of 1.5 kg, as the superficial velocity is further increased after swirling, lifting of particles from the distributor was observed near the central cone at a certain velocity. The point corresponding to the starting of the lifting of particles from the distributor observed is identified as LS in the case of SRVD. For a bed weight of 2.0 kg, the lifting of particles could not be clearly observed due to a higher bed height.

It can be observed from figures 5.5.6 to 5.5.9 that, the superficial velocity corresponding to the starting of wave and swirl motion is independent of the bed

weight considered (1.5 kg and 2.0 kg).

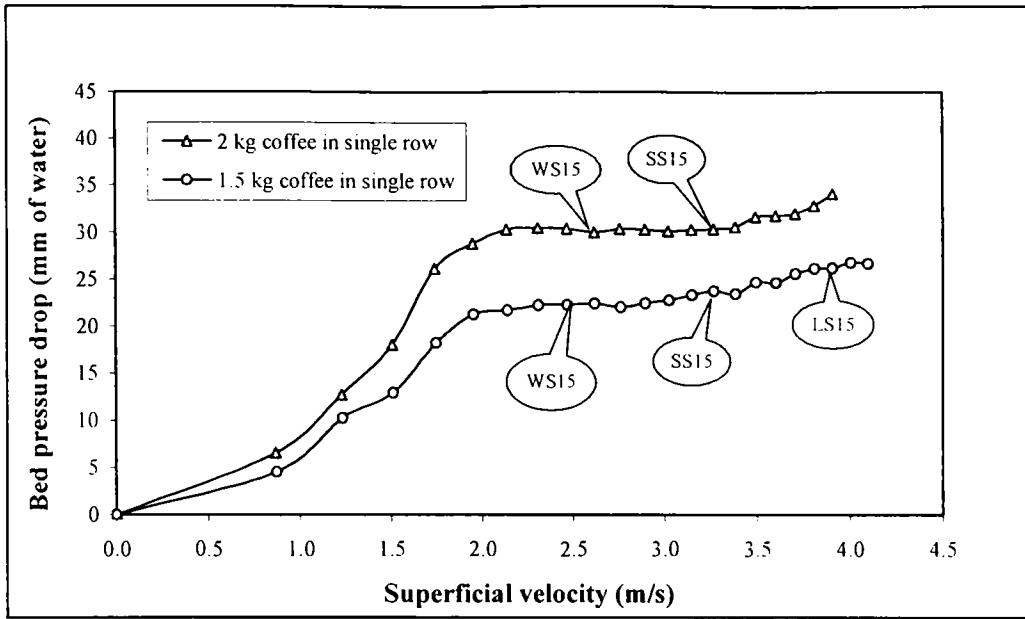


Figure 5.5.6 Effect of bed weight in beds with single row vane type distributor having vane angle $\theta = 15^\circ$ (bed material – coffee beans)

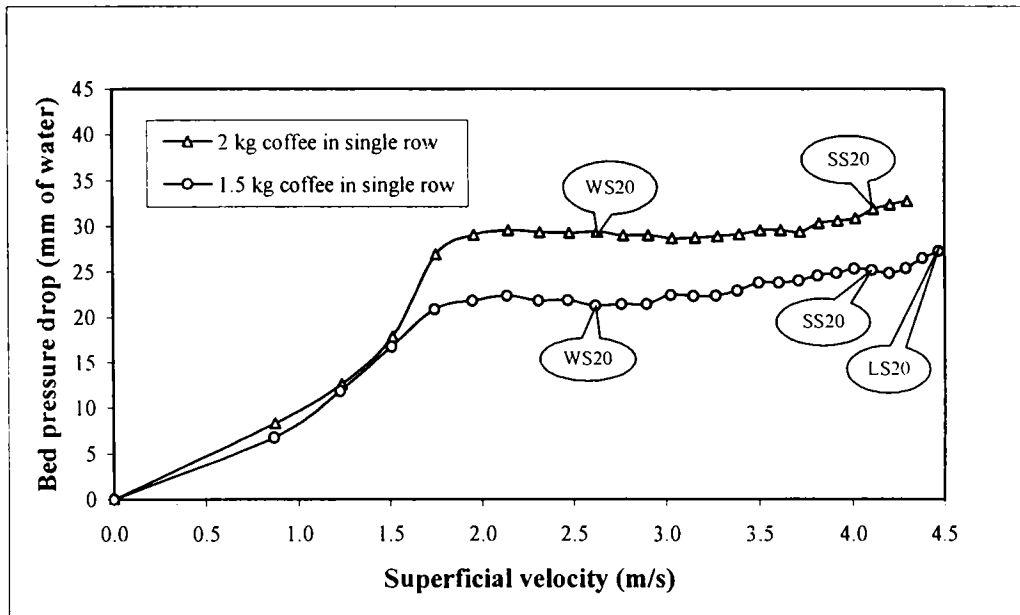


Figure 5.5.7 Effect of bed weight in beds with single row vane type distributor having vane angle $\theta = 20^\circ$ (bed material – coffee beans)

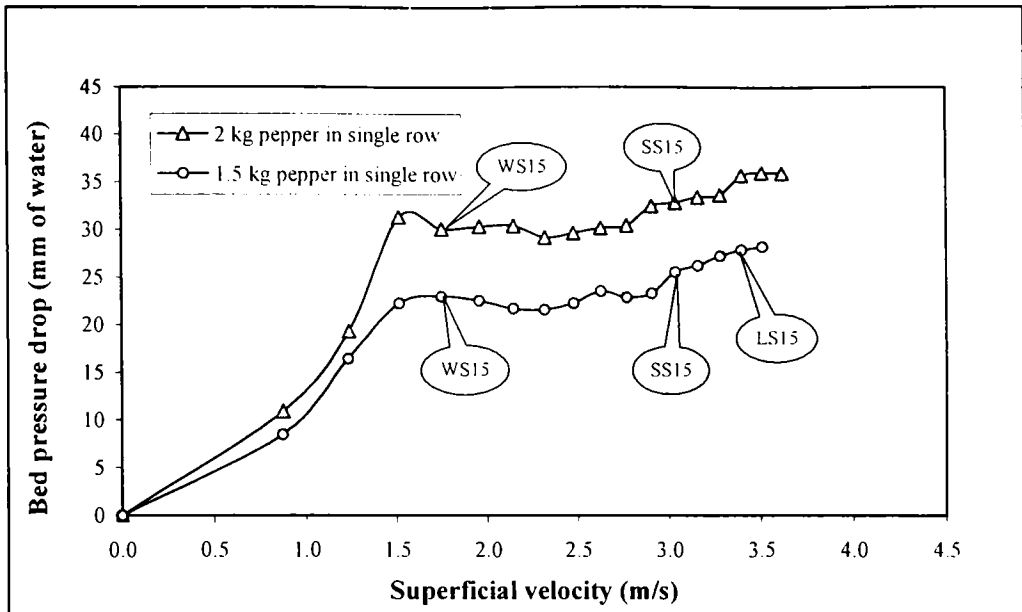


Figure 5.5.8 Effect of bed weight in beds with single row vane type distributor having vane angle $\theta = 15^\circ$ (bed material – pepper)

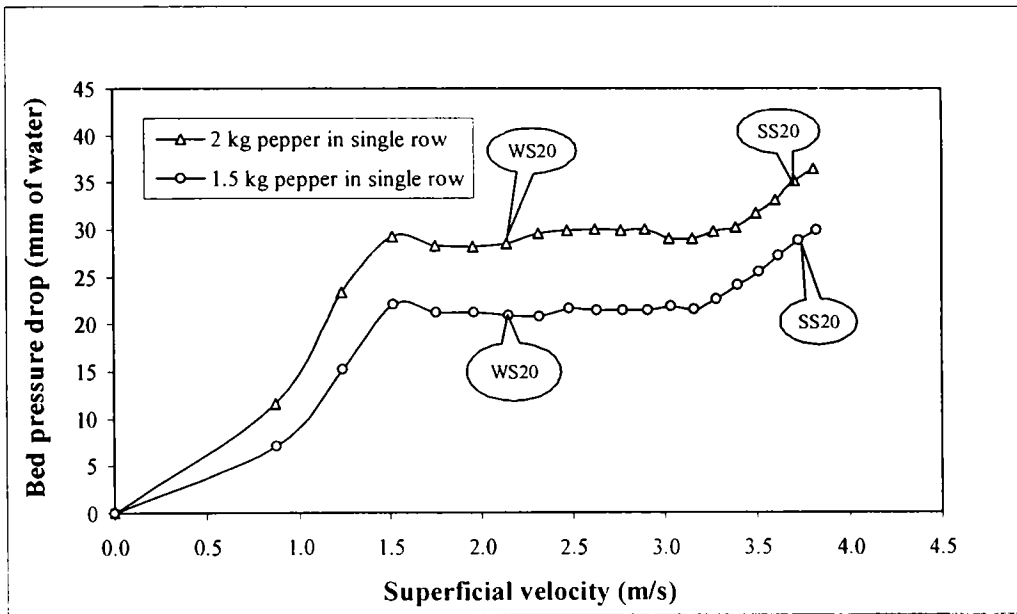


Figure 5.5.9 Effect of bed weight in beds with single row vane type distributor having vane angle $\theta = 20^\circ$ (bed material – pepper)

For single row vane type distributor with a bed weight of 1.5 kg, as the superficial velocity is further increased after swirling, lifting of particles from the distributor was observed near the central cone at a certain velocity. The point corresponding to the

starting of the lifting of particles from the distributor observed is identified as LS in the case of SRVD. For a bed weight of 2.0 kg, the lifting of particles could not be clearly observed due to a higher bed height.

It can be observed from figures 5.5.6 to 5.5.9 that, the superficial velocity corresponding to the starting of wave and swirl motion is independent of the bed weight considered (1.5 kg and 2.0 kg).

Figures 5.5.10 to 5.5.13 compares the effect of vane angle on the variation of bed pressure drop for single row vane type distributors.

The swirl motion starts at an early superficial velocity in the case of lower vane angle. Once the swirl motion starts, with an increase in superficial velocity, the rate of increase in bed pressure drop is more for a lower vane angle. For a given mass flow rate of air, the horizontal component of the momentum of air coming out of the distributor is more with a lower vane angle.

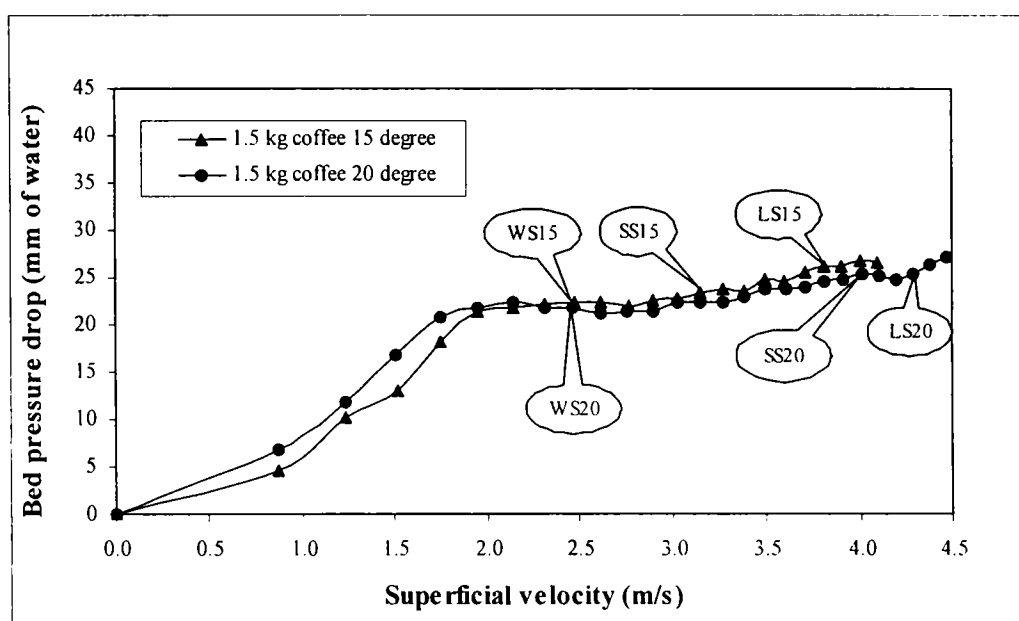


Figure 5.5.10 Comparison of the variation of bed pressure drop with superficial velocity between 15⁰ and 20⁰ single row vane type distributors (bed material -1.5 kg coffee beans)

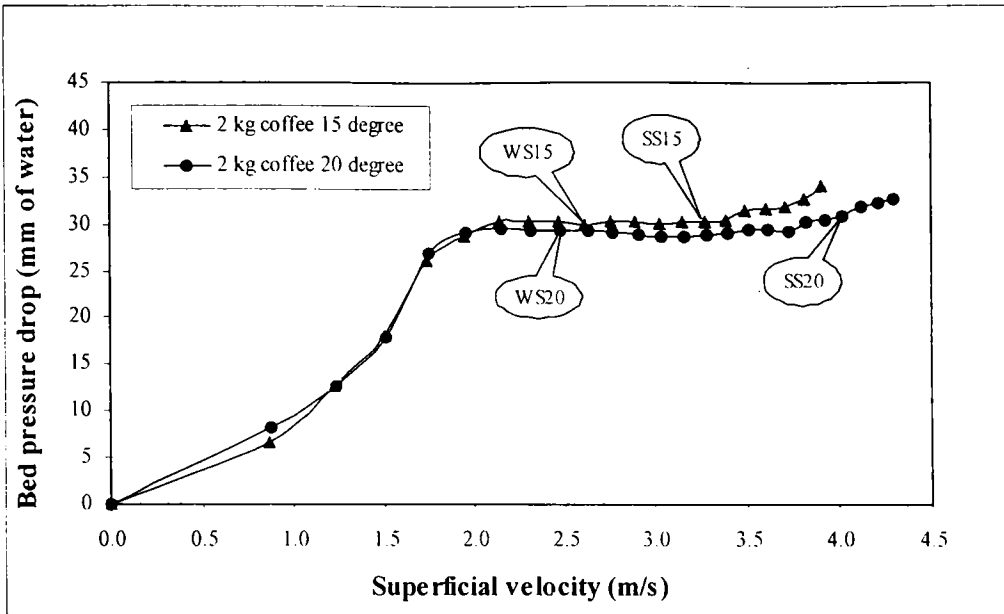


Figure 5.5.11 Comparison of the variation of bed pressure drop with superficial velocity between 15⁰ and 20⁰ single row vane type distributors (bed material –2.0 kg coffee beans)

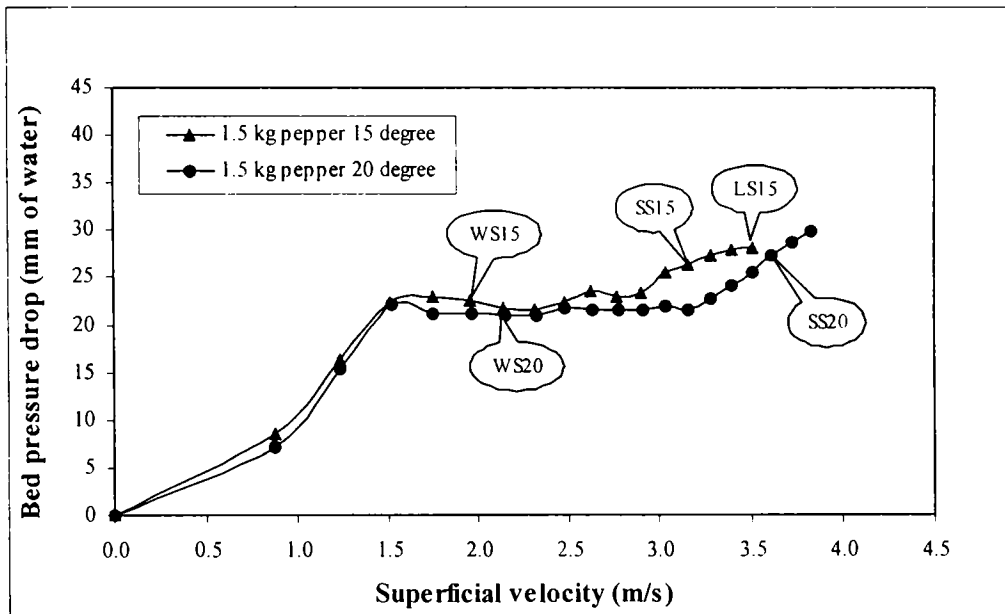


Figure 5.5.12 Comparison of the variation of bed pressure drop with superficial velocity between 15⁰ and 20⁰ single row vane type distributors (bed material –1.5 kg pepper)

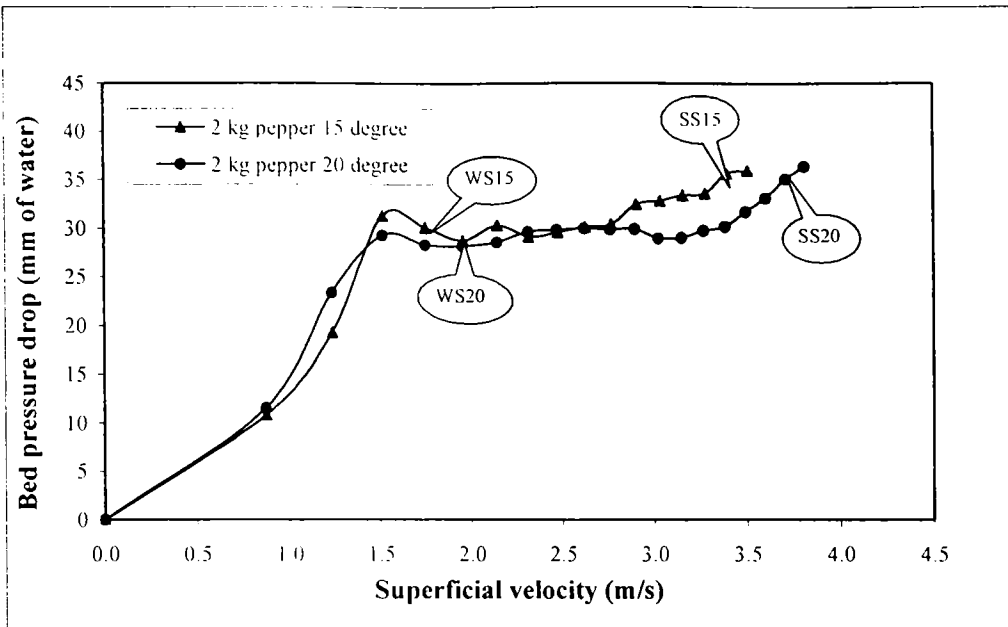


Figure 5.5.13 Comparison of the variation of bed pressure drop with superficial velocity between 15⁰ and 20⁰ single row vane type distributors (bed material –2.0 kg pepper)

A higher horizontal momentum causes higher swirl velocity in the bed, which results in an increase in the particle-wall friction. Further, with an increase in swirl velocity in the bed, the bed height at the outer periphery will be increased due to the movement of particles from the inner region to the outer region. The combined effect of particle-wall friction and increase in the bed height at the outer periphery causes a higher bed pressure drop.

5.5.2 Behaviour of Inclined Hole Type Distributor

Inclined hole type distributors (IHD) designed has higher percentage useful area of the distributor compared to single row vane type distributor. For the distributor considered, the useful distributor area of IHD is 94 % while that for SRVD is 64 %. The percentage area of opening for inclined hole type distributor with 15⁰ and 20⁰ hole angles is 3 % and 5 % respectively. On the other hand, the percentage area of

opening of single row vane type distributor with corresponding vane angles is 19 % and 25 % respectively.

Unlike single row vane type distributors, no wave motion was observed in inclined hole type distributors. For a given superficial velocity, the mass flow rate is higher in IHD compared to SRVD due the higher percentage useful area of the distributor in IHD. Further, for a given mass flow rate, the momentum of air coming out of the distributor is more in IHD due to a lower percentage area of opening in IHD compared to SRVD. Hence, even at the minimum fluidization velocity, the air coming out of the IHD attains a momentum sufficient to cause swirl motion. It could be further observed that, as superficial velocity increases, swirl motion, which starts from the inner radius of the bed, progresses towards the outer radius.

Figure 5.5.14 compares the variation of bed pressure drop with superficial velocity in the case of IHD15 for two different bed weights (2 kg and 1.5 kg coffee beans).

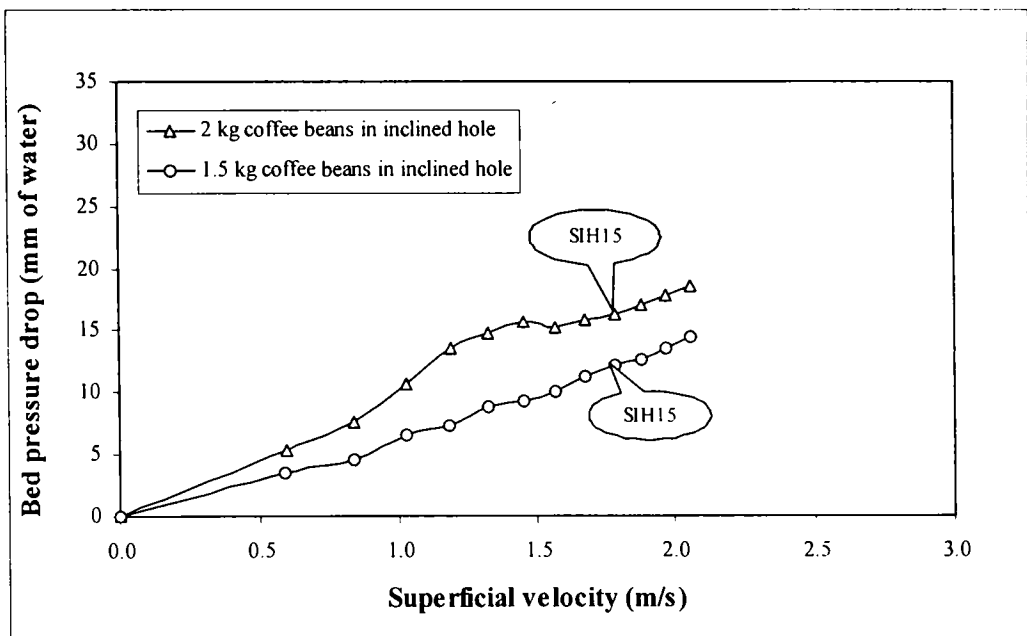


Figure 5.5.14 Effect of bed weight in inclined hole –type distributor having vane angle $\theta = 15^\circ$ (bed material – coffee beans)

The superficial velocity corresponding to the start of swirl is identified as SIH in this figure. As expected, the SIH value is the same for both bed weights. The bed pressure drop increases with increase in superficial velocity for IHD as seen in figure 5.5.14. Hence the minimum fluidizing velocity could not be clearly established experimentally in the case of IHD.

A similar study has been carried out by changing the bed particle to pepper as well as by changing to the distributor with a hole angle of 20° and the above discussion is applicable in these cases also. The comparison similar to that given in figure 5.5.14 is presented in figures 5.5.15 to 5.5.17.

From figures 5.5.14 to 5.5.17, it can be stated that, in general, the rate of increase in the variation of bed pressure drop increases with an increase in the superficial velocity in swirl region. Further, the rate of increase in the variation of bed pressure drop is higher for a lower bed weight.

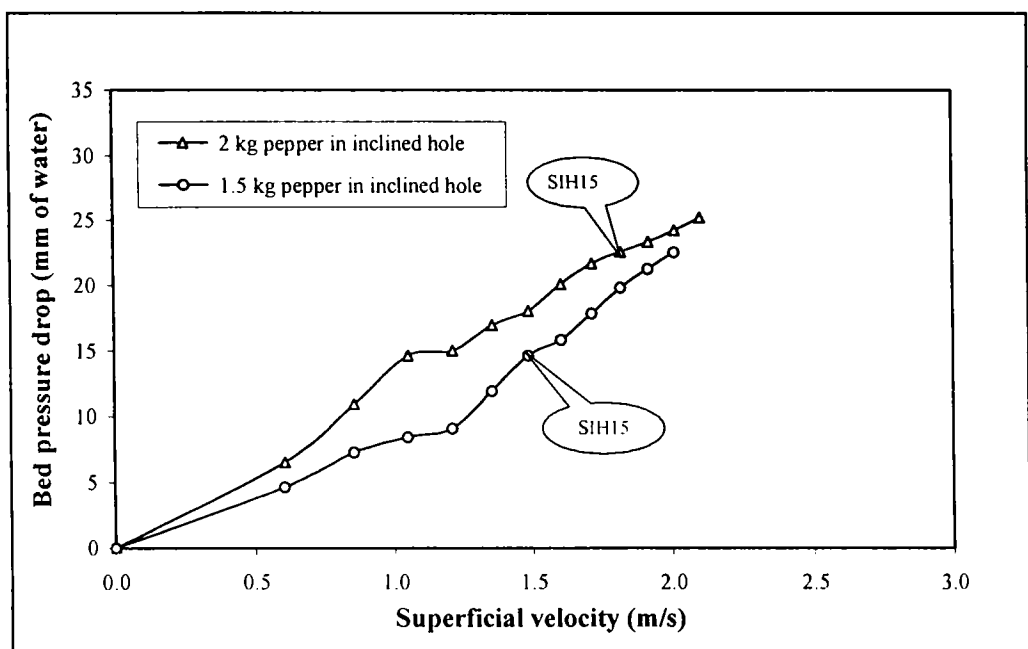


Figure 5.5.15 Effect of bed weight in inclined hole –type distributor having vane angle $\theta = 15^\circ$ (bed material – pepper)

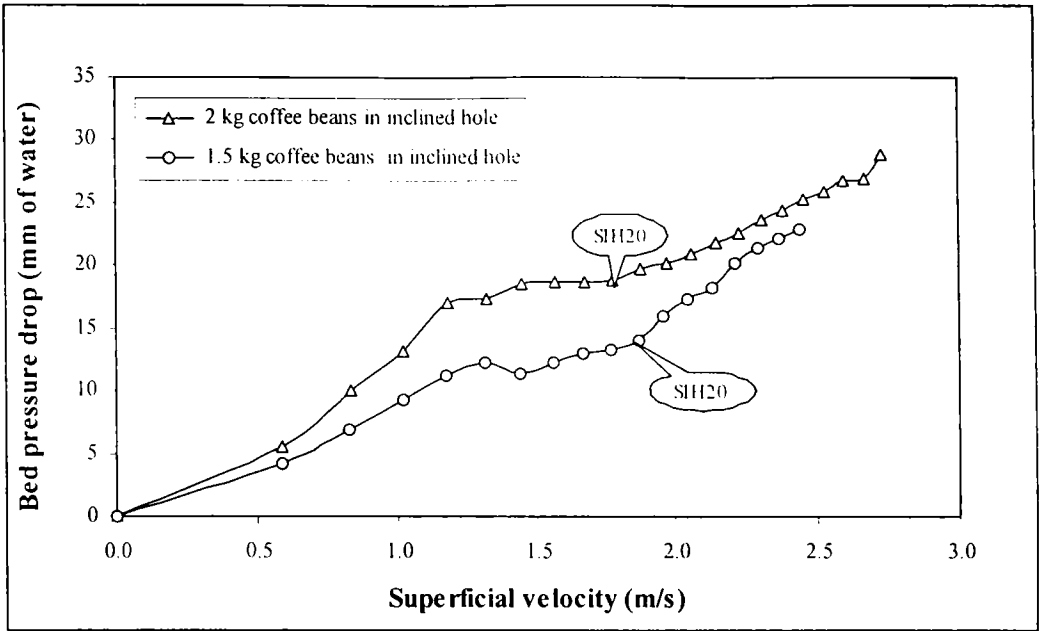


Figure 5.5.16 Effect of bed weight in inclined hole –type distributor having vane angle $\theta = 20^{\circ}$ (bed material – coffee beans)

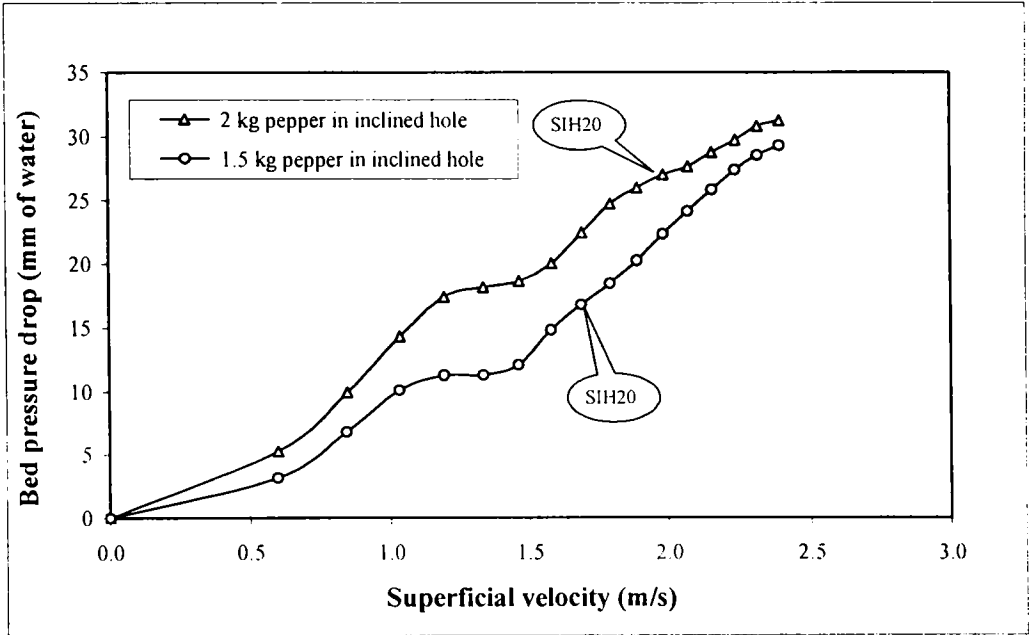


Figure 5.5.17 Effect of bed weight in inclined hole –type distributor having vane angle $\theta = 20^{\circ}$ (bed material – pepper)

A typical case of particle separation and the corresponding phenomenon of air bypassing at higher superficial velocity in IHD20 is shown in figure 5.5.18. The bed particle used in this case was 1.5 kg pepper.

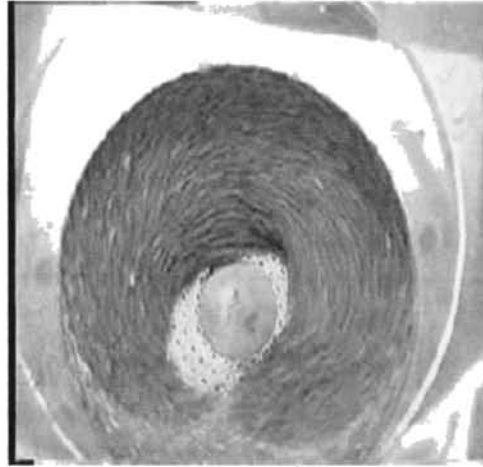


Figure 5.5.18 Inclined hole type distributor showing bypassing of air

5.5.3 Behaviour of Three Row Vane type Distributor

The three row vane type distributors (TRVD) designed have 91 percentage useful area. The percentage area of opening for TRVD with 15° and 20° vane angles is 17 % and 22 % respectively.

When the superficial velocity was increased within the swirl region, lifting of the bed was observed in TRVD for both 1.5 kg and 2.0 kg bed weight. Further, the lifting from the distributor was more at the inner radius, where the phenomenon of particle lifting started.

Figure 5.5.19 compares the variation of bed pressure drop with superficial velocity for three row vane type distributor having vane angle $\theta = 15^{\circ}$ (TRVD15) with perforated plate distributor (conventional). In both cases, the bed material used was 2 kg of coffee beans. The superficial velocity corresponding to the beginning of wave motion, swirl motion and lifting of the bed has been identified as WT, ST and LT respectively in the case of TRVD.

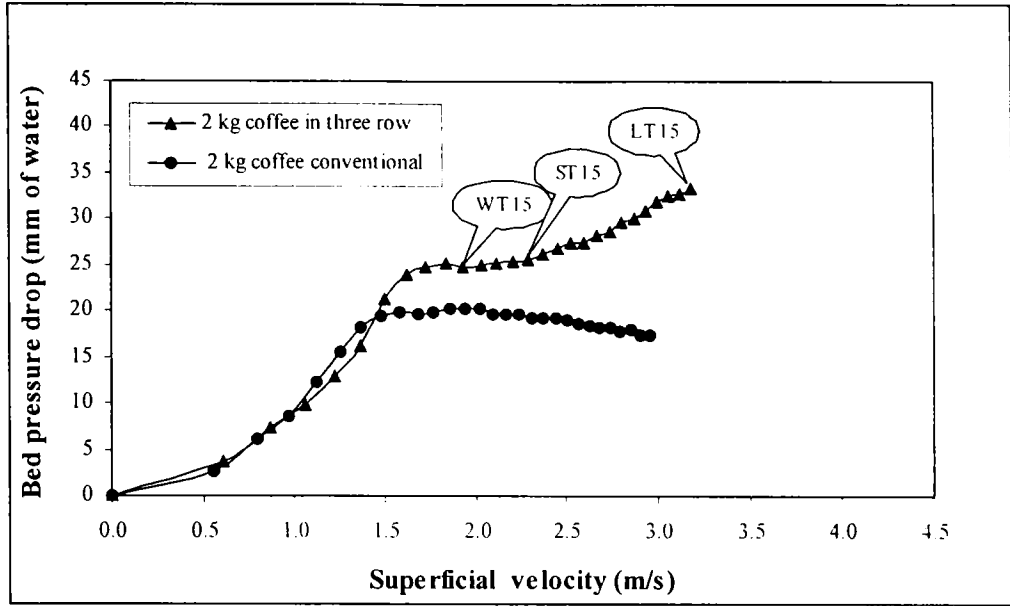


Figure 5.5.19 Comparison of the variation of bed pressure drop with superficial velocity in three row vane type distributor having vane angle $\theta = 15^\circ$ and conventional distributor (bed material- 2 kg coffee beans)

A similar study has been carried out by changing the bed particle to pepper as well as by changing the distributor with a 20° vane angle. A comparison similar to that given in figure 5.5.19 is presented in figures 5.5.20 to 5.5.22.

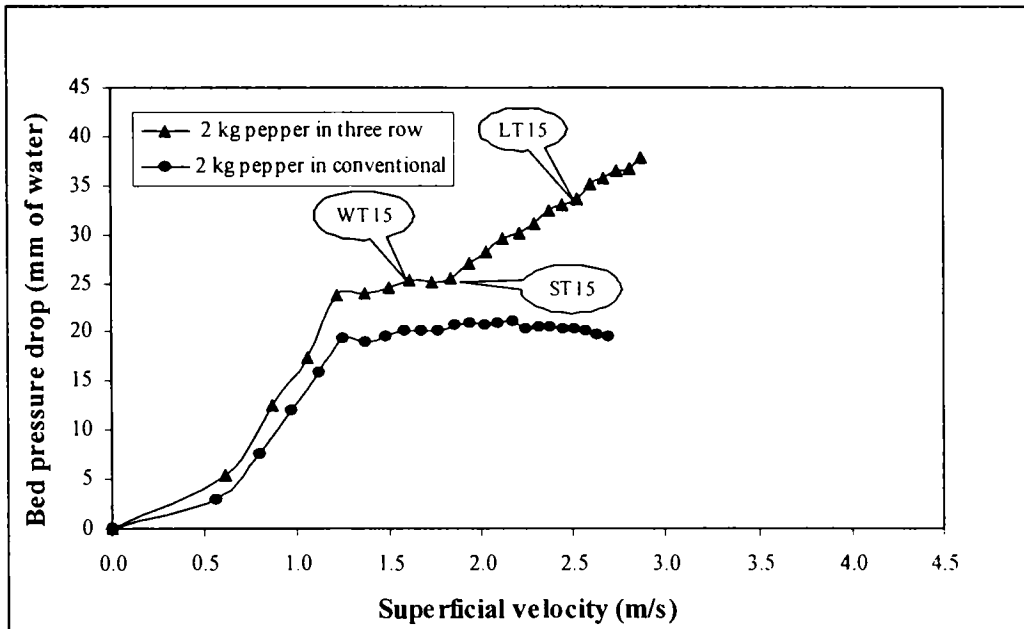


Figure 5.5.20 Comparison of the variation of bed pressure drop with superficial velocity in three row vane type distributor having vane angle $\theta = 15^\circ$ and conventional distributor (bed material- 2 kg pepper)

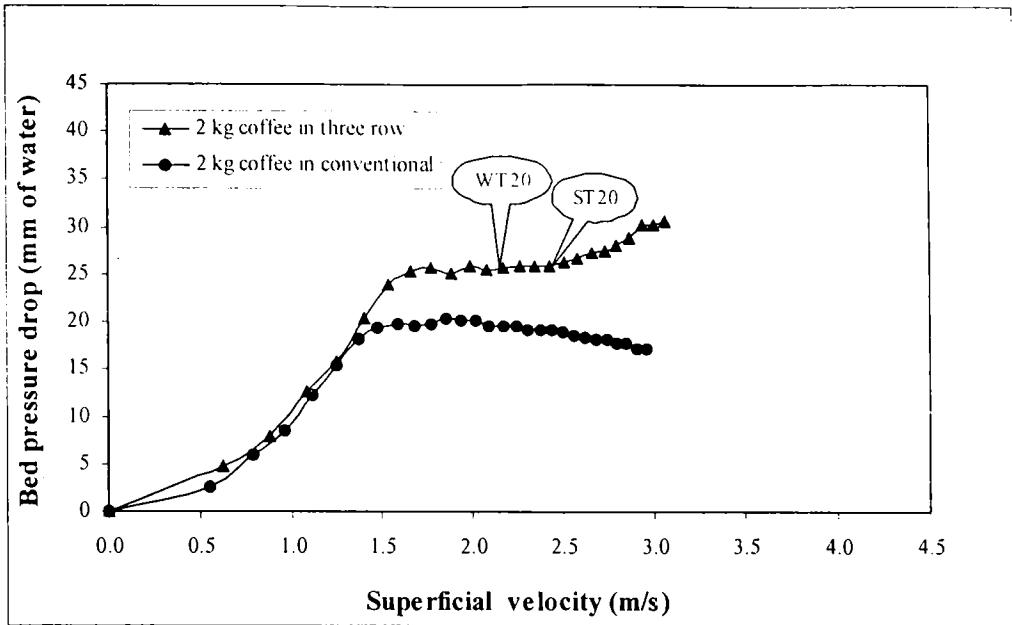


Figure 5.5.21 Comparison of the variation of bed pressure drop with superficial velocity in three row vane type distributor having vane angle $\theta = 20^\circ$ and conventional distributor (bed material- 2 kg coffee beans)

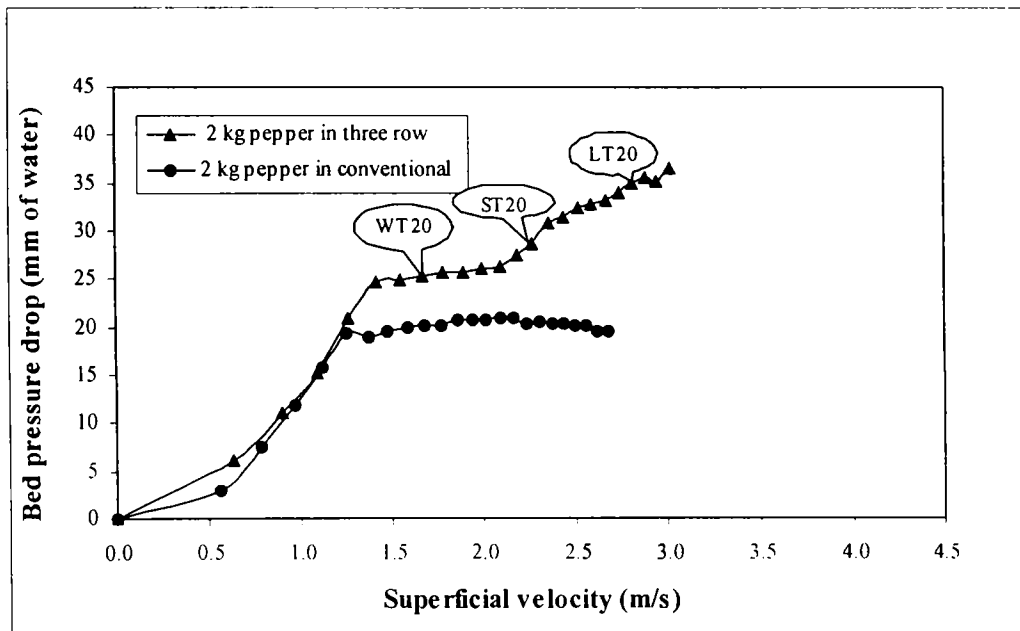


Figure 5.5.22 Comparison of the variation of bed pressure drop with superficial velocity in three row vane type distributor having vane angle $\theta = 20^\circ$ and conventional distributor (bed material- 2 kg pepper)

The general behaviour of the variation of bed pressure drop with superficial velocity of TRVD is similar to that of SRVD. Between the wave and swirl motions, the bed pressure drop is almost constant over the initial region and it increases towards the end. In the swirl region, however, the bed pressure drop increases with an increase in the superficial velocity.

The influence of bed weight in bed pressure drop is compared in figures 5.5.23 to 5.5.26 for two bed weights, namely 2.0 kg and 1.5 kg in TRVD 15 and TRVD 20 with two types of particles (coffee beans and pepper).

The general behaviour of the variation of bed pressure drop with superficial velocity is similar for both the bed weights considered (Figures 5.5.23 to 5.5.26). The superficial velocity corresponding to the starting of wave and swirl motion as well as lifting of particles is almost the same for both the bed weights considered. This shows that for bed weights above 1.5 kg, the above phenomena in the swirling fluidized bed are independent of bed weight.

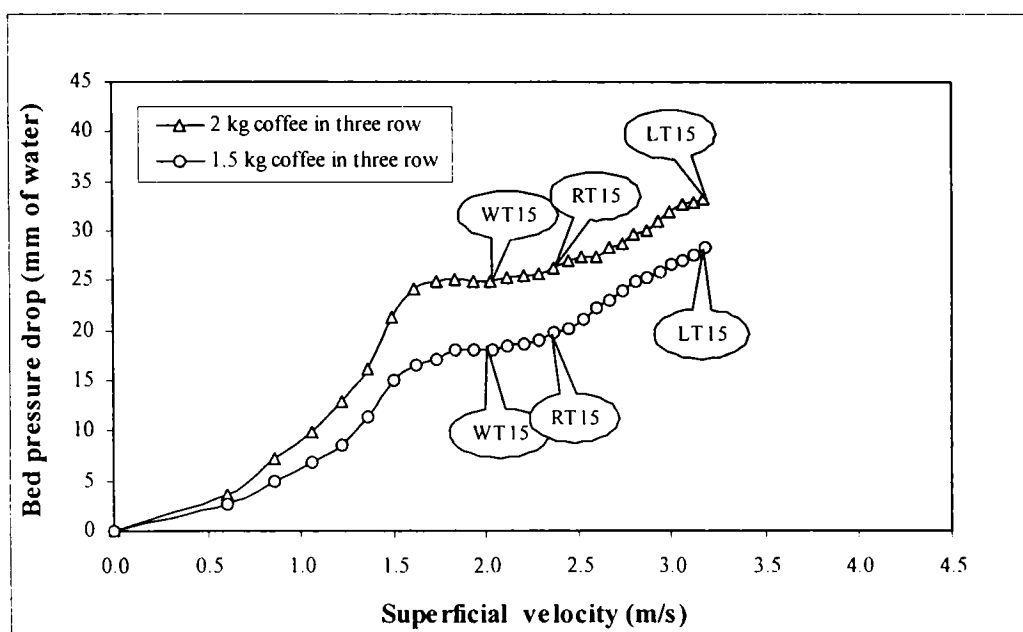


Figure 5.5.23 Effect of bed weight on bed pressure drop in three row vane type distributor having vane angle $\theta = 15^\circ$ (bed material – coffee beans)

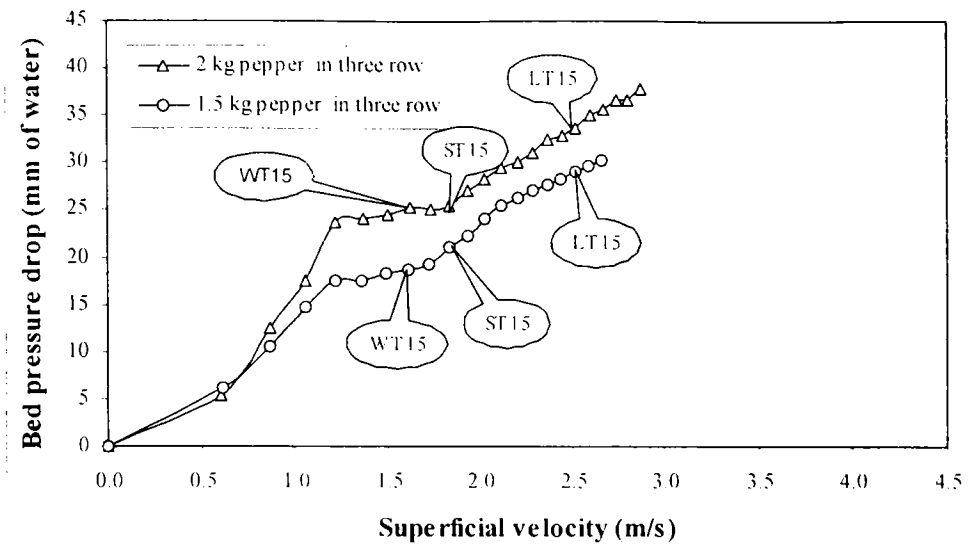


Figure 5.5.24 Effect of bed weight on bed pressure drop in three row vane type distributor having vane angle $\theta = 15^{\circ}$ (bed material – pepper)

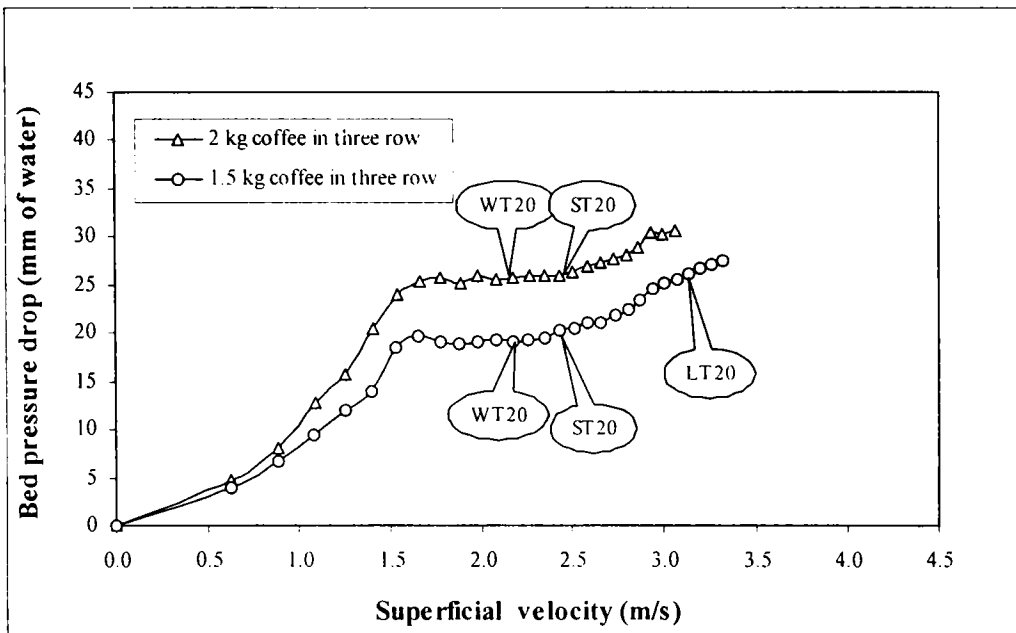


Figure 5.5.25 Effect of bed weight on bed pressure drop in three row vane type distributor having vane angle $\theta = 20^{\circ}$ (bed material – coffee beans)

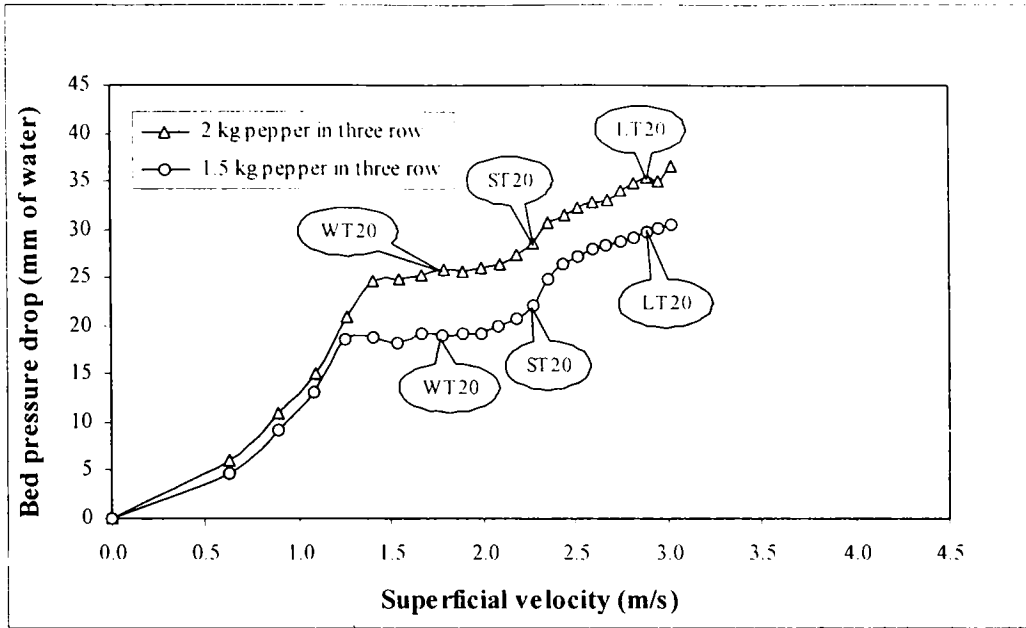


Figure 5.5.26 Effect of bed weight on bed pressure drop in three row vane type distributor having vane angle $\theta = 20^\circ$ (bed material – pepper)

Figure 5.5.27 to 5.5.30 compares the effect of change in vane angle on the variation of bed pressure drop in the case of three row vane type distributors. Once swirl motion starts, the rate of increase of bed pressure drop is more for a lower vane angle. A similar behaviour was observed in the case of single row vane type distributor also.

Figures 5.5.31 to 5.5.34 compares the variation of bed pressure drop with superficial velocity of single row and three row vane type distributors with a vane angle of 15° . Coffee beans and pepper with 1.5 kg as well as 2.0 kg bed weights were considered for the comparison. A similar comparison with a vane angle of 20° is presented in figures 5.5.35 to 5.5.38.

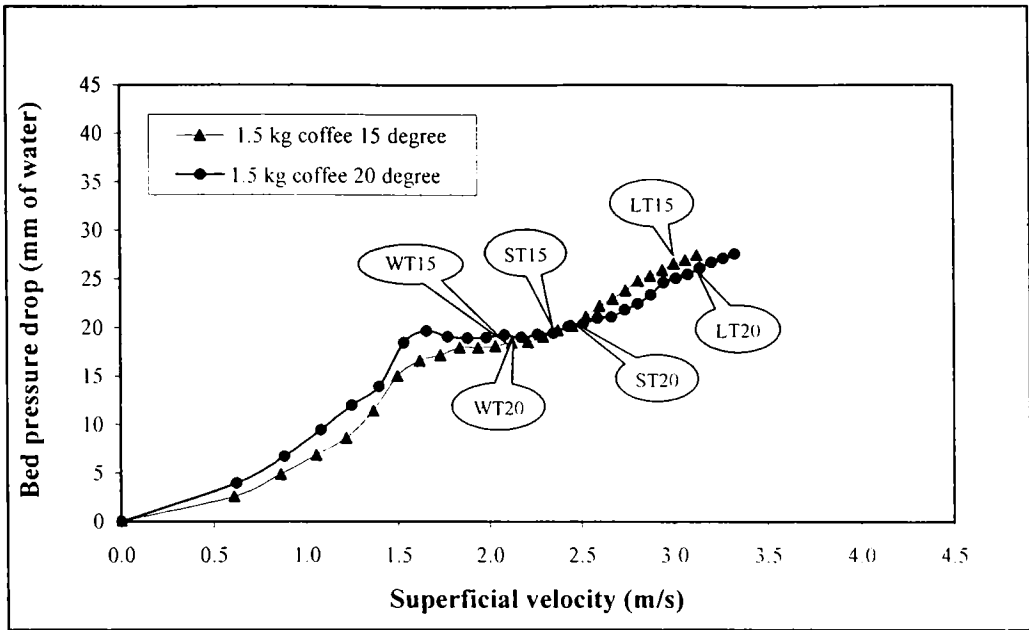


Figure 5.5.27 Comparison of the variation of bed pressure drop with superficial velocity between 15° and 20° three row vane type distributors (bed material –1.5 kg coffee beans)

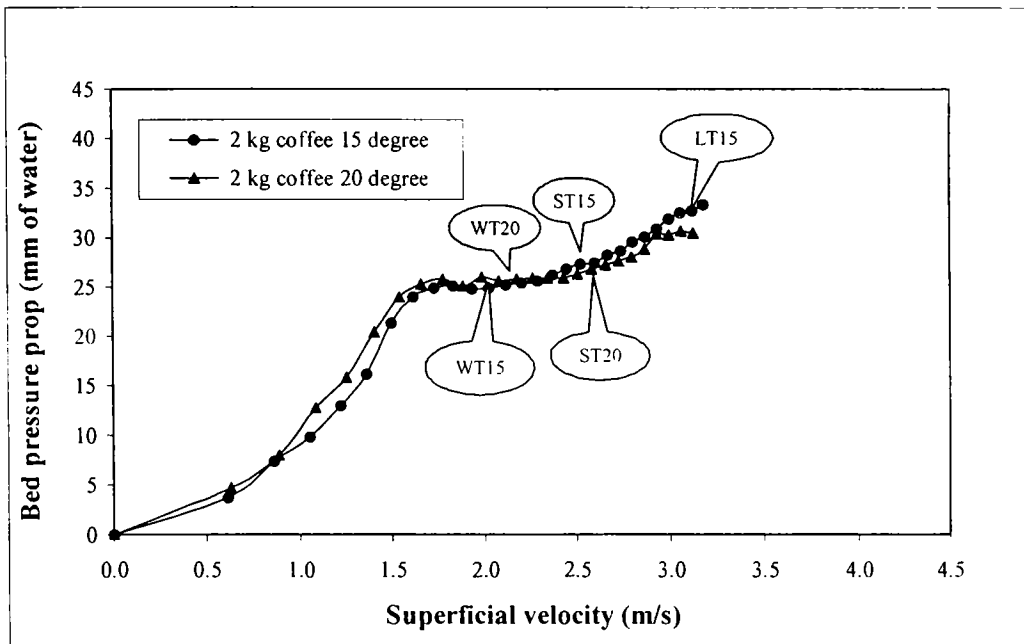


Figure 5.5.28 Comparison of the variation of bed pressure drop with superficial velocity between 15° and 20° three row vane type distributors (bed material –2.0 kg coffee beans)

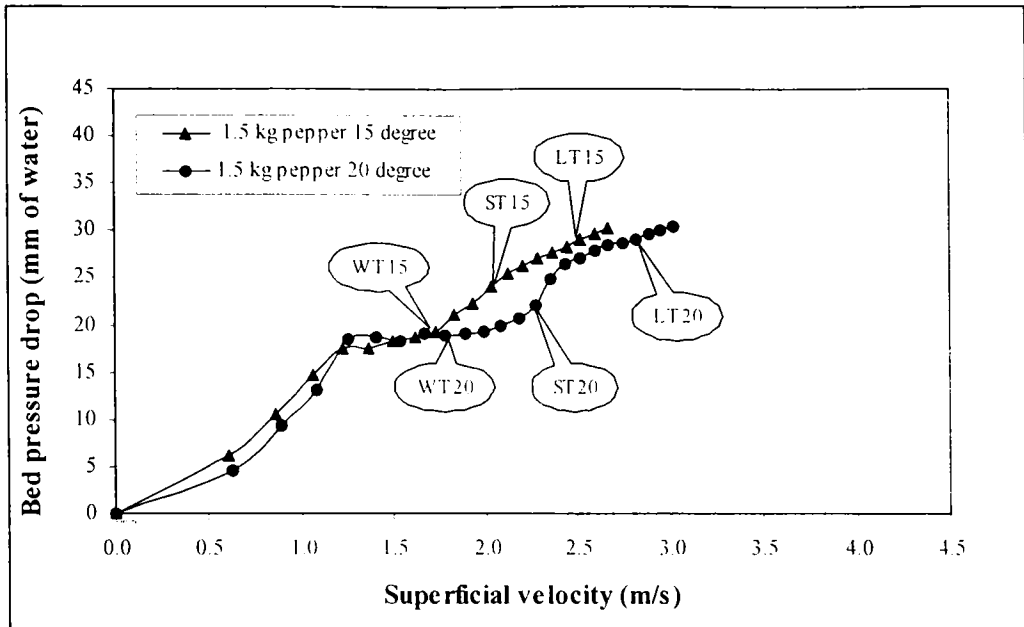


Figure 5.5.29 Comparison of the variation of bed pressure drop with superficial velocity between 15° and 20° three row vane type distributors (bed material –1.5 kg pepper)

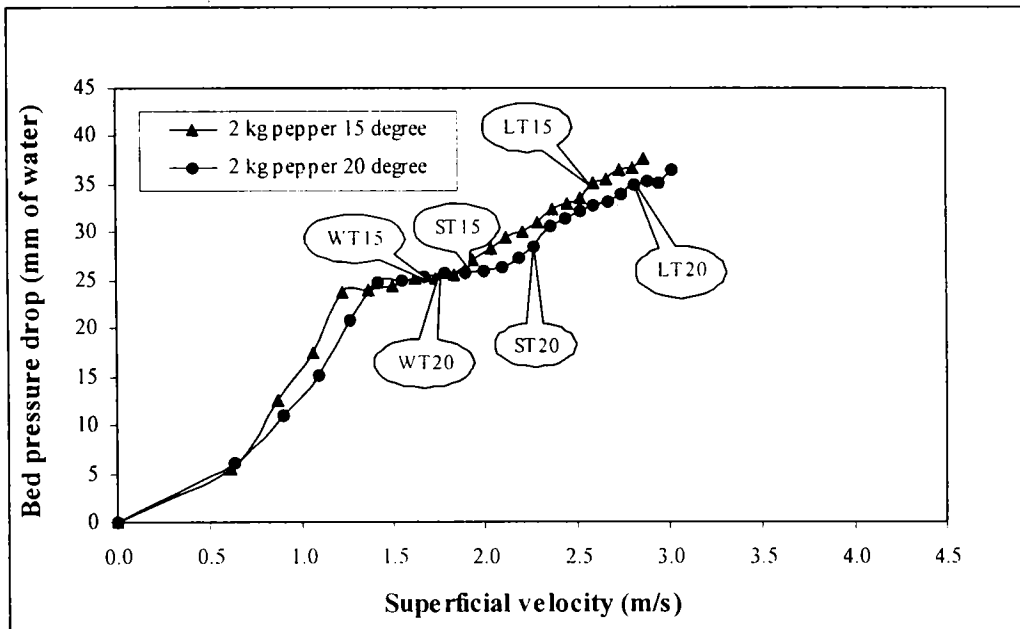


Figure 5.5.30 Comparison of the variation of bed pressure drop with superficial velocity between 15° and 20° three row vane type distributors (bed material –2.0 kg pepper)

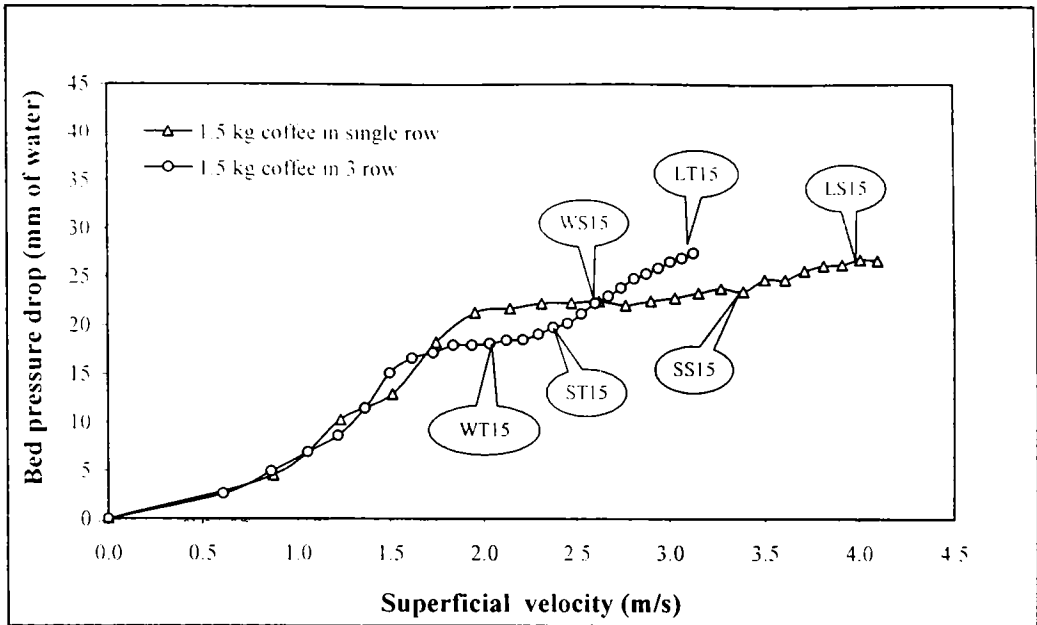


Figure 5.5.31 Comparison of the variation of bed pressure drop with superficial velocity between single row and three row vane type distributors with vane angle 15° (bed material–1.5 kg coffee beans)

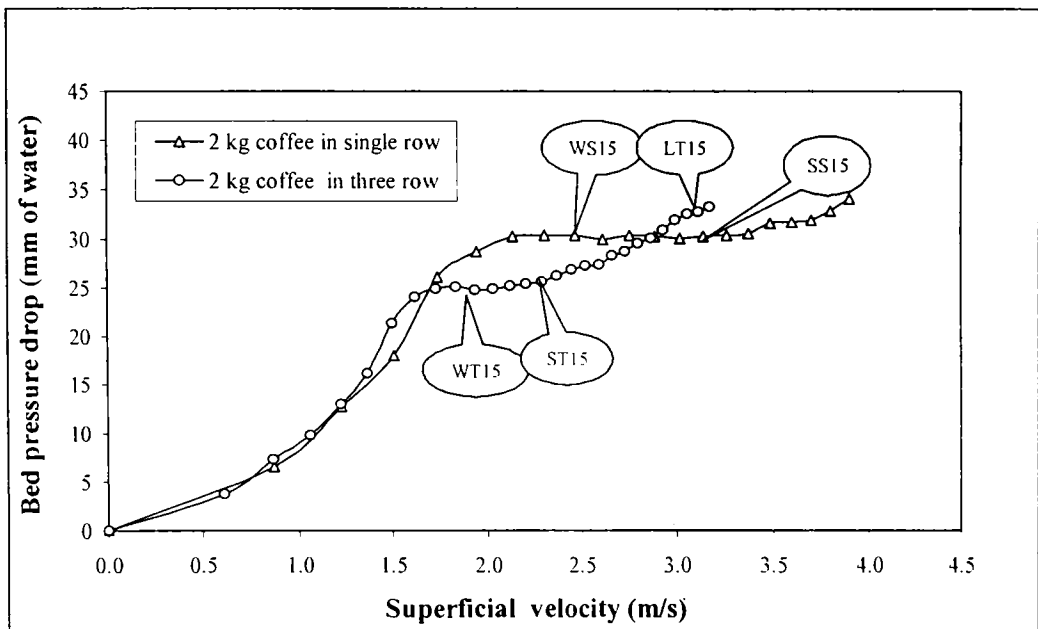


Figure 5.5.32 Comparison of the variation of bed pressure drop with superficial velocity between single row and three row vane type distributors with vane angle 15° (bed material –2.0 kg coffee beans)

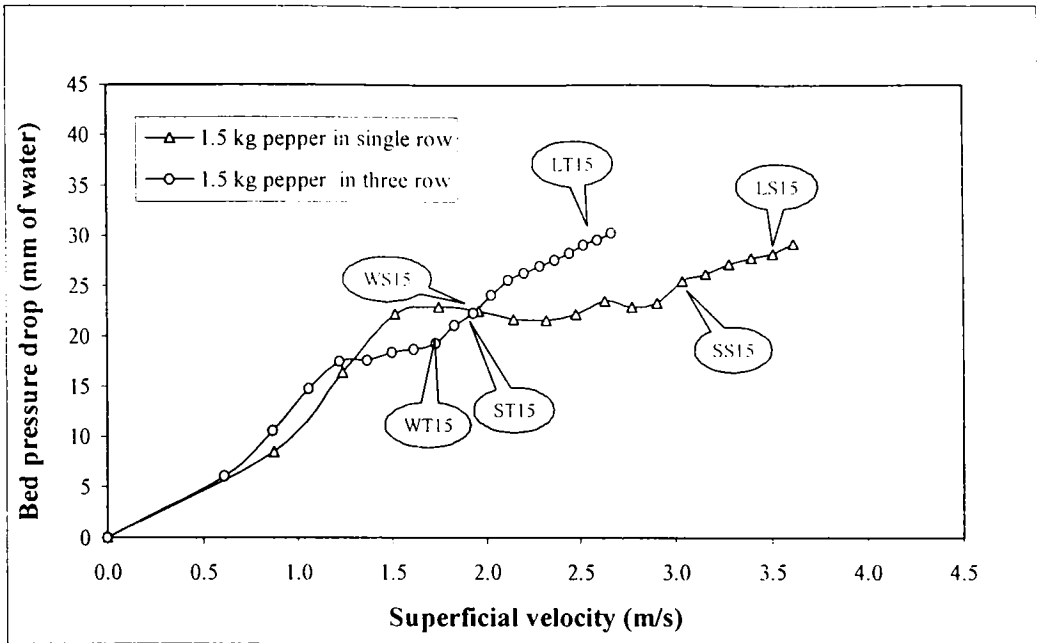


Figure 5.5.33 Comparison of the variation of bed pressure drop with superficial velocity between single row and three row vane type distributors with vane angle 15° (bed material –1.5 kg pepper)

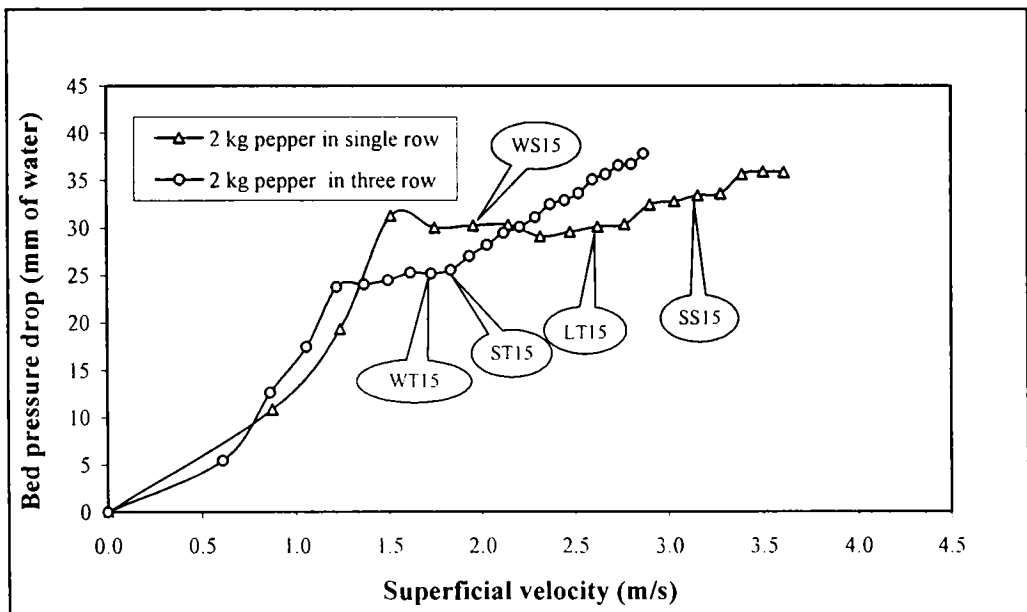


Figure 5.5.34 Comparison of the variation of bed pressure drop with superficial velocity between single row and three row vane type distributors with vane angle 15° (bed material –2.0 kg pepper)

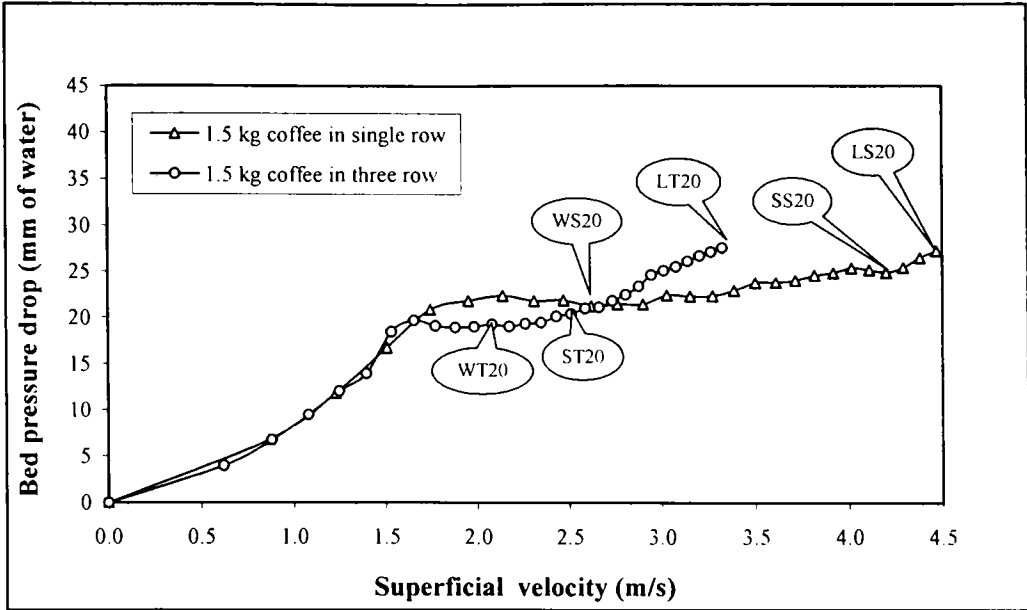


Figure 5.5.35 Comparison of the variation of bed pressure drop with superficial velocity between single row and three row vane type distributors with vane angle 20° (bed material –1.5 kg coffee beans)

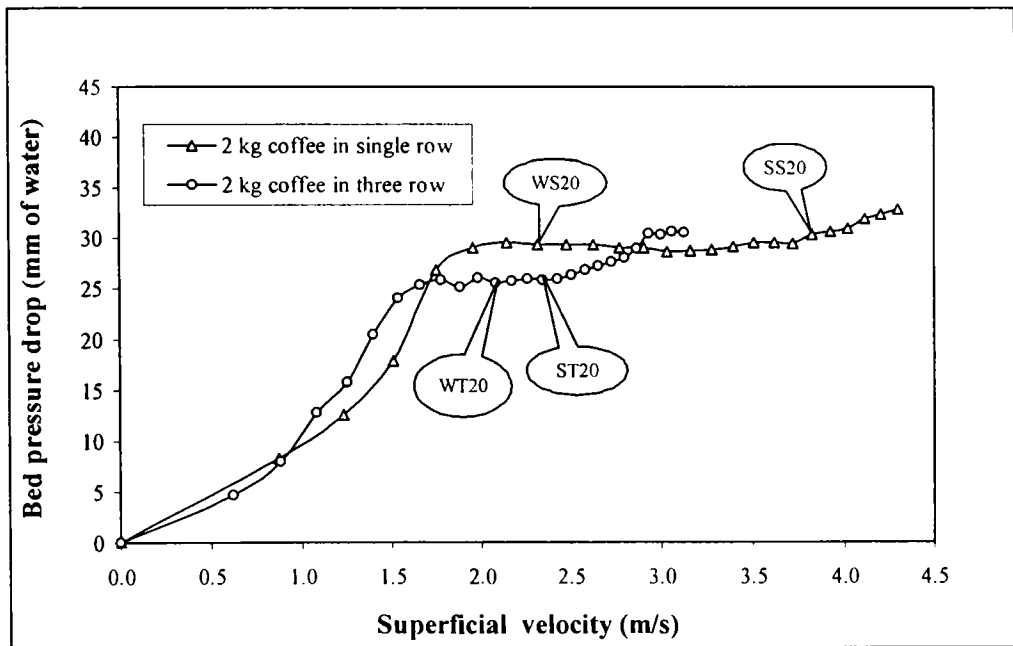


Figure 5.5.36 Comparison of the variation of bed pressure drop with superficial velocity between single row and three row vane type distributors with vane angle 20° (bed material –2.0 kg coffee beans)

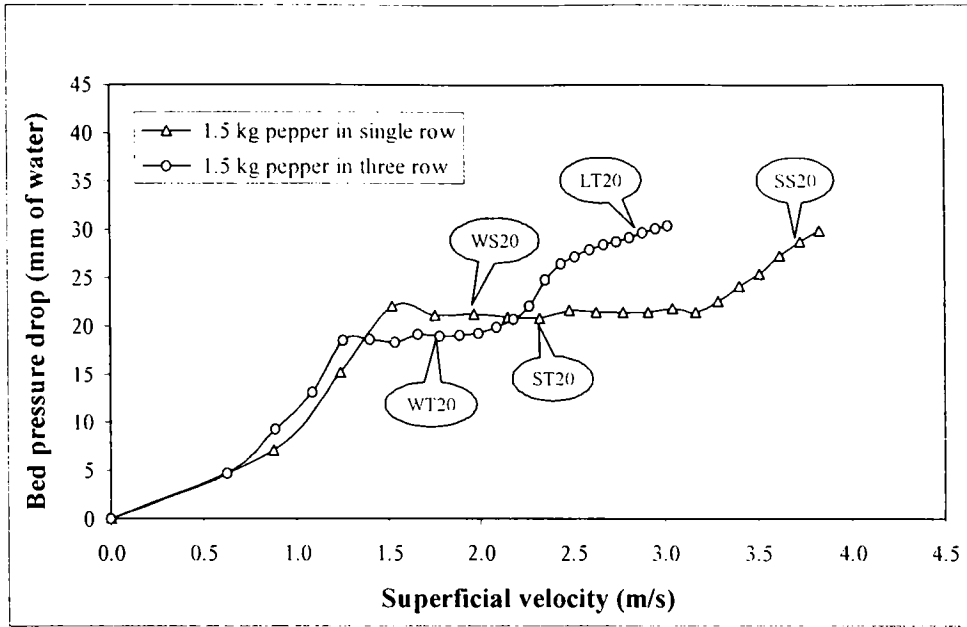


Figure 5.5.37 Comparison of the variation of bed pressure drop with superficial velocity between single row and three row vane type distributors with vane angle 20° (bed material –1.5 kg pepper)

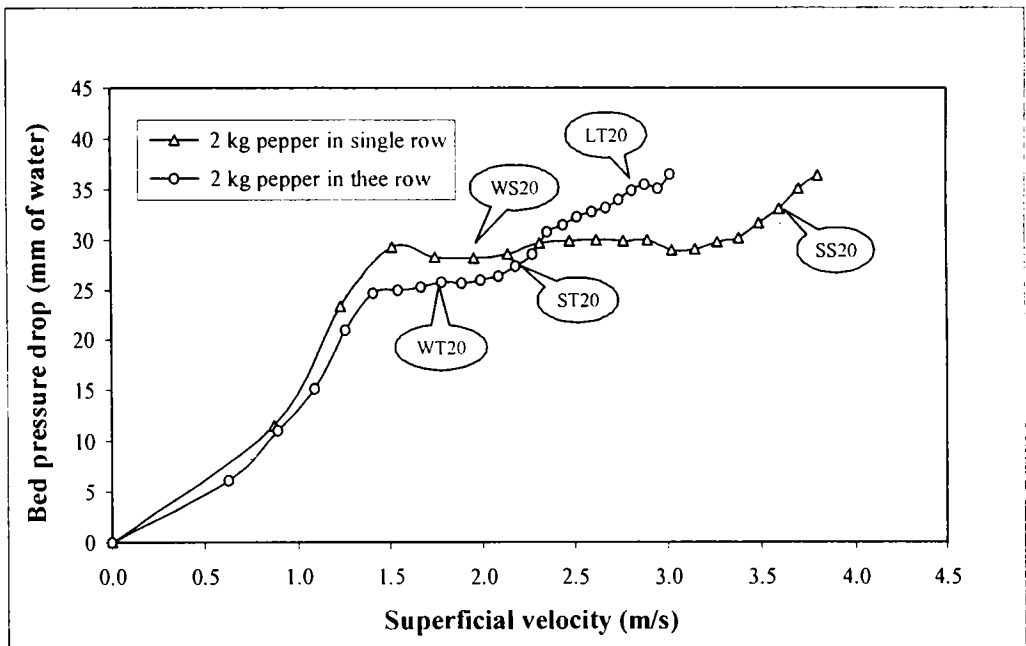


Figure 5.5.38 Comparison of the variation of bed pressure drop with superficial velocity between single row and three row vane type distributors with vane angle 20° (bed material –2.0 kg pepper)

From figures 5.5.31 to 5.5.38, it can be concluded that compared to a single row vane type distributor, the bed pressure drop for a three row vane type distributor is less in the wave region. This is due to the low static bed height in TRVD. The wave motion and swirl motion starts at a lower superficial velocity for three row vane type distributors compared to single row vane type distributors. This is because, in the case of TRVD for the same superficial velocity, the air coming out of the distributor is having a higher momentum (due to a higher mass flow rate and higher velocity of air coming out of the distributor in TRVD).

5.6 VARIATION OF BED PRESSURE DROP WITH SUPERFICIAL VELOCITY ALONG RADIAL DIRECTION FOR THREE ROW VANE TYPE DISTRIBUTORS

The formation of vortex in swirling fluidized bed causes a variation of bed height in the radial direction and this variation increases with an increase in the swirl velocity. Hence a variation in the bed pressure drop along the radial direction is always to be expected in a swirling fluidized bed when the gas velocities are considerably more than at minimum fluidisation.

The variation of bed pressure drop along the radial direction in the case of three row vane type distributors has been studied using two bed materials (coffee beans and pepper). Both coffee beans and pepper behaved in a similar manner and hence only coffee beans is considered for the present discussion.

Typical results showing the variation of bed pressure drop in the case of coffee beans are presented in figures 5.6.1 to 5.6.8. Curves 1, 2, 3 and 4 in these figures correspond to the variation of bed pressure drop with superficial velocity at radial distances of 150 mm, 116 mm, 78 mm and 44 mm from the centre respectively. The study has been carried out with two distributor angles (15° and 20°) and for different bed weights varying from 1.5 kg to 3.0 kg.

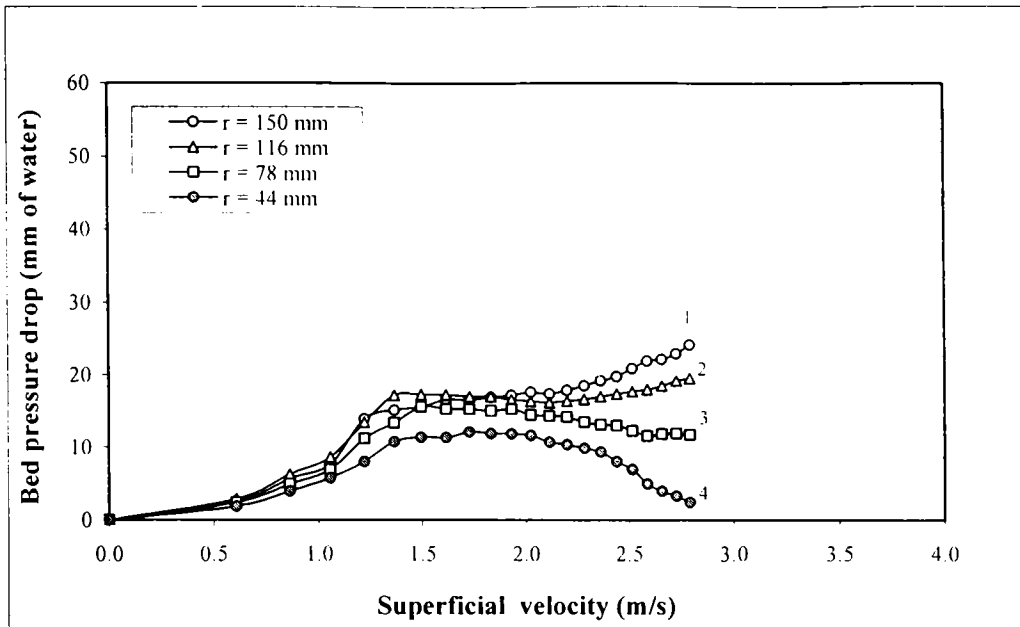


Figure 5.6.1 Variation of bed pressure drop with superficial velocity at different radial positions in three row vane type distributor - vane angle 15° and bed material - 1.5 kg coffee beans

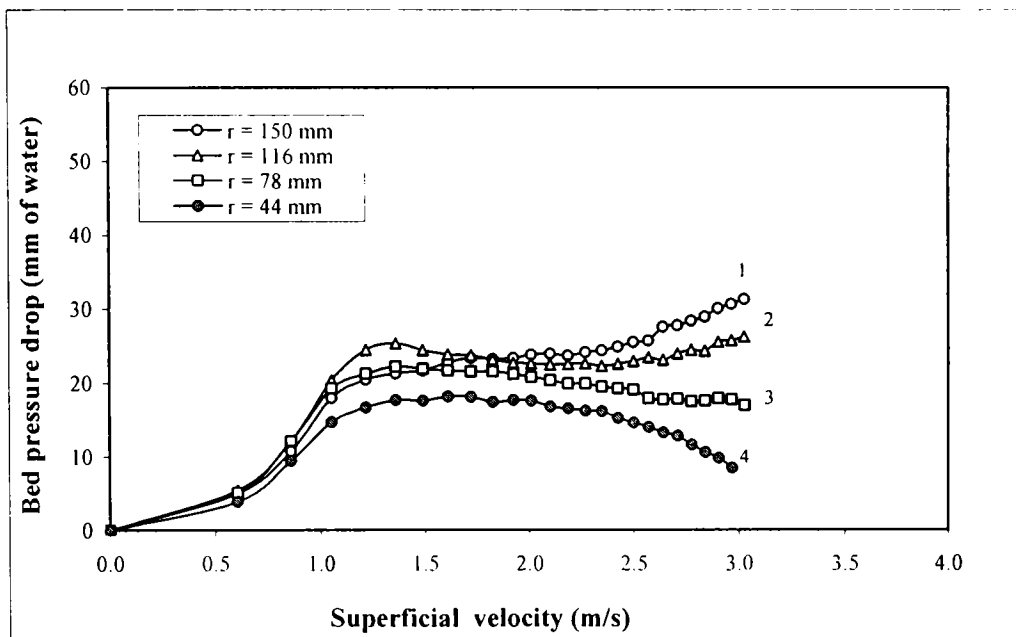


Figure 5.6.2 Variation of bed pressure drop with superficial velocity at different radial positions in three row vane type distributor - vane angle 15° and bed material - 2.0 kg coffee beans

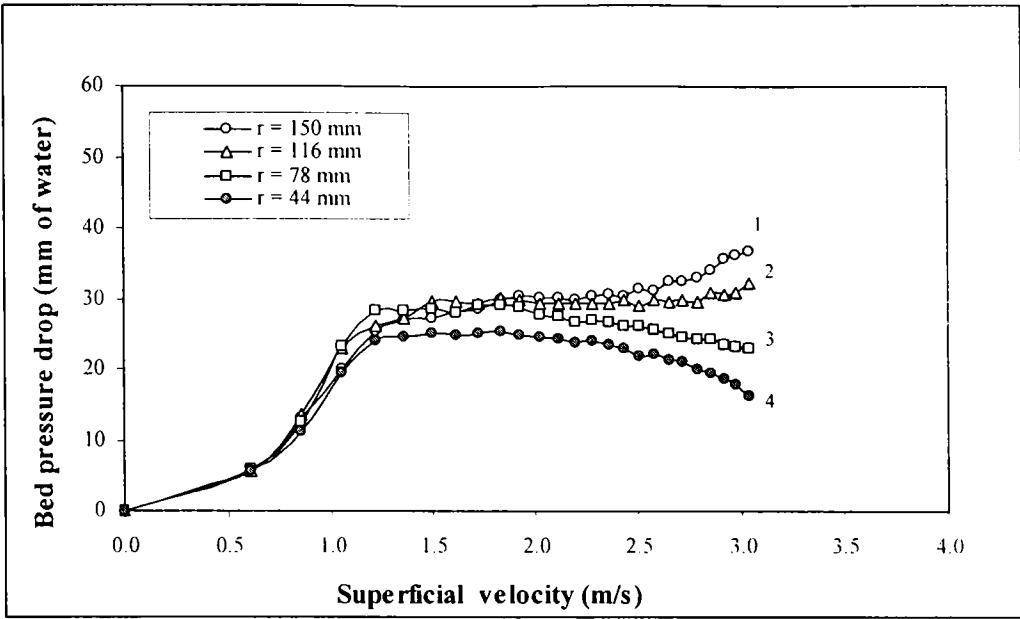


Figure 5.6.3 Variation of bed pressure drop with superficial velocity at different radial positions in three row vane type distributor - vane angle 15° and bed material – 2.5 kg coffee beans

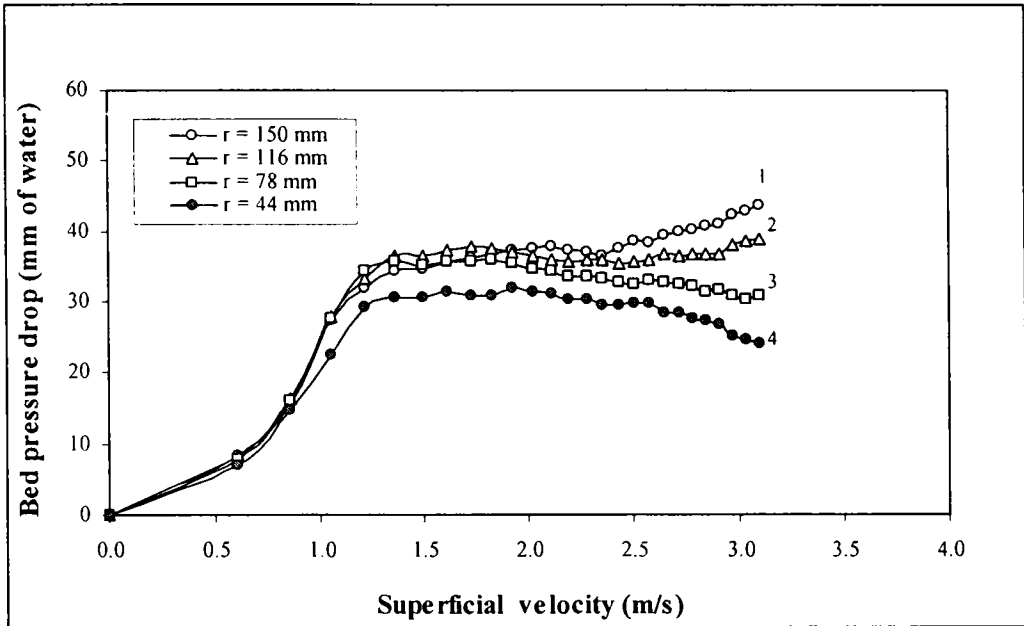


Figure 5.6.4 Variation of bed pressure drop with superficial velocity at different radial positions in three row vane type distributor - vane angle 15° and bed material – 3.0 kg coffee beans

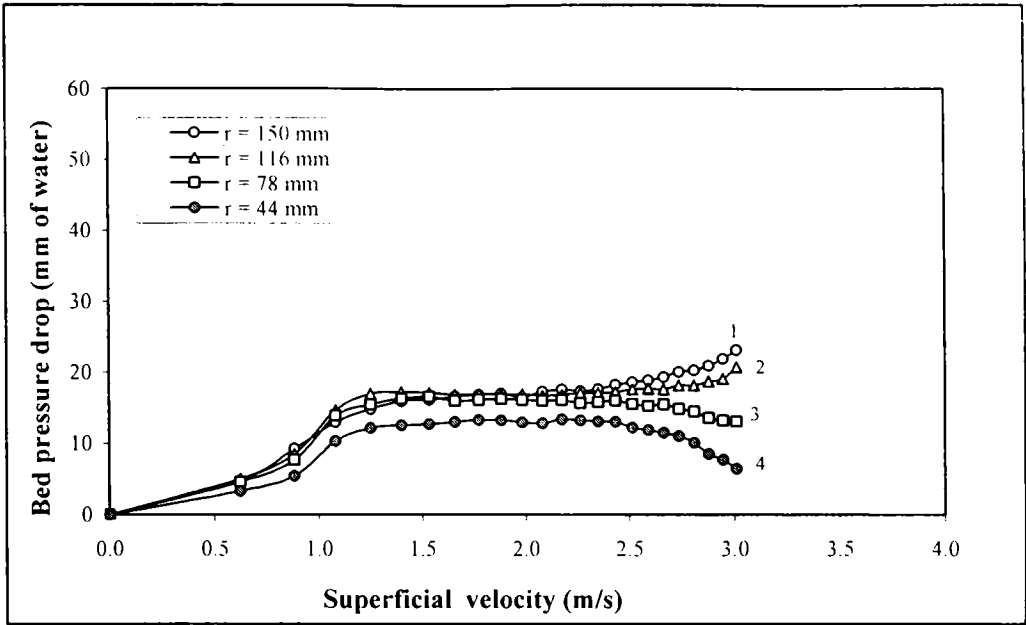


Figure 5.6.5 Variation of bed pressure drop with superficial velocity at different radial positions in three row vane type distributor - vane angle 20° and bed material – 1.5 kg coffee beans

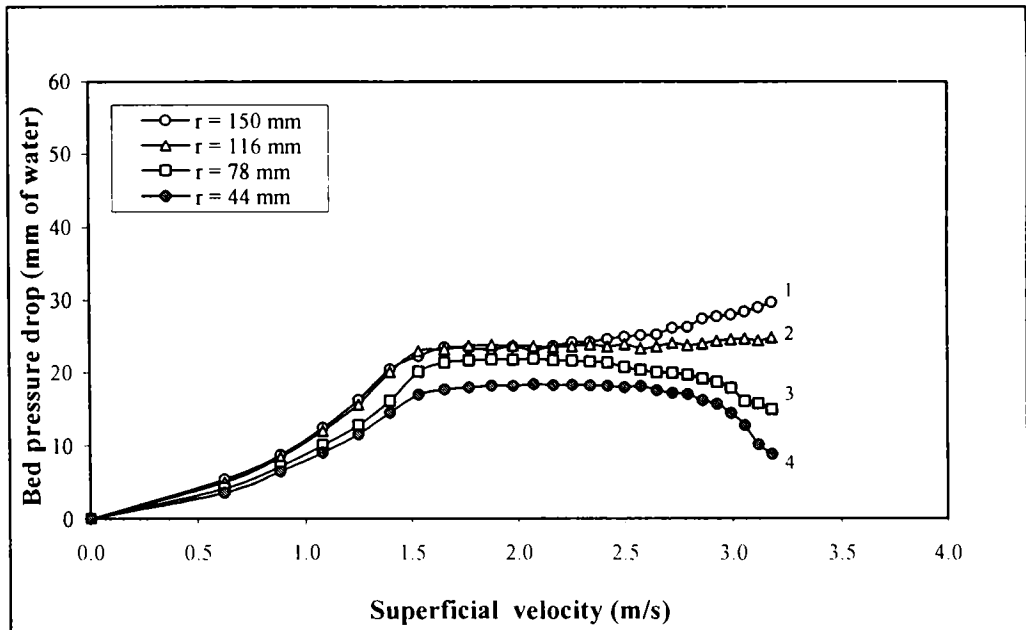


Figure 5.6.6 Variation of bed pressure drop with superficial velocity at different radial positions in three row vane type distributor - vane angle 20° and bed material – 2.0 kg coffee beans

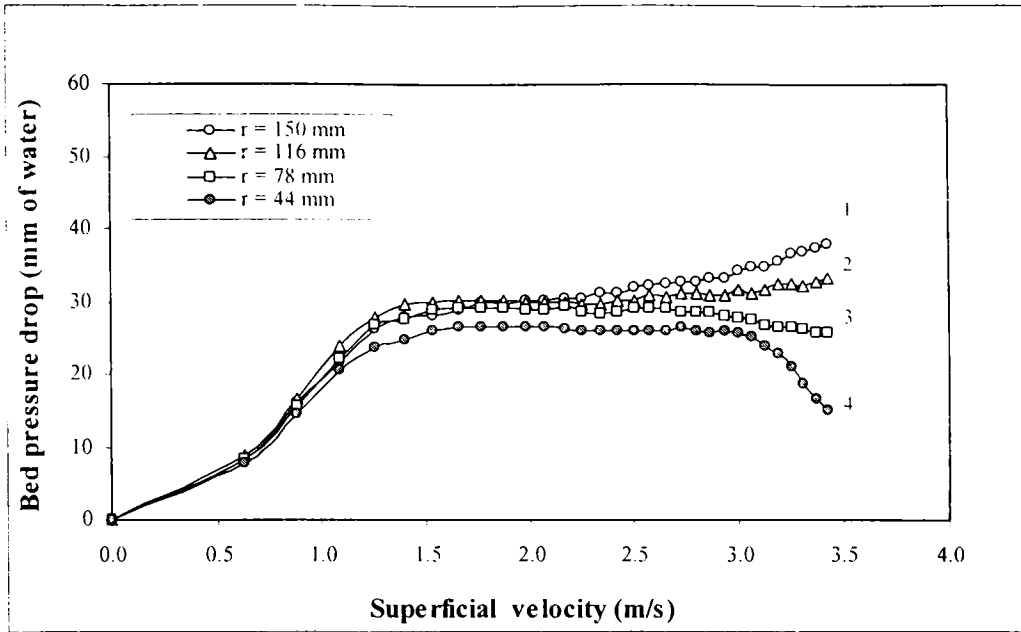


Figure 5.6.7 Variation of bed pressure drop with superficial velocity at different radial positions in three row vane type distributor vane angle 20° and bed material – 2.5 kg coffee beans

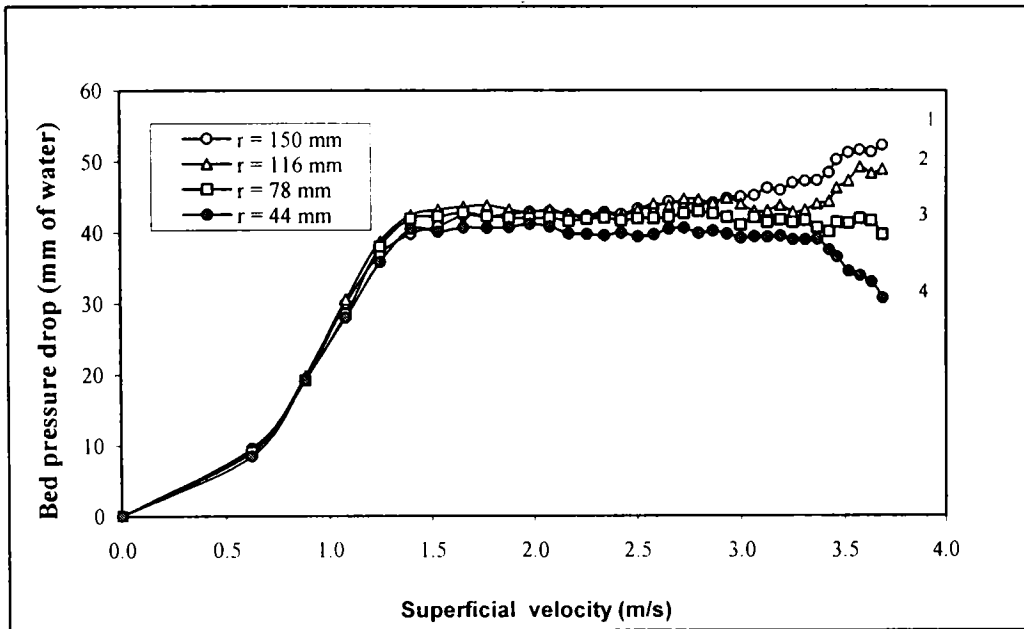


Figure 5.6.8 Variation of bed pressure drop with superficial velocity at different radial positions in three row vane type distributor - vane angle 20° and bed material – 3.0 kg coffee beans

In general, it can be said that, the bed pressure drop increases with an increase in the

superficial velocity up to the minimum fluidizing velocity. Beyond the minimum fluidizing velocity and up to the beginning of the swirl motion, there is no significant variation in the bed pressure drop with an increase in the superficial velocity.

However, if the superficial velocity is increased in the swirl region, the bed behaves differently. It is to be noted that, while the bed pressure drop increases with superficial velocity in the outer region of the bed, it decreases in the inner region. The rate of reduction in the bed pressure drop in the inner region of the bed is greater with a higher superficial velocity in the swirl region. Due to the lower bed pressure drop in the inner region of the bed, the air might get by-passed through the inner boundary of the bed (around the cone) which may reduce the efficiency of gas-particle contact in the bed.

Depending on the process for which the bed is used, by-passing of air may affect the bed performance, particularly for drying processes. This means that the maximum superficial velocity is to be limited in the swirl region to have an optimum bed performance for drying process.

5.7 VARIATION OF BED HEIGHT WITH SUPERFICIAL VELOCITY IN INCLINED HOLE TYPE DISTRIBUTORS

Once the swirling starts, the bed height variation with superficial velocity is different in the swirling fluidized bed compared to a conventional bed. Unlike inclined hole type distributors, vane type distributors have a wave region and assessment of bed height in the wave region is difficult. Hence inclined hole type distributors are considered for the study of the variation of bed height with superficial velocity. The bed height considered in the present study was the average readings from three scales placed symmetrically to the outer periphery of the bed column.

Variation of bed height with superficial velocity has been recorded with two bed materials and bed weights (coffee beans and pepper, each with 1.5 kg and 2.0 kg) and the same was compared with the bed height variation in a conventional bed. Typical behaviour is shown in figures 5.7.1 and 5.7.2, which corresponds to coffee beans and pepper respectively with a bed weight of 2.0 kg.

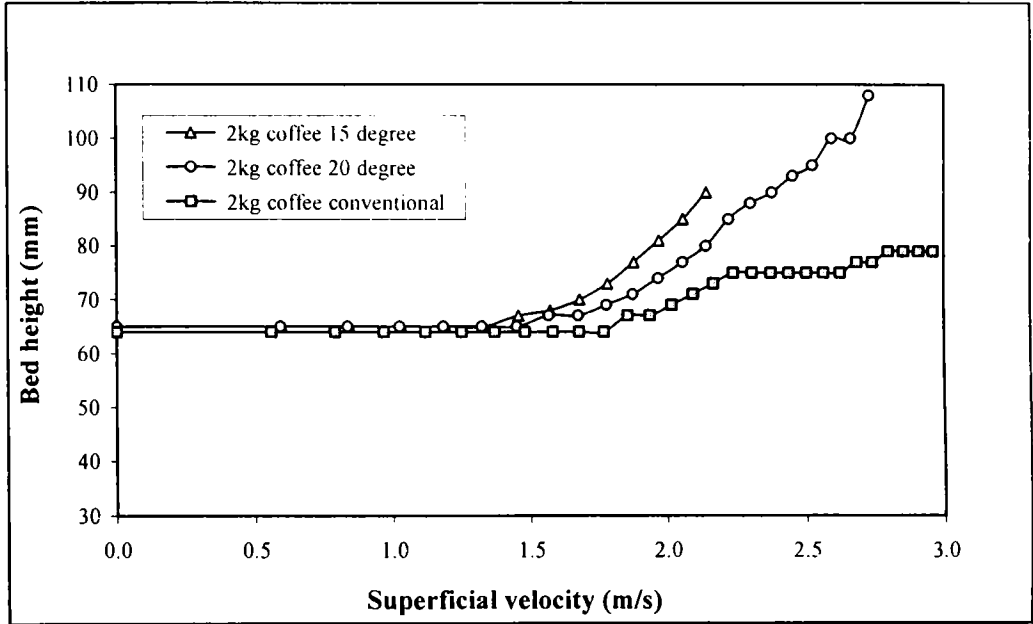


Figure 5.7.1 Variation of bed height with superficial velocity in inclined hole type -distributors – bed material - 2 kg coffee beans

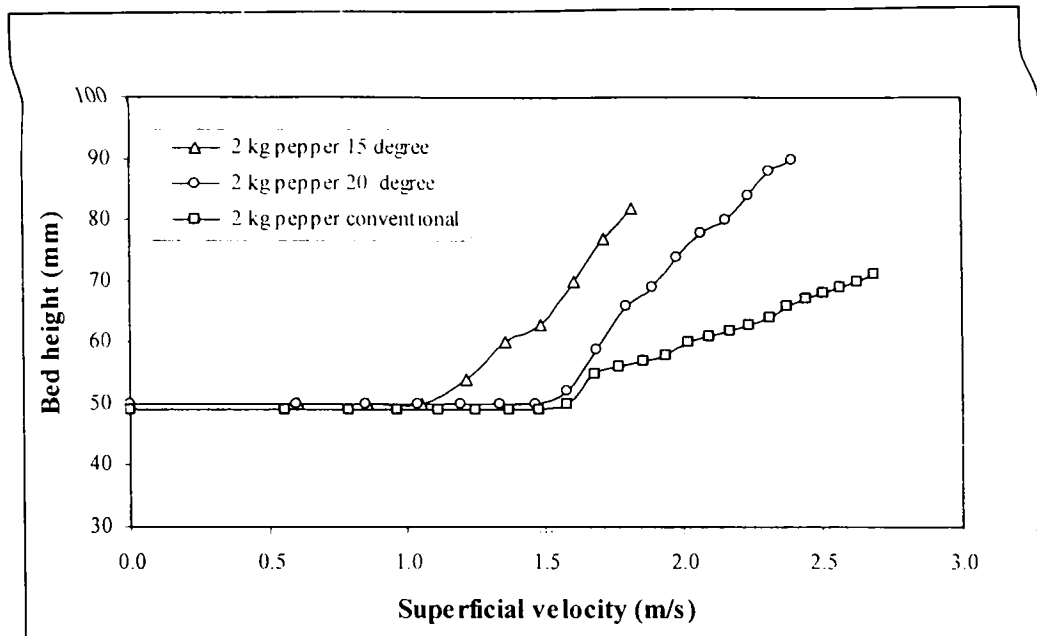


Figure 5.7.2 Variation of bed height with superficial velocity in inclined hole type distributors- bed material - 2 kg pepper

There is no significant variation in the bed height from the static bed height up to a certain superficial velocity beyond the minimum fluidizing velocity for conventional bed. However, on increasing the superficial velocity to about $1.23 U_{mf}$, a sudden increase in the bed height can be seen in figures 5.7.1 and 5.7.2. After this increase, the bed height increases with an increase in the superficial velocity. The reason for not much expansion of bed immediately after the minimum fluidization is due to the fact that the bed is shallow and that Geldart's D type particles were used in the present study.

For inclined hole type distributors, the bed height starts increasing at a lower superficial velocity compared to the conventional bed. Further, with a lower hole angle, the superficial velocity at which the increase in bed height starts is still lower. It is to be noted that in the case of inclined hole type distributors, the percentage area of opening is lower and a correspondingly higher jet velocity develops within the bed. The air passing through the openings closer to the center of the distributor will have

sufficiently higher jet velocity to cause fluidization and swirl motion at the inner region. With an increase in the superficial velocity, this fluidized region will expand outwards and thus the whole bed will get fluidized. Due to the swirl motion at the inner region, particles will get shifted towards the bed wall. Since the bed height was measured at the outer boundary of the bed (bed wall), the increase in bed height could be observed at a lower superficial velocity compared to that in the case of conventional bed. With a lower hole angle, the swirl velocity increases and due to the above reasons, an increase in bed height at a still lower superficial velocity can be expected.

It may be further noted that the bed height measured in the case of inclined hole type distributors is the combined effect of bed expansion and the shifting of particles from the inner region to the outer region. As a result, it can be seen that the rate of increase in the bed height with superficial velocity is higher for inclined hole type distributors compared to conventional distributor.

5.8 BED BEHAVIOUR IN THREE RAW VANE TYPE DISTRIBUTORS

The swirling fluidized bed can be used for different processes such as drying, granulation, combustion etc. The air-solid mixing and lateral mixing of particles are more effective in swirling fluidized bed compared to conventional bed due to the swirl and toroidal motion. As the superficial velocity is increased from zero to the maximum, the swirling fluidized bed may undergo three different stages namely stagnant, wave motion and swirl motion.

The formation of wave and swirl motion in a swirling fluidized bed can be explained as follows. When air enters through the distributor at an angle θ with the horizontal, it will have two components: horizontal and vertical. The vertical component, $V\sin\theta$, causes fluidization and the horizontal component, $V\cos\theta$, causes rotation of the

particles. At low velocity, the bed behaves as a packed bed and the horizontal movement of the air will be obstructed by the particles. So the entire flow percolates upwards. When the airflow rate is increased, the bed reaches the minimum fluidizing condition. At this point, the particles are, on an average, no longer in contact with each other. The particle-particle friction essentially disappears and the particles are free to move relative to each other at this stage. The momentum of air in the horizontal direction moves the particles around the annulus in the horizontal direction. When the particles start moving, the air transfers its horizontal angular momentum to the particles. However, once the particles begin to swirl, some of the angular momentum of particles is lost against the wall-particle friction and air-particle friction, which leads to a wave motion in the bed which is a transition stage prior to the swirl motion. With an increase in superficial velocity, the angular momentum of air will be sufficient to overcome the frictional resistance and the bed swirls steadily. A typical wave formation in a swirling fluidized bed is shown in figure 5.8.1.

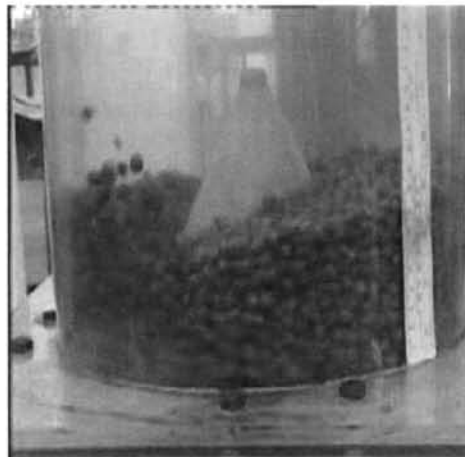


Figure 5.8.1 Typical wave formation in a swirling fluidized bed

Here the particles from left side of the bed are taken away and are accumulated on the right side. These heaps and lows will change with time and thus forms a wave motion in the bed. However, once swirl motion starts, these heaps and lows will disappear.

Different processes need different types of bed behaviour and hence it is important to identify the velocity regime over which a particular behaviour occurs. No wave regime was observed in inclined hole- type distributors. This was due to low percentage area of opening and a corresponding high air jet velocity. In the case of single row vane type distributors, wave regime was observed for a wide range of superficial velocity and swirl was observed only at a higher superficial velocity. This was due to the higher percentage area of opening and a lower useful area of the single row vane type distributor. On the other hand, three row vane type distributors showed the three different stages as the superficial velocity was increased from zero to the maximum. Hence, experiment was conducted to identify different regimes in the bed in the case of three row vane type distributors only.

For a particular bed material and bed weight, the air flow was increased slowly from zero and the superficial velocity corresponding to the beginning of wave motion and swirl motion were observed, details of the experimental procedure are explained in section 4.3.7. Coffee beans and pepper were used for the study and the bed weight was varied from 500 g to 1300 g. Figures 5.8.2 to 5.8.5 show the plot of different regimes in the case of three row vane type distributors with different bed materials.

Table 5.8.1 presents the superficial velocity corresponding to the starting of wave and swirl motion. The superficial velocity required for the starting of wave motion and swirl motion are more for a distributor with higher vane angle. Further, the wave and swirl starts at a lower superficial velocity in the case of pepper. This early starting of wave/swirl motion may be due to a lower surface area for pepper. It is to be noted that compared to coffee beans, pepper has higher sphericity and particle density with a lower particle size.

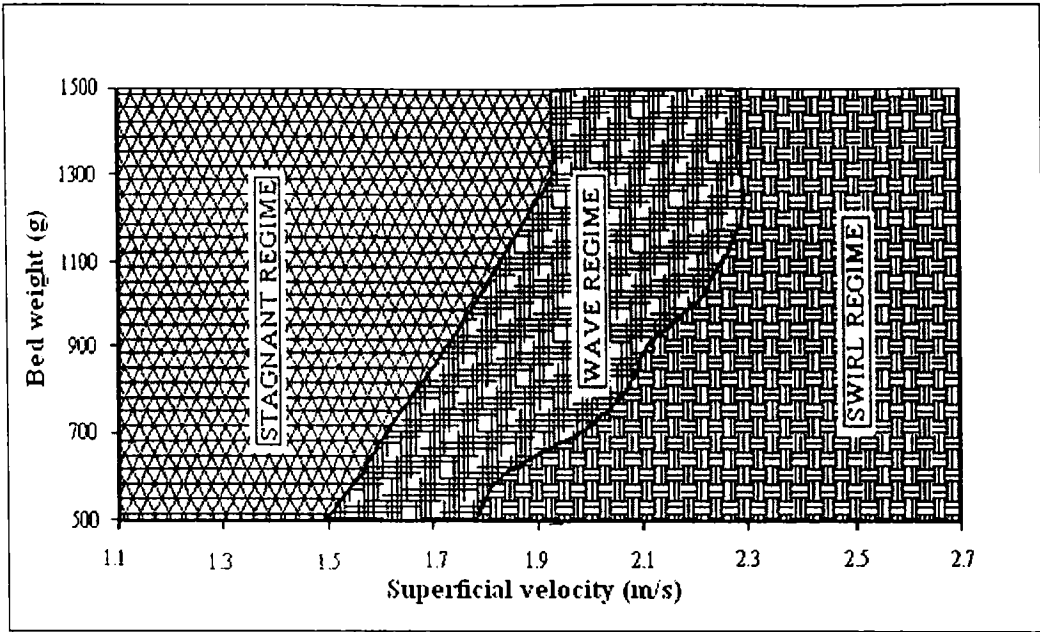


Figure 5.8.2 Different regimes in three row vane type distributor - vane angle 15° and bed material coffee beans

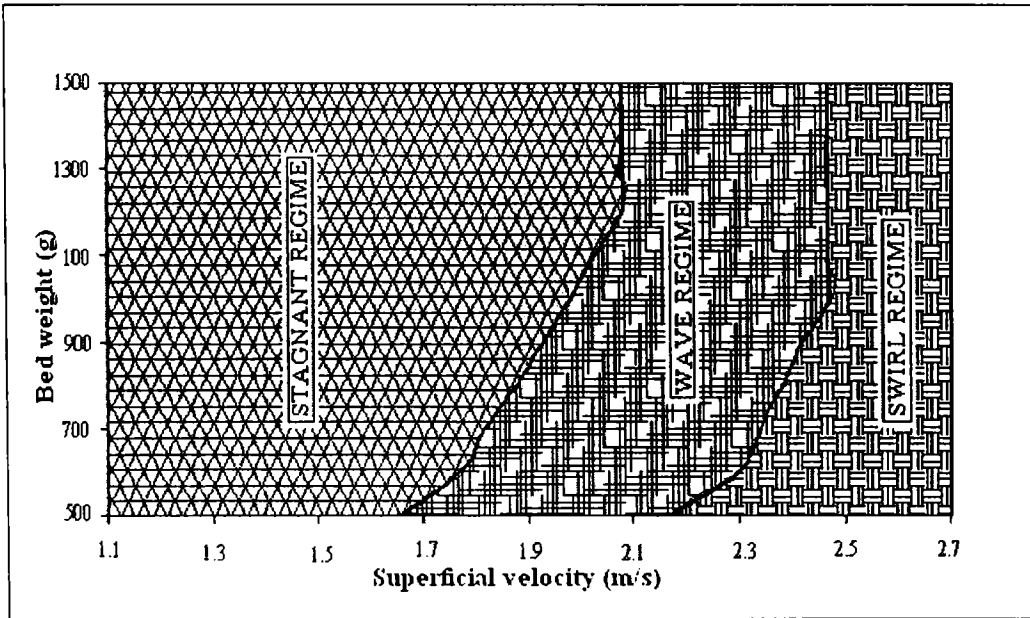


Figure 5.8.3 Different regimes in three row vane type distributor - vane angle 20° and bed material coffee beans

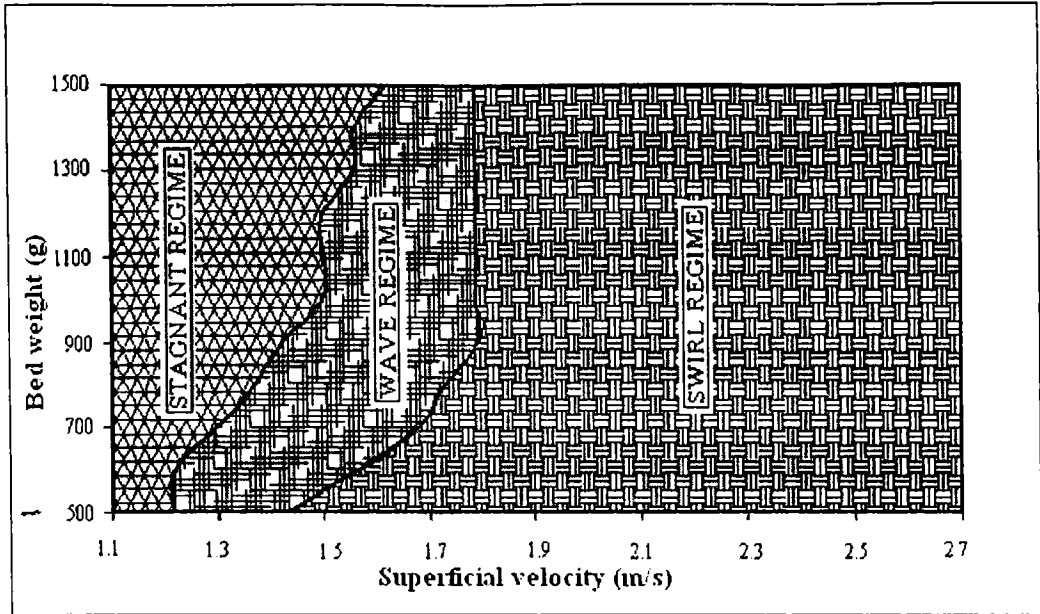


Figure 5.8.4 Different regimes in three row vane type distributor - vane angle 15° and bed material pepper

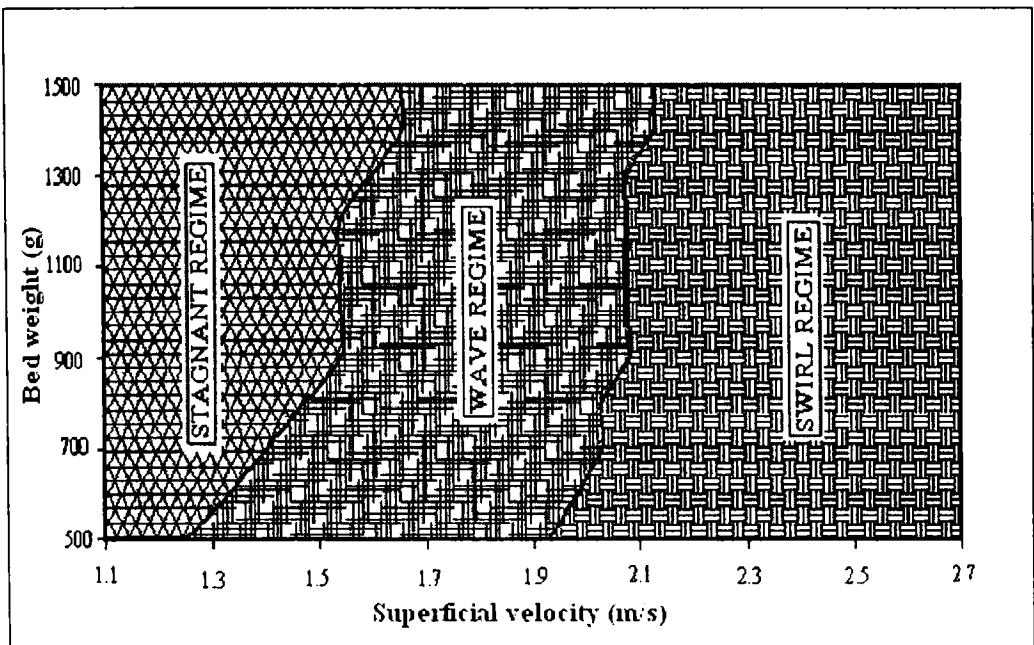


Figure 5.8.5 Different regimes in three row vane type distributor - vane angle 20° and bed material pepper

G9116

Table 5.8.1 Superficial velocity corresponding to the starting of wave motion and swirl motion

Sl. No	Bed weight (g)	Superficial velocity for three row distributor with 15 degree vane angle (m/s)				Superficial velocity for three row distributor with 20 degree vane angle (m/s)			
		Coffee Beans		Pepper		Coffee Beans		Pepper	
		Wave starts	Swirl starts	Wave starts	Swirl starts	Wave starts	Swirl starts	Wave starts	Swirl starts
1	500	1.49	1.78	1.22	1.43	1.66	2.17	1.25	1.93
2	600	1.56	1.83	1.22	1.56	1.77	2.30	1.33	1.98
3	700	1.61	1.98	1.30	1.68	1.82	2.34	1.40	2.03
4	800	1.67	2.07	1.37	1.73	1.88	2.38	1.47	2.03
5	900	1.73	2.11	1.42	1.79	1.93	2.42	1.54	2.08
6	1000	1.78	2.20	1.50	1.79	1.98	2.47	1.54	2.08
7	1100	1.83	2.25	1.50	1.79	2.03	2.47	1.54	2.08
8	1200	1.88	2.29	1.50	1.79	2.08	2.47	1.54	2.08
9	1300	1.93	2.29	1.56	1.79	2.08	2.47	1.60	2.08
10	1400	1.93	2.29	1.56	1.79	2.08	2.47	1.66	2.13
11	1500	1.93	2.29	1.62	1.79	2.08	2.47	1.66	2.13

The superficial velocity corresponding to the beginning of wave and swirl motion increases with an increase in the bed weight and after a certain bed weight, they become constant and are independent of bed weight. Identification of the constant superficial velocity corresponding to the wave and swirl motion in a fluidized bed is important, particularly for processes like drying of agricultural produces for determining the optimum bed weight. For example, agricultural produces, on drying, weighs as low as 25 % of the initial weight. So, for a particular bed behaviour (swirl or wave motion), the optimum bed weight must be selected in such a way that even after drying, the expected bed behaviour is obtained.

5.9 CONCLUSIONS

Based on the above discussions, the following conclusions are made, which are presented based on the hydrodynamic parameters studied.



5.9.1 Distributor pressure drop

1. The distributor pressure drop is lower in the case of distributors with an area of opening higher than about 17 %. A further increase in the area of opening will not reduce the distributor pressure drop considerably.
2. In the present study, for the distributor with 17 % area of opening and corresponding to the maximum measured superficial velocity of 4.33 m/s, the distributor pressure drop obtained was 55.25 mm of water.

5.9.2 Air velocity in empty bed

In the case of three row vane type distributors and based on the observations of air velocity along the radial distance and at two planes located at 5 mm and 10 mm above the distributor, it can be concluded that,

1. In general, while the radial component of velocity decreases, the tangential component increases with an increase in the radial distance.
2. The radial component of the velocity reduces suddenly within a certain radial distance and beyond this distance; the radial component is almost the same. The sudden change in the value of radial component starts at a shorter radial distance in the case of a lower plane.
3. The tangential component of the velocity increases with increase in the radial distance and beyond a certain radial distance the rate of increase is not significant.
4. In the case of an empty swirling fluidized bed, the air flow is available over the full annular space up to a certain height above the distributor and beyond this height, the air swirls within a narrow annular width at the outer boundary.
5. There is a limitation over the maximum height of bed material which may swirl effectively in a swirling fluidized bed, which depends on the particle

characteristics also. Further, it is expected to have a no swirl top layer region in the bed if the bed height is more than a certain height.

5.9.3 Minimum fluidizing velocity of vane type distributors

1. For the bed particles considered the vane type distributors gives a higher minimum fluidizing velocity compared to perforated type distributors and the value dependent on the vane angle also.
2. Compared to perforated plate distributor, a variation as high as 30.8 % has been observed (for single row - 15° vane angle- coffee beans) in the present study.

5.9.4 Variation of bed pressure drop with superficial velocity

Based on the study on the variation of the bed pressure drop with superficial velocity with respect to different distributors, namely perforated plate, single row vane type, inclined hole type and three row vane type, the following conclusions could be arrived at:

1. Swirling bed fluidizes large particle (Geldart D type particles) effectively compared to conventional bed.
2. Compared to single row vane type distributors, with out affecting the quality of fluidization, the useful area of distributor could be increased with inclined hole type and three row vane type distributors. For the present study, this increase is respectively 29 % and 27 %.
3. Wave region has not been observed in inclined hole type distributors, unlike vane type distributors.
4. The swirl motion in inclined hole type distributors starts from the inner region of the bed and progresses to the outer region while, in the case of vane type distributors, it starts from the outer region of the bed and

- progresses to the inner region.
5. The major parameters that influence the superficial velocity corresponding to the starting of wave and/or swirl motion in a swirling fluidized bed are
 - a. Vane/hole angle
 - b. Percentage area of opening
 - c. Percentage useful area of the distributor.
 6. The swirl starts at a lower superficial velocity for a lower vane/hole angle as well as for a lower percentage area of opening. However, the swirl starts at a lower superficial velocity for a higher percentage useful area of the distributor.
 7. For both single row and three row vane type distributors, up to the formation of the wave motion, the variation of bed pressure drop with superficial velocity is similar to that of the conventional bed. Between the wave and swirl motions, the bed pressure drop is almost constant over the initial region and it increases towards the end. In the swirl region, however, the bed pressure drop increases with an increase in the superficial velocity.
 8. Once swirl motion starts, the rate of increase in bed pressure drop in the case of single row and three row vane type distributors is higher for 15° vane angle compared to 20° .

5.9.5 Variation of bed Pressure drop With superficial velocity along radial direction

In the case of three row vane type distributors and in the swirl region,

1. The bed pressure drop increases with superficial velocity in the outer region of the bed and it decreases in the inner region.
2. The rate of reduction in the bed pressure drop in the inner region of the bed is

higher with a higher superficial velocity.

3. Due to the lower bed pressure drop in the inner region of the bed, the air might get by-passed through the inner boundary of the bed (around the cone).
4. Depending on the process for which the bed is used, the maximum superficial velocity is to be limited to have an optimum bed performance.

5.9.6 Variation of bed height with superficial velocity

In case of swirling fluidized bed,

1. The variation of bed height with superficial velocity is the combined effect of bed expansion and the shifting of particles from the inner region.
2. The rate of increase in the bed height with superficial velocity is higher in the case of swirling fluidized beds compared to conventional bed.
3. The rate of increase in bed height with superficial velocity is also influenced by the hole angle.

5.9.7 Bed behaviour in three row vane type distributors

1. The superficial velocity corresponding to the beginning of wave and swirl motion increases with an increase in the bed weight and after a certain bed weight, they become constant and are independent of bed weight.
2. Identification of the constant superficial velocity corresponding to the wave and swirl motion in a fluidized bed is important, particularly for processes like drying of agricultural produces for determining the optimum bed weight.

CHAPTER 6

CONCLUSIONS

6.1 INTRODUCTION

Seven distributors have been designed and fabricated. They include single row vane-type distributor, inclined hole-type distributor, three row vane-type distributor and perforated plate distributor. For all types, except the perforated plate distributor, two distributors were fabricated with vane/hole angles of 15° and 20° .

Large particles (Geldart D-type) have been selected for the hydrodynamic study. Particles have been selected from locally available agricultural produce namely coffee beans and black pepper.

Basic hydrodynamic characteristics of swirling fluidized bed have been studied and compared using the different distributors fabricated. The major variables considered in the present study include the percentage area of opening, angle of air injection and useful area of the distributor.

The major conclusions drawn from the present investigations are presented in this chapter.

6.2 CONCLUSIONS

1. The distributor pressure drop decreases with an increase in the percentage area of opening.
2. One of the methods of increasing the percentage area of opening is by using vane type distributors.
3. The distributor pressure drop is lower in the case of distributors with an area of opening higher than about 17 %. A further increase in the area of opening will not considerably reduce the distributor pressure drop.

4. In the present study, for the distributor with an area of opening 17 %, and corresponding to the maximum measured superficial velocity of 4.33 m/s, the distributor pressure drop obtained was 55.25 mm of water.
5. Single row vane type distributors have limitation over the useful area of the distributor. However, by using multiple rows, the useful area of distributor can be increased.
6. In the present study, a useful area of 91 % could be achieved in three row vane type distributor as against 64 % useful area in the case of single row vane type distributor.
7. The air flow in a swirling fluidized bed is essentially three dimensional.
8. The radial component of velocity, which supports the radial mixing of the particles decreases with an increase in radial distance.
9. The tangential component of velocity, which causes swirl motion, increases with an increase in radial distance.
10. The swirling bed fluidizes large particles (Geldart D-type particles) effectively compared to conventional bed.
11. The major parameters that influence the superficial velocity corresponding to the starting of wave and/or swirl motion in a swirling fluidized bed are
 - a. Vane/hole angle
 - b. Percentage area of opening
 - c. Percentage useful area of the distributor.
12. For vane-type distributors, up to the formation of the wave motion, the variation of bed pressure drop with superficial velocity in the static bed is similar to that of the conventional bed. Between the wave and swirl motions, the bed pressure drop is almost constant over the initial region and it increases towards the end. In the swirl region, however, the bed pressure drop increases with an increase in the

superficial velocity.

13. The swirl starts at a lower superficial velocity for a lower vane/hole angle as well as for a lower percentage area of opening.
14. The swirl starts at a lower superficial velocity for a higher percentage useful area of the distributor.
15. Once swirl motion starts in vane type distributors, the rate of increase in bed pressure drop is higher for a lower vane angle.
16. In a swirling fluidized bed, once swirl motion starts, the bed pressure drop increases with superficial velocity in the outer region and it decreases in the inner region. So, with higher superficial velocity, the air might get by-passed through the inner boundary of the bed (around the cone).
17. Depending on the process for which the bed is used, the maximum superficial velocity is to be limited to have an optimum bed performance.
18. Due to the combined effect of bed expansion and the shifting of particles from the inner region, the rate of increase in the bed height with superficial velocity is higher in the case of swirling fluidized bed compared to conventional bed.
19. The superficial velocity corresponding to the beginning of wave and swirl motion increases with an increase in the bed weight and after a certain bed weight, they become constant and are independent of bed weight.
20. For determining the optimum bed weight, identification of the constant superficial velocity corresponding to the wave and swirl motion in a fluidized bed is important, particularly for processes like drying of agricultural produces.

6.3 SUGGESTIONS FOR FUTURE WORK

In the present study, the openings in the distributor are made in such a way that the air entering to the bed at any radial distance is tangential. It is felt that by appropriately

varying the entry angle of the air, by-passing of the air through the inner region of the bed can be delayed. A detailed study can be carried out on this aspect.

Study on the effectiveness of plenum chamber in achieving a uniform distribution of air is required for large diameter beds (say 1m and above).

Wave motion in a swirling fluidized bed is a transition stage between fluidization and swirl motion. A study can be carried out to determine the area of opening such that the swirling bed could be designed at will with or without wave motion.

APPENDIX A

CALIBRATION OF TREE HOLE PROBE

A1 GENERAL

Calibration of the three-hole probe, essentially to establish the independence of Reynolds number on the probe measurements, has been carried out in a wind tunnel within the range of the following parameters.

- Velocity - 30 m/s and 70 m/s
- Yaw angle - -30° to $+30^\circ$ with an interval of 2°

The corresponding calibration curves are shown in figure A1. The calibration coefficients are defined as follows

$$\bar{P} = \frac{(P_R + P_L)}{2} \quad (\text{A.1})$$

$$D = P_C - \bar{P} \quad (\text{A.2})$$

$$K_\alpha = \frac{(P_L + P_R)}{D} \quad (\text{A.3})$$

$$K_q = \frac{(\bar{P} + P_{\text{Static}})}{D} \quad (\text{A.4})$$

$$K_0 = \frac{(P_{\text{Total}} + P_C)}{D} \quad (\text{A.5})$$

where P_L , P_C and P_R are pressure in the left, central and right holes respectively. P_{Total} and P_{static} are respectively the total and static pressures in the calibration tunnel. Figure A1 shows the variation of K_α , K_q and K_0 with α , where α is the angle between the flow vector and probe hydrodynamics.

The experimental yaw angle, static and total pressure can be found out through interpolation and these details are as follows.

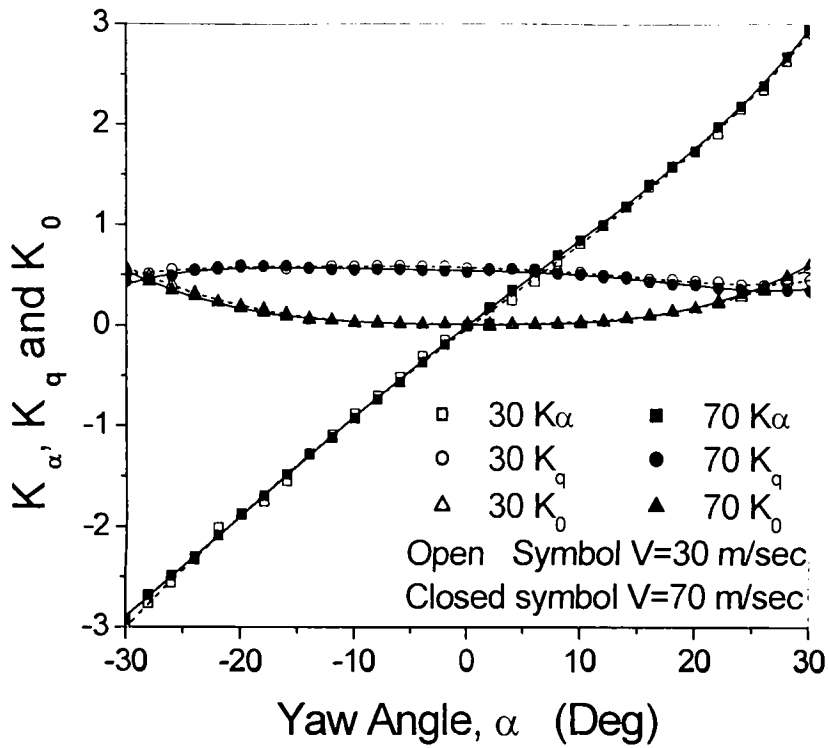


Figure A1 Calibration curve of three hole probe

K_α can be calculated using measured values of pressure from the experiment and corresponding α can be interpolated from the calibration curve of K_α Vs. α . The intersection of constant α line with K_q and K_0 curves of the calibration curves gives values of interpolated K_q and K_0 and using these values static and total pressure can be determined with the following equations.

$$P_{\text{Total}} = P_C + K_0 \times D \quad (\text{A.6})$$

$$P_{\text{Static}} = \bar{P} - K_q \times D \quad (\text{A.7})$$

Knowing the values of the P_{Total} , P_{Static} and α , the velocity components can be calculated with the following equations.

$$V = \sqrt{\frac{2 \times (P_{\text{Total}} - P_{\text{Static}})}{\rho}} \quad (\text{A.8})$$

$$V_r = V \times \sin(\alpha_{\text{ref}} + \alpha) \quad (\text{A.9})$$

$$V_t = V \times \cos(\alpha_{\text{ref}} + \alpha) \quad (\text{A.10})$$

where α_{ref} is the initial setting angle of the probe measured from the tangential direction.

APPENDIX B

CALIBRATION CERTIFICATE OF MICRO-MANOMETER

B2 GENERAL

The calibration details of digital micro-manometer are presented below.

Furness Controls Limited
CERTIFICATE OF CALIBRATION

Page 1 of 1 pages
 Date 17 March 2004
 Certificate
 Number C-17921

This is to certify that the following instrument has been tested in accordance with the standards laid down and adhered to by Furness Controls Ltd., Bexhill, England. It was calibrated using standards whose calibration is traceable to European standards. Ambient temperature was 20 ± 2 °C. Dry air was used for pressure calibration. This certificate is issued by Furness Controls Limited which holds ISO 9002 certification for the administration of its quality management system. The instrument is ~~is not~~ within the manufacturer's specification. (*delete as appropriate)

Sales Order No : 36018
 Customer : SARTECH INTERNATIONAL
 Instrument : AIRPRO
 Instrument type: FC0520
 Supply voltage : Battery
 Serial No : 0402176

Pressure range : -600 to 600 Pa

Reference Pressure Pa	Instrument calibrated Display Pa	deviation 0	% of R
600.130	-599.7	-0.4	-0.07
480.197	-480.0	-0.2	-0.04
359.757	-360.2	0.4	0.11
239.623	-240.0	0.4	0.17
120.239	-120.4	0.2	0.17
0.000	0.0	0.0	
120.202	120.2	-0.0	0.00
240.049	240.3	0.3	0.12
360.113	360.1	-0.0	0.00
480.758	480.6	-0.2	-0.04
601.539	600.5	-1.0	-0.17

Reference instruments used to carry out calibration of the above unit.

Pressure standard : FRS4HR serial number (FCPS017), RS36, Calibration uncertainty better than 0.01% of reading + 0.002 Pa
 Electrical multimeter : Thurlby 1905a - FCL ref. number WS96
 Calibration accuracy 0.01% + 1digit.

Approved sign. : G Thorogood

sign : 

History of traceability to National Standards and a list of approved signatories are available from Furness Controls Ltd.

The uncertainties are for a confidence level of not less than 95%

APPENDIX C

UNCERTAINTY ANALYSIS

C1 INTRODUCTION

Uncertainty analysis is the prediction of the uncertainty limit, based on the scatter in the data used for the calculation of the result. Any measurement, irrespective of the type of instrument used, possesses certain amount of error, while acquiring the data. These errors are propagated through the data reduction, resulting in uncertainty. Some instruments have better accuracy than others. Uncertainty in measurement can be defined as the maximum error, which might be expected between the measured value and the true value of the measured parameter. Authors, Moffat (1985), Holman and Gajda (1989), Govardhan (1997), Coleman and Steele (1989) and Poti and Rabe (1988) have recommended methods to calculate the two sources of errors namely, bias (fixed) errors and precision (random) errors.

Bias error is the difference between the mean value and the true value. Bias error remains constant for a given configuration. Precision error is the scatter observed in the measurement that fall in to a Gaussian distribution about a mean value in a multiple sample. Statistical analysis shows that the standard deviation of the distribution is the value which best represent the measure of precision. Total error is the combined effect of the above two errors.

All measuring instruments have both bias and precision errors. The errors are calculated for entire data path from the measurement source to the output device, including probe, calibration source and individual errors. Overall system measurement error is calculated by combining each individual error component using the following equations.

$$B = \sqrt{\sum_{k=1}^N (B_k)^2} \quad (C.1)$$

$$P = \sqrt{\sum_{k=1}^N (P_k)^2} \quad (C.2)$$

$$U = \pm \sqrt{(B^2 + t_{95} \times P^2)} \quad (C.3)$$

where,

N = Number of readings of the sample population

k = Variable under consideration

B = Bias error of the variable consideration

P = Precision error of the variable under consideration

U = Total uncertainty

t_{95} = 95th percentile point for the two tailed student 't' distribution.

C2 ERROR IN THE CALCULATION OF VELOCITY USING THREE HOLE PROBE

The sources of error associated with the use of three hole probe are listed below.

1. Turbulence effect
2. Reynolds number and Mach number affect
3. Effect of pressure and velocity gradients
4. Wall vicinity effect
5. Effect of probe blockage and probe stem
6. Finite dimensions of the probe sensing area
7. Misalignment in the reference direction
8. Interpolation errors

Chue (1975) discussed these errors in detail. All the errors except 7 and 8 would be due to the inherent characteristics of the air flow or the probe.

The probe has been calibrated in a calibration tunnel, where the turbulence is very low. The magnitude of error expected in the probe calibration coefficients would be of the order of $\pm 0.6\%$ for 10% turbulence intensity. The error would be slightly more if the turbulence intensity is more. There would be errors in the angles and pressures interpolated. The value of the error in the total velocity would be approximately 0.35%, while the errors in velocity components vary depending on the yaw angle.

The probe was calibrated at two Reynolds numbers corresponding to a high and a low velocity likely to be encountered in the experimental program. The effect of Reynolds number was negligible. Hence, the error due to Reynolds number effect for this probe was assumed to be negligible. As the error caused by neglecting the effect of compressibility for the Prandtl probe amounts to about $\pm 1\%$ at a Mach number of 0.28, the magnitude of error could be expected to be the same for the three hole probe. Since the measurements carried out during the present investigations were at Mach numbers less than 0.2. The errors induced would therefore be negligible.

The three hole probe used in the present investigations was calibrated in a uniform flow. In the boundary layer region, the steep gradients present in pressure and velocity would cause large error. This could result in the following errors; (i) the probe sensing the pressure reading at location different from the geometric centre of the probe, (ii) each of the three holes would be located in a differing pressure field and hence induce an error known as spatial error, (iii) the presence of the probe in a velocity gradient causing deflection of the stream lines toward the region of lower velocity gradient causing deflection of the stream lines toward the region of lower velocity resulting in recording of pressures in excess of the existing values at the same location in the absence of the probe. In the present case this effect is negligibly small as the readings are taken 8 mm away from the wall.

The probe could be subjected to the displacement effect, which may be assumed to be the same as that of Pitot tube. In the case of Pitot tube the displacement of the probe measurement point, δ , from the probe geometric centre was found to be about 21% of the tube diameter. In the present investigation the tube diameter for the central hole was 0.8 mm and hence the value of δ for the probe was about 0.17 mm. Since this amounts to a small value and affects all measurement positions equally, it is not of much significance. Whenever probe has to be placed near a solid surface, for example near the bed wall, the flow will accelerate in that region and induce an error in the measurement known as wall vicinity effect. It was seen that the wall vicinity effect would cause an error in the yaw angle of the order of about ± 0.5 degree and a maximum error in the pitch angle about ± 2.5 degrees. Although the probe was not calibrated for the effect of pitch angle on the calibration constant, it is assumed negligible, as the maximum pitch angle is 2.5 degrees. The maximum errors induced for static pressure and velocity would be about 4 percent and 5 percent respectively. The error would be negligible beyond 2 probe thickness from the wall. The pressures sensed by the probe would also induce a maximum error of about 6% in the pressures and 5% in the velocities computed near the wall.

The flow blockage for a probe would be about 2.4% of the annular space. This flow blockage would result in an increase of the radial velocity by the same amount. Hence, the amount of error induced in the computed values would be of the order of about 2.4%. Probe stem supporting the probe would cause interference with the flow near the tip. Results obtained from the earlier researchers have shown that the error induced would be negligible when the distance between the probe tip was more than three times the stem diameter. In the present investigations, the probe tip was at about

9 mm away from the stem axis and the stem diameter was 2.6 mm and hence the effect of the stem interference was minimal.

Misalignment of the probe with the reference direction would also induce error in the pressures sensed by the probe. The probe was aligned properly so that the error in the reference direction would not exceed ± 0.2 degrees and hence the consequent error in the probe measurements would be very small. Another source of error is due to the interpolation method used. To estimate the magnitude of this error, some calibration data was fed as input to the interpolation program. The interpolated values of static and stagnation pressures and their components of velocities were compared with those values actually measured. The agreement was found to be excellent. The variables and the corresponding instruments used to measure them are given in table C1.

Table C1 Variable and instruments considered for measurement

Measured variable	Quantity	Instrument
T_a	Ambient temperature	Thermocouple
P_a	Ambient pressure	Barometer
α	Flow angle	protractor
ΔP	Pressure difference	Inclined manometer

The bias and precision errors for the above interments, except for the pressure probes, are given in the table C2.

Table C2 Bias and precision error of instruments

Instrument	Bias Error	Precision Error
Thermocouple	0.2 ⁰ C	0.5 ⁰ C
Barometer	2 mm of Hg	0.5 mm of Hg
Protractor	0.5 ⁰	0.125 ⁰
Inclined manometer	1 mm of water	0.25 mm of water

C3 ERROR IN PRESSURE MEASUREMENT

From the errors mentioned above, the major sources of error in pressure probe measurements can be identified as those caused by turbulence and blockage effects and hence they are considered as bias errors caused by installation effects. The corresponding values are presented in table C3

Table C3 Bias error in pressure measurement

Error source	Bias error
Turbulence	0.35%
Probe blockage	2.40 %
Inclined - manometer	0.5 mm of water

The precision error by the unsteadiness in the pressures was obtained by sampling 20 values of pressures were measured and the precision error was found to be 2.5 %. Considering the precision error in the inclined manometer, this was given as 0.25 mm. So, the total uncertainty in the pressure measurement can be calculated using equations C1 to C3 and the value obtained is $\pm 3.52 \%$

C4 ERROR IN MEASUREMENT OF ANGLE

The major sources of errors in the measurements of angle α and their corresponding bias errors are given in table C4. The total bias error in α thus works out to be $\pm 0.75 \%$

Table C4 Bias error in measurement of angle

Error Source	Bias Error
Inclined manometer	1 mm of water
Protractor	0.5^0

The precision errors, due to unsteadiness in the flow, for α is obtained by taking 20 samples and is found to be 2 %. Considering the precision errors in the inclined manometer and protractor, which are 0.5 mm of water and 0.125 degree and nominal values are 200 mm of water and 90 degrees respectively, the total uncertainty involved in the angle measurement can be calculated as $\pm 0.77\%$.

C5 ERROR IN VELOCITY MEASUREMENT

The expression for velocity and its consequent simplification is given in equation C4.

$$V \text{ (velocity)} = \left[\frac{2 \times (\text{dynamic pressure})}{\text{density}} \right]^{1/2} = \left[\frac{2(\Delta P)}{\rho} \right]^{1/2} \quad (\text{C.4})$$

where,

$$\rho = \frac{(\text{ambient pressure})}{(R) \times (\text{ambient temperature})} = \frac{P_a}{R \times T_a}, \text{ R being the gas constant}$$

$$\text{Now, V can be written as a (constant)} \times \left[\frac{\Delta P \times T_a}{P_a} \right]^{1/2}.$$

The bias B_V in the velocities can be written in terms of the biases in the other variables and the same is presented in equation C5.

$$\frac{B_V}{V} = \left[\frac{1}{4} \times \left(\frac{B_{\Delta P}}{\Delta P} \right)^2 + \frac{1}{4} \times \left(\frac{B_{T_a}}{T_a} \right)^2 + \frac{1}{4} \times \left(\frac{B_{P_a}}{P_a} \right)^2 \right]^{1/2} \quad (\text{C.5})$$

The expression for the precision error P_V is the similar to that of the bias error with B being replaced by P with the corresponding suffixes. The bias and precision errors of different measurement for the calculation of velocity are present in table C5. The total uncertainty involved in the velocity measurement can be calculated as $\pm 0.36\%$.

Table C5 Bias and precision error – velocity calculation

Variable	Bias Error	Precision Error
ΔP	1 mm of water	0.25 mm of water
T_a	0.2 °C	0.05 °C
P_a	2 mm of Hg	0.5 mm of Hg

C6 CONCLUSION

Result of the uncertainty analysis in connection with the measurement using three hole probe is summarized below.

1. Total uncertainty in pressure measurement = $\pm 3.52\%$
2. Total uncertainty in the measurement of angle = $\pm 0.77\%$
3. Total uncertainty in velocity calculation = $\pm 0.36\%$

APPENDIX D

VIDEO CLIPPING

D1 INTRODUCTION

Behaviour of fluidized bed with different types of distributors considered in the present study is presented in the form of video clippings in the attached compact disc and it's details are given in table D1.

Table D1 Details of video clipping

Sl. No.	File Name	Distributor Type	Particle Used
1	PPD-PB	Perforated plate	Polystyrene Beads
2	PPD-PP	Perforated plate	Pepper
3	PPD-CB	Perforated plate	Coffee Beans
4	PPD-CC	Perforated plate	Coca Beans
5	SRVD-PP	Single row vane type	Pepper
6	SRVD-CB	Single row vane type	Coffee Beans
7	SRVD-CC	Single row vane type	Coca Beans
8	IHD-PP	Inclined hole type	Pepper
9	IHD-CB	Inclined hole type	Coffee Beans
10	IHD-CC	Inclined hole type	Coca Beans
11	TRVD-PP	Three row vane type	Pepper
12	TRVD-CB	Three row vane type	Coffee Beans
13	TRVD-CC	Three row vane type	Coca Beans

REFERENCES

1. **Agarwal J. C., Davis W. L., and King D. T.**, (1962), "Fluidized -bed Coal dryer", *Chemical Engineering Progress*, Vol.58, No. 11, pp 85-90.
2. **Binod Sreenivasan and Vijay R. Raghavan**, (2002), "Hydrodynamics of a swirling fluidised bed", *Chemical Engineering and Processing*, Vol.41, pp 99- 106.
3. **Birk R. H., Camp G. A. and Hutchinson L. B.**, (1990), "Design of an Agglomeration Resistant Gas Distributor", *AIChE Symposium series*, Vol 86, pp 16-21.
4. **Botterill J. S. M., Teoman Y. and Yüregir K. R.**, (1982), "The Effect of Operating temperature on the Velocity of Minimum Fluidization, Bed Voidage and General Behaviour", *Powder Technology*, Vol.31, pp 101-110.
5. **Botterill J. S. M., Teoman Y. and Yuregir K. R.**, (1982), "The Effect of temperature on the Fluidized bed behaviour", *Chemical Engineering*, Vol.15, pp 227-238.
6. **Bouratoua R., Molodtsov Y., and Koniuta A.**,(1993), "Hydrodynamic Characteristics of a Pressurized Fluidized Bed", *Proceedings of the 12th International Conference on Fluidized Bed Combustion*, San Diego, California, 9-13 May, Vol 1, pp 63-70.
7. **Chen Y. M.**, (1987), "Fundamentals of a Centrifugal Fluidized Bed", *AIChE Journal*, Vol. 23, No. 5, pp 249-252.
8. **Chue S. H.**, (1975), "Progress in Aerospace", *Pressure Probe for Fluid Measurement*, Pergamon press, Vol.16, pp 147-223.
9. **Chyang C. S. and Huang C.C.**, (1991), "Pressure Drop across a Perforated-Plate Distributor in a Gas Fluidized Bed", *Journal of Chemical Engineering of Japan*, Vol. 33, No. 2, pp 722-728.
10. **Coleman H. W., and Steele Jr. W. G.**, (1989), "Experimentation and Uncertainty Analysis for Engineers".
11. **Desai A, H. Kikukawa and Pulsifer A. H.**, (1977), "The Effect of temperature upon minimum fluidizing velocity", *Powder Technology*, Vol 16, pp 143-144.
12. **Fan L.T, Chang C. C. and Yu Y. S., Teruo Takahashi and Zennosuke Tanaka**,(1985), "Incipient Fluidization Condition for a Centrifugal Fluidized Bed", *AIChE Journal*, Vol. 31, No. 6, pp 999-1009.
13. **Fakhimi S., Sohrabi S. and Harrison D.**, (1983), "Entrance Effect at a Multi-orifice Distributor in Gas Fluidized Beds", *The Canadian Journal of Chemical Engineering*, Vol 61, June, pp 364-369.

14. **Geldart D., and Bayens J.** (1985). "The design of distributors for gas-fluidized beds", *Powder Technology*, Vol. 42, pp 67.
15. **Govardhan M.** (1997). "Uncertainty Analysis of Experimental Data", *QIP Short Term Course on Modern Measurement Techniques of Turbomachinery*, Indian Institute of Technology, Madras.
16. **Hatamipour M.S. and Mowla D.** (2002), "Shrinkage of carrots during drying in an inert medium fluidized bed", *Journal of Food Engineering*, Vol 55, pp 247-252.
17. **Hiby J. W.**, (1967), "Periodic Phenomena Connected with Gas-Solid Fluidization", pp 99-106.
18. **Holman J. P. and Gajda Jr.** (1989). "Experimental Methods for Engineers", Mc Graw Hill.
19. **Howard J. R.**, (1989), "Fluidized Bed Technology Principles and Applications", Adam Higher, Bristol, New York.
20. **Kao J., Pfeffer R. and Tardos G. I.**, (1987), "On Partial Fluidization in Rotating Fluidized Beds", *AIChE Journal*, Vol 33, pp 858-866.
21. **Kroger D. G., Levy E. K. and Chen J. C.**, (1979), "Flow Characteristics in Packed and Fluidized Rotating Bed", *Powder Technology*, Vol 24, pp 9.
22. **Mathur A., Saxena S. C. and Zhang Z. F.**, (1986), "Hydrodynamic Characteristics of Gas Fluidized Beds over a Broad Temperature Range", *Powder Technology*, Vol 47, pp 247-256.
23. **Moffat R. J.**, (1985), "Using Uncertainty-analysis in the Planning of an Experiment", *ASME Journal of Fluid Engineering*, Vol 107, pp 173-180.
24. **Nakamura M., Hamada Y. and Toyama S.**, (1985), "An Experimental Investigation of Minimum Fluidization Velocity at Elevated Temperatures and Pressure", *The Canadian Journal of Chemical Engineering*, Vol 63, pp 8.
25. **Niamnuy C. and Devahastin S.** (2004), "Drying kinetics and quality of coconut dried in a fluidized bed", *Journal of Food Engineering*, Vol 66, pp 267- 271.
26. **Otero R. A. and Munoz C. R.**, (1974), "Fluidized Bed Gas Distribution of Bubble Cap Type", *Powder Technology*, Vol 9, pp 279-287.
27. **Ouyang F. and Levenspiel O.**, (1986), "Spiral Distributor for Fluidized Beds", *Ind. Eng. Che. Process Des. Dev.*, Vol 25, pp 504-507.
28. **Özbey M. and Söylemez M.S.**, (2004), "Effect of swirling flow on fluidized bed drying of wheat grains", *Energy Conversion and Management*, Vol 46, pp 1495-1512.

29. **Poti N. D. and Rabe D. C.**, (1988), "Verification of Compressor Data Accuracy by Uncertainty analysis and Testing Methods", *ASME Journal of Turbomachinery*, Vol 110, pp 265-269.
30. **Prakash S., Jha S.K. and Datta N.**, (2004), "Performance evaluation of blanched carrots dried by different dries", *Journal of Food Engineering*, Vol 62, pp 305-313
31. **Qureshi A. E. and Creasy D. E.**, (1979), "Fluidized Bed Gas Distributors", *Powder Technology*, Vol 22, pp 113-119.
32. **Sadasivan S., Barreteau D. and Laguerie C.**, (1980), "Studies on frequency and magnitude of fluctuation of pressure drop in gas-solid fluidized beds", *Powder Technology*, Vol 26, pp 67-74.
33. **Sathiyamoorthy D. and Rao CH. S.**, (1981), "The Choice of Distributor to Bed Pressure Drop Ratio in Gas Fluidised Beds", *Powder Technology*, Vol 30, pp 139-143.
34. **Sathiyamoorthy D. and Rao CH. S.**, (1978), "Gas Distributor in Fluidized Bed", *Powder Technology*, Vol 20, pp 47-52.
35. **Sathiyamoorthy D. and Rao CH. S.**, 1979, "Multi-Orifice Plate Distributors in Gas Fluidised Beds- A Model for Design of Distributors",
36. **Saxena S. C., Chatterjee A. and Patel R. C.**, (1979), "Effect of Distributors on Gas-Solid Fluidization", *Powder Technology*, Vol 22, pp 191-198.
37. **Saxena S. C., Rao N. S. and Zhou S. J.**, (1990), "Fluidization Regime Delineation in Gas- Fluidized Bed", *AIChE Symposium Series*, Vol 86, n 276, pp 95-102.
38. **Senadeera W., Bheshe R. B. Gordon Young and Bandu Wijesinghe**, (2003), "Influence of shapes of selected vegetable materials on drying kinetics during fluidized bed drying", *Journal of Food Engineering*, Vol 58, pp 277-283.
39. **Shi Y. F. and Fan L. T.**, (1984), "Effect of Distributor to Bed Resistance Ratio on Uniformity of Fluidization", *AIChE Journal*, Vol 30, No. 5, pp 860-867.
40. **Shi M.H., Wang H. and Hao Y.L.**, (2000), "Experimental investigation of the heat and mass transfer in a centrifugal fluidized bed dryer", *Chemical Engineering Journal*, Vol 78, pp 107-113.
41. **Shu J., Lakshmanan V.I. and Dodson C.E.**, (2000), "Hydrodynamic study of a toroidal fluidized bed reactor", *Chemical Engineering and Processing*, Vol 39, pp 499-506.
42. **Siegel R.**, (1976), "Effect of Distributor Plate-to-Bed Resistance Ratio on Onset of Fluidized Bed Channeling", *AIChE, Journal*, Vol 22, No.2, pp 590.

43. **Singh B., Rigby G. R. and Callcott T. B.**, (2000), "Measurement of minimum fluidization velocities at elevated temperature", *Trans. Instn Chemical Engineering*, Vol 51, pp 93-96.
44. **Sutherland J. P.**, (1964), "The measurement of pressure drop across a gas fluidized bed", *Chemical Engineering Science*, Vol 19, pp 839-841.
45. **Takahashi T., Tanaka Z., Itoshima A. and Fan L. T.**, (1984), "Performance of Rotating Fluidized Bed", *Journal of Chemical Engineering Japan, Powder Technology*, Vol 17, pp 333-335.
46. **Topuz A, Mesut Gur and Zafer Gul M.**, (2004), "An experimental and numerical study of fluidized bed drying of hazelnuts", *Journal of Applied thermal engineering*, Vol. 24, pp 1535-1547.
47. **Upadhyay S. N., Saxena S. C. and Ravetto F. T.**, (1981), "Performance Characteristics of Multijet Tuyere Distributor Plate", *Powder Technology*, Vol 30, pp 155-159.
48. **Vikram G., Martin H. and Raghavan V.R.**, (2003), "The Swirling Fluidized Bed –An Advanced Hydrodynamic Analysis", *Proceedings of the 4th National Workshop and Conference on CFB Technology and Revamping of Boilers in India*, Bangalore Engineering College, June 3-4, pp 9-19.
49. **Virr M. J.**, (1985), "Advanced Shallow Bed Heat Exchangers", *Industrial Heat Exchangers Exposition and Symposium Proceedings, American Society of Metals, Pittsburgh*, pp 81-97.
50. **Vreedenberg H. A.**, (1958), "Heat transfer between a fluidization bed and a horizontal tube", *Chemical Science*, Vol 9, pp 52-60.
51. **Wen C. Y., Krishnan R., Khosravi R. and Dutta S.**, (1978), "Dead Zone Height near the Grid of Fluidized Bed in Fluidization", J F Davidson and D L Keairns, Eds, Cambridge Uni. Press, pp 32.
52. **Whitehead A. B., Davidson J. F. and Harrison D.**, (1971), "Problems in Large Scale Fluidized Beds in Fluidization", Eds Academic Press, pp 781.
53. **Wu S. Y., and Baeyens J.**, (1991), "Effect of operating temperature on minimum fluidization velocity", *Powder Technology*, Vol. 67, pp 217-220
54. **Yacono C. and Angelino H.**, (1978), "The Influence of Gas Distributor on Bubble Behaviour Comparison between Ball Distributor and Porous Distributor in Fluidization", J F Davidson and D L Keairns, Eds, Cambridge University Press, pp 25.
55. **Yang J.S, Liu Y.A. and Squires**, (1987), "Pressure Drop across Shallow Fluidized Beds: Theory and Experiment", *Powder Technology*, Vol 53, pp 79-89.